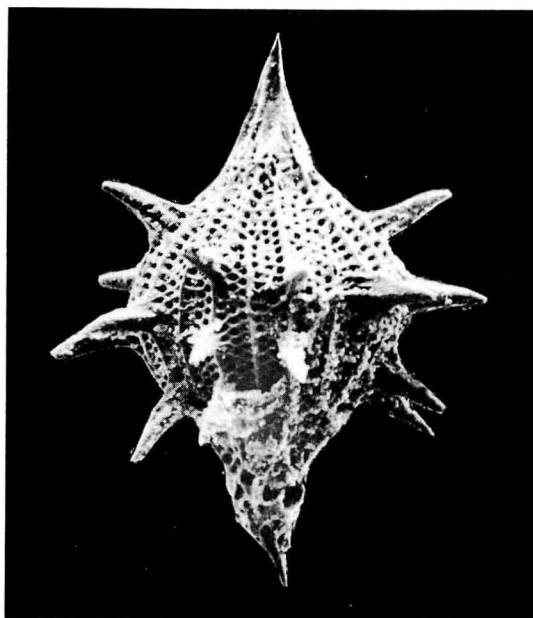


日本古生物学会 報告・紀事

Transactions and Proceedings
of the
Palaeontological Society of Japan

New Series No. 138



日本古生物学会
Palaeontological Society of Japan
July 15, 1985

Co-Editors

Takashi HAMADA and Hisayoshi IGO

Officers for 1985—1986

President: Toshimasa TANAI

Honorary President: Teiichi KOBAYASHI

Councillors: Kiyotaka CHINZEI, Takashi HAMADA, Tetsuro HANAI, Yoshikazu HASEGAWA, Itaru HAYAMI, Hisayoshi IGO, Junji ITOIGAWA, Tadao KAMEI, Tatsuaki KIMURA, Tamio KOTAKA, Kei MORI, Ikuwo OBATA, Tsunemasa SAITO, Yokichi TAKAYANAGI, Toshimasa TANAI

Members of Standing Committee: Kiyotaka CHINZEI (Membership), Takashi HAMADA (Co-Editor of Transactions), Yoshikazu HASEGAWA (Foreign Affairs), Itaru HAYAMI (Planning), Hisayoshi IGO (Co-Editor of Transactions), Tatsuaki KIMURA (Finance), Ikuwo OBATA (General Affairs), Yokichi TAKAYANAGI (Editor of "Fossils"), Juichi YANAGIDA (Editor of Special Papers)

Auditor: Yoshiaki MATSUSHIMA

The fossil on the cover is *Unuma (Spinunuma) echinatus* ICHIKAWA and YAO, a Middle Jurassic multisegmented radiolaria from Unuma, Gifu Prefecture, central Japan (photo by A. YAO, × 260).

All communication relating to this journal should be addressed to the

PALAEONTOLOGICAL SOCIETY OF JAPAN

c/o Business Center for Academic Societies,

Yayoi 2-4-16, Bunkyo-ku, Tokyo 113, Japan

795. EARLY PALEOGENE SILICOFLAGELLATES AND EBRIDIANS FROM THE ARCTIC OCEAN*

HSIN YI LING

Department of Geology, Northern Illinois University, DeKalb, Illinois 60115

Abstract. Subsequent to the finding of Upper Cretaceous (Maastrichtian?) submarine sediments from FL-437, another unusual core, FL-422, was recognized from the Fletcher's Ice Island T-3 in the Alpha Ridge region of the Arctic Ocean. In spite of a superficial lithological resemblance to the previous FL-437 cored sediments, the silicoflagellate and ebridian assemblage identified from the FL-422 marine deposits is best considered as Early Paleogene age. Its microfloral composition is distinctly different from all the previously published records of this group of siliceous microfossils of other parts of the world. The following new taxa are proposed:

Dictyocha arctios, *D. curta*, and *Ammodochium fletcheri*. This report of Early Paleogene silicoflagellates and ebridians reconfirms the existence of pre-Miocene deep-sea sediments in the Alpha Ridge area of the Arctic Ocean, thus providing paleoceanographic evidence about geophysical and tectonic paradigm of the Arctic Ocean floor.

Introduction

The recovery of an unusual sediment core, FL-437 (Text-fig. 1), from the Alpha Ridge area of the Arctic Ocean, and the subsequent age identification of the sediments as Late Cretaceous (Maastrichtian?) based on the contained silicoflagellate assemblage (Ling *et al.*, 1973), provided the first documentation of the occurrence of pre-Pliocene sediments in the Arctic Basin.

Another interesting deep-sea sediment core, FL-422 (Text-fig. 1), was recovered from the same area and its unique nature was apparent even at preliminary examination when a Paleocene-Eocene age was suggested (Clark, 1974; Kitchell and Clark, 1982). First, the sediments are silicoflagellate-diatom ooze and second, the silicoflagellate assemblage is distinctive when it

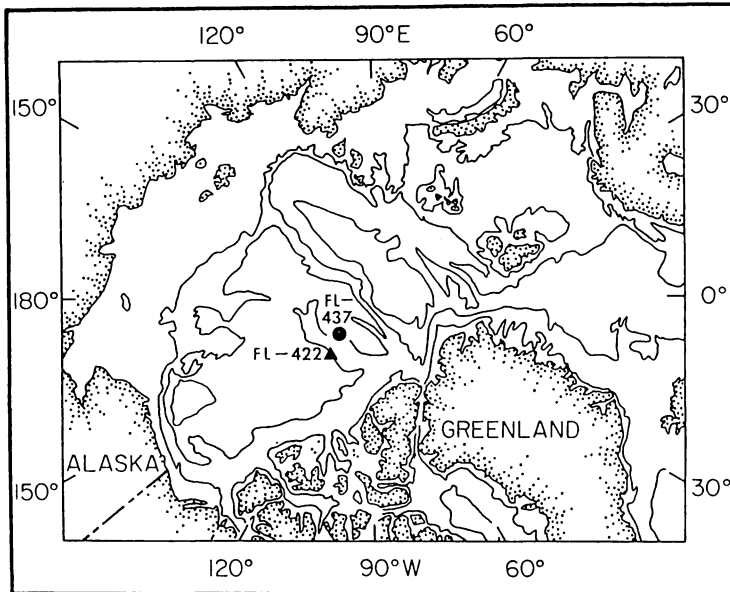
is compared with the available records of this group of microfossils from other parts of the world, including those from the land outcrops and submarine deposits.

This paper reports the silicoflagellate and ebridian assemblage including new taxa, refines the earlier age estimate to Early Paleogene, and discusses its significance with sea-floor spreading and plate tectonic paradigm of the Arctic Ocean.

Material studied

Core FL-422 was collected at 84°53.48'N, 142°32.87'W at a water depth of 2,049 meters from the Fletcher's Ice Island T-3 on July 20, 1969 (Text-fig. 1). The core is 364 cm long. The uppermost 12 cm is a "normal" Arctic gray-brown (10YR 4/4) lutite, rich in typical cold-water planktonic foraminifera, "*Globigerina*"

*Received September 3, 1983.



Text-fig. 1. Index map of Arctic Ocean showing the location of core FL-422 studied in this paper. The position of the Late Cretaceous (Maestrichtian?) silicoflagellate-bearing sediment core FL-437 is also indicated.

pachyderma. Below this is 169 cm of yellow to yellow orange (10YR 6/6) siliceous oozes with some darker clasts. Four samples from this sequence revealed that they contained up to 60% montmorillonite with 10–20% illite, chlorite and kaolinite. Underlying this middle unit is 183 cm of dark brown to black (10YR 2/1) siliceous oozes, more like normal Pleistocene Arctic sediments. All contacts may be unconformable (Clark, 1974; Kitchell and Clark, 1982). As in previous investigations from the area (Ling *et al.*, 1973), cores were cut into 15 cm segments and numbered consecutively upward. Samples were also taken at 5 cm intervals throughout the cores for paleomagnetic polarity measurement. All the samples showed normal polarity, with the exception of 9 samples from 22 to 57 cm below the top of the core, which showed reverse polarity. This polarity sequence could not be correlated with any known Pleistocene-Pliocene magnetic sequences in the Arctic (Clark, 1971, 1974).

In the cored sediments, specimens of planktonic foraminifera, "*Globigerina*" *pachyderma* and a few *Globigerina quinqueloba* were found.

"*G.*" *pachyderma* were abundant in the upper 12 cm (segment 24), and although rare, were also found in the next lower 18 cm and in the bottom segment of the core (Clark, 1974).

Systematic paleontology

Utilizing procedures similar to the previous studies for this group of siliceous microfossils (*e.g.*, Ling, 1970, 1972; Ling *et al.*, 1973), cored sediments (from the center of each 15 cm segment) were chemically treated prior to the detailed examination under the microscope. Terminology employed throughout the present paper for silicoflagellates is as described previously (Ling, 1972), and for those ebridians, after Deflandre (1934, 1951), Ling (1972), and Loeblich, III. *et al.* (1968). Observation under a scanning electron microscope, JSM-U3, was made for some selected taxa to examine their surface microstructures.

Slides containing type specimens with USNM numbers will be deposited in the National Museum of Natural History, Smithsonian Insti-

tution, Washington, D.C. and all the remaining slides and negatives of the scanning electron microscopy used for the present investigation will be deposited permanently in the micropaleontology collection of the Department of Geology, Northern Illinois University, DeKalb, Illinois.

Order Siphonotestales Lemmermann, 1901a

Genus *Corbisema* Hanna, 1928

Corbisema apiculata (Lemmermann)

Pl. 10, Figs. 1, 2.

Dictyochoa triacantha var. *apiculata* Lemmermann, 1901b, p. 259, pl. 10, figs. 19, 20.

Corbisema apiculata (Lemmermann), Frenguelli, 1940 (in part), fig. 12 h; Ling, 1972, pp. 151, 152, pl. 23, figs. 13-17.

Corbisema hastata hastata (Lemmermann)

Pl. 10, Figs. 3, 4.

Dictyochoa triacantha var. *hastata* Lemmermann, 1901b, p. 259, pl. 10, figs. 16, 17.

Corbisema hastata hastata (Lemmermann), Bukry 1976a, p. 892.

Corbisema sp. cf. *C. inermis minor* (Glezer)

Pl. 10, Figs. 5, 6.

Dictyochoa triacantha var. *apiculata* fa. *minor* Schulz, Gemeinhardt, 1930, p. 42, fig. 31.

Not *Dictyochoa triacantha* var. *apiculata* fa. *minor* Schulz, 1928, p. 249, figs. 29 a, b.

Not *Dictyochoa triacantha* var. *inermis* f. *minor* Glezer, 1966, p. 231, pl. 8, figs. 3-5; pl. 31, fig. 7.

Not *Corbisema inermis minor* (Glezer), Bukry, 1976a, p. 892, pl. 5, fig. 47.

Remarks:—The specimens from the core FL-422 appear to be identical to the form observed by Gemeinhardt (1930) from Oamaru, New Zealand. These specimens possess round apices of the basal body ring as well as very short but definite radial spines at the apices. The specimens, beyond any doubt, closely resemble those illustrated by Glezer (1966) from various locali-

ties of Russia ranging in ages from Early Paleocene through Early Oligocene, and by Bukry (1976a) from the Paleocene section of Hole 327A of the Falkland Plateau. However, the present Arctic specimens can be differentiated from them by its possession of definite short radial spines at the three apices and by the less elevated apical structure.

Corbisema triacantha (Ehrenberg)

Pl. 10, Fig. 7; Pl. 12, Fig. 1.

Dictyochoa triacantha Ehrenberg, 1844, p. 80.

Corbisema triacantha (Ehrenberg), Hanna, 1931, p. 198, pl. D, fig. 1.

Genus *Dictyochoa* Ehrenberg, 1838

Dictyochoa sp.

Pl. 10, Figs. 8-11; Pl. 12, Figs. 2-4.

Description:—Basal body ring, rhombic, with well developed radial spines of approximately equal length to the respective axis; lateral rods, also well developed, intersecting nearly perpendicular to the outline of the basal ring in either apical or abapical view, joined on the apical side of the basal ring, and extending well beyond the basal ring; major and minor axes intersect slightly obliquely; apical bar, short, generally on the direction of major axis, but some also on minor axis; neither apical or basal accessory spines present.

The surface microstructure of the species shows a reticulate pattern on the abapical side of the basal ring (Pl. 12, Figs. 2, 3), but a nearly smooth, or very weak, if present, reticulate pattern on the apical side (Pl. 12, Fig. 4); whereas the apical bar and lateral rods are finely reticulate on the apical side (Pl. 12, Fig. 4), and definitely reticulate on the abapical side (Pl. 12, Fig. 3).

Remarks:—Undoubtedly the present species is similar to *D. frenguelli* Deflandre (1950, p. 66, 82, figs. 188-193) or *D. f.* var. *frenguelli* by Glezer (1966, p. 240, pl. 11, fig. 9) in its general configuration. However, it differs from

them by its larger size, much developed lateral rod extensions, and the rhombic rather than quadrate or square-shaped basal ring. It also lacks basal accessory spines.

Bukry (1984) referred the specimens of the present taxon to his two subspecies, *Dictyocha aspera martini* and *D. fibula formicata*. The major difference of these two subspecies is the orientation of an apical bar either on or transversal to major axis. Unfortunately, the present Arctic specimens show both directions, although preference seems to be along the major axis. SEM observation of the specimens failed to reveal any difference on their surface microstructure.

Thus the present species includes a part of *Dictyocha aspera martini* (Bukry, 1975, p. 854, pl. 2, figs. 5?, 6, 8 (only); 1984, p. 199, fig. 1e). As to *Dictyocha fibula formicata*, Bukry (1975, p. 854) differentiated it from *D. frenguelli* of Deflandre (1950) by an absence of "a modified apical plate", but in the original description, Deflandre (1950, pp. 66–67) stated only: ". . . baguette apical courte, typiquement élargie mais non aplatie, l'aire apicale formée restant creuse; . . ." and never mentioned the presence of such a plate structure. Therefore, further comparative study, particularly samples from the southern ocean, is necessary in order to clearly the taxonomy of the present Arctic species.

Dictyocha arctios Ling, n. sp.

Pl. 10, Figs. 12-15.

Description:—Basal ring, square, with a slight indentation in the outline where the lateral rods originate; radial spines, longer or approximately equal in length with the diagonal dimension of the basal ring; lateral rods straight, intersecting near the center to form a letter X, or with a very short apical bar; apical spine projects upward; both apical and basal accessory spines, absent.

Derivation of name:—The new species is named after the Arctic Ocean.

Remarks:—The general appearance of this new species calls to mind some of the specimens

illustrated previously by various workers as *D. staurodon* Ehrenberg. Therefore, the following discussion is in order.

A silicoflagellate species, *Dictyocha staurodon*, was originally proposed by Ehrenberg (1844, p. 71; p. 80) and illustrated later by him (1854, pl. 18, fig. 58) from a Miocene sample of Richmond, Virginia. His specimen showed a rhombic basal ring, short radial spines, basal accessory spines, and above all, a very small square-shaped apical window. The presence of this apical structure was later confirmed by Locker (1974, p. 640, pl. 3, fig. 10) after his reexamination of the original Ehrenberg's collection. He correctly identified the species as *Distephanus crux* under the widely accepted present-day classification scheme, and this reassignment has already been adopted, e.g., Bukry (1977, p. 687).

A literature survey has revealed that the following forms have been incorrectly assigned to *Dictyocha staurodon*:

1. forms with long radial spines, straight lateral rods and with an apical spine only; Schulz (1928, fig. 34 C) from Bremia.
2. forms with long radial spines, straight lateral rods and with both apical and basal accessory spines: Lemmermann (1901b, pl. 10, fig. 22; 1903, fig. 91) from the Atlantic. Gemeinhardt (1930, fig. 38b) from Bremia.
3. forms with long radial spines and an apical accessory spine, but with curved lateral rods and basal accessory spines either present or absent: Schulz (*op. cit.*, figs. 34a, b) and Gemeinhardt (*op. cit.*, fig. 38a) from Dolje.
4. forms with short radial spines but straight lateral rods and an apical accessory spine as *f. minor*: Schulz (*op. cit.*, fig. 38d) from Kusnetz; or without an apical spine, Mandra (1968, p. 253, fig. 65) from California and Zanon (1934, p. 66, figs. 9, 10) from Italy.
5. forms with short radial spines and both apical and basal accessory spines but curved lateral rods: Schulz (*op. cit.*, fig. 34f) and Gemeinhardt (*op. cit.*, fig. 38c) from the Atlantic Ocean.

A specimen from Bremia illustrated by

Schulz (*op. cit.*, fig. 34c), referred to as "Bremia bei Kavna, Hungary," and as Sarmatian Stage by Loeblich, III. *et al.*, (*op. cit.*, p. 17) may undoubtedly be conspecific with the present species. However, it seems reasonable to propose them as separate species in view of first, their chronostratigraphic differences, Paleogene vs. Miocene; and second, because thus far there is no subsequent record of the species from any part of the world, including the submarine deposits recovered by DSDP.

Measurements:—Length on major axis of basal body ring, 36-42 μm ; of basal spines, 24-36 μm .

Types:—Holotype, USNM 395821; Isotype, USNM 395822.

Dictyocha sp. cf. *D. carentis incerta* (Glezer)

Pl. 10, Figs. 16, 17; Pl. 13, Figs. 1-3.

Dictyocha frenguelli var. *carentis* fa. *incerta*
Glezer, 1964, p. 52, pl. 1, figs. 15, 16; Glezer, 1966, pp. 241, 242, pl. 11, figs. 14-16.

Dictyocha cf. *D. carentis* Glezer, Perch-Nielsen, 1975a (in part), p. 686, pl. 4, fig. 6 (only).

Remarks:—It is agreed with Perch-Nielsen (1975a) and Bukry (1976a, p. 893) that Glezer's variety should be raised to specific rank. Separation seems warranted because *D. frenguelli* — proposed originally by Deflandre (1950) from the Eocene diatomites of Isenski, Singhiliewski (or Cenghileevsky) and Kamischev of Russia — is quite different from the present taxon in its apical configuration as well as in its dimensions. Based on the observation of specimens under both transmitted and scanning electron microscopes, it is advisable to consider the present taxon as having the following characteristics: (1) the shape of the basal body ring is circular; (2) the radial spines are all short, of equal dimension, and truncated at the distal end, and (3) it is very small in size.

The specimens from the Arctic deep-sea sediments are thus apparently closely related to Glezer's *forma* from the Urals (but, according to her, from Eocene to early Oligocene). Judging from her illustrations, however, the Russian specimens seem to possess an apical plate (see

particularly her figures 16 of 1964 and 1966) instead of thick lateral rods, and an apical bar short if present.

Perhaps it would be advisable in the future to remove the present taxon from *D. carentis* because of the differences in the shape of basal body ring (circular vs. square) and the nature of radial spines (short and thick vs. long and pointed). However, such action should wait until an actual comparative study of Russian samples can be made.

Dictyocha curta Ling, n. sp.

Pl. 10, Figs. 18-21.

Description:—Basal body ring, square, with smoothly rounded apical corners; radial spines short, occasionally truncated at the distal end, and located near the middle of the side, not at the corners like other species; an apical bar, very short, but parallel to a set of the basal ring; neither apical nor basal accessory spines present.

Derivation of name:—The species name is derived from *curtus*, Latin for short, referring to the very short radial spines for the species.

Remarks:—This tiny *Dictyocha* is characterized by its square-shaped basal body ring, the unusual position of radial spines at the middle of four sides and not at the corners like numerous other silicoflagellates, and a short apical bar which is parallel to a pair of sides of basal body ring.

Measurements:—Length of a side of basal body ring, 15-22 μm ; of basal spines, 1-4 μm .

Types:—Holotype, USNM 395823; Isotype, USNM 395824.

Dictyocha deflandrei Frenguelli ex Glezer

Pl. 10, Fig. 22; Pl. 11, Figs. 1, 2.

Dictyocha deflandrei Frenguelli, 1940, figs. 14 a-d.

Dictyocha deflandrei var. *deflandrei* (Frenguelli), Glezer, 1966, p. 244, pl. 12, figs. 12, 16; pl. 32, fig. 4.

D. d. var. *completa* f. *completa* Glezer, 1966, pp. 244, 245, pl. 12, figs. 14, 15.

D. d. var. completa f. producta Glezer, 1966, pp. 245, 246, pl. 12, figs. 17-19.

Remarks:—A square-shaped basal ring with four developed radial spines and an apical plate (but without window) characterize the species. The three varieties and forma listed above from Russia are here combined confirming them as an intraspecific variation. Basal accessory spines may or may not be present.

Bukry observed triangular to hexagonal variants of the species from Legs 28 (1975a) and 29 (1975b) DSDP samples from the southern oceans.

Dictyocha fibula Ehrenberg

Pl. 11, Figs. 3-6.

Remarks:—As in my previous studies (e.g., Ling, 1970, 1972, 1973, 1975, 1977), a broad species concept is applied for specimens whose apical bar lies in the direction of major axis. Radial spines are either short or long.

Dictyocha obliqua Glezer

Pl. 11, Figs. 7, 8.

Dictyocha obliqua Glezer, 1964, p. 57, pl. 2, fig. 10; 1966, p. 246, pl. 13, figs. 1-5.

Remarks:—Although there are some differences (such as the minor axis is less oblique toward the major axis and an apical plate is almost exclusively in the direction of the major axis), it is considered here that the present Arctic forms are conspecific with those forms reported from Late Eocene through Early Oligocene of Russia observed by Glezer.

Dictyocha sp. cf. *D. rotundata* Jousé

Pl. 11, Figs. 9-12.

Description:—A basal body ring, generally smooth, semi-square to square without radial spines; an apical plate nearly square connected by short, broad lateral rods which originate from the corners of the basal ring; basal accessory spines absent.

Remarks:—This tiny silicoflagellate shows some superficial resemblances to forms reported from Late Eocene to Early Oligocene of Russia by Jousé (1955, *vide* Loeblich, III., *et al.*, 1968, p. 111, pl. 21, fig. 8), and by Glezer (1964, p. 53, pl. 1, figs. 17, 18; 1966, p. 243, pl. 11, figs. 17-20), but all the above Russian specimens show circular basal body rings.

Intraspecific variations observed during the present examination are: (1) the shape of the basal body ring; and (2) the proportion of the size of the apical plate relative to the basal body ring, as shown in the illustration. It should be noted that, thus far, only the subspecies, *D. rotundata secta* Glezer, has been reported from outside of Russia, *i.e.* the Norwegian Sea (Site 343) by Bukry (1976b), Martini and Müller (1976, as *D. rotundata* Jousé), but not the type of the species, *D. rotundata* Jousé (1955, 3a, *vide* Loeblich, III., *et al.*, *op. cit.*; Glezer, 1964, p. 53, pl. 1, figs. 17, 18; 1966, pl. 11, figs. 17-20).

Dictyocha spinosa Deflandre

Pl. 11, Figs. 13, 14.

Corbisema spinosa Deflandre, 1950, p. 65/82, figs. 178-182.

Dictyocha spinosa (Deflandre), Glezer, 1966, pp. 238, 239, pl. 10, figs. 6-8.

Remarks:—The specimens from the Arctic agree well with those reported by Deflandre from Barbados and Glezer from Russia. However, the Arctic specimens are larger than those previously reported specimens.

Genus *Distephanus* Stöhr, 1880

Distephanus speculum (Ehrenberg)

Pl. 11, Figs. 15, 16.

Dictyocha speculum Ehrenberg, 1838, p. 129, pl. 4, fig. Xn.

Distephanus speculum (Ehrenberg), Haeckel, 1887, p. 1565.

Remarks:—Considering the well-known long geological range and the widely accepted ecological habitat of cold-water forms (Gemeinhardt,

1930), it is somewhat surprising to find that only a few specimens were encountered in the studied submarine deposits from the Arctic Basin.

Order *Stereotestales* Lemmermann, 1901a

Genus *Ammodochium* Hovasse, 1932a

Ammodochium fletcheri Ling, n. sp.

Pl. 11, Figs. 17-20; Pl. 13, Fig. 5.

Description:—Ovoidal in outline in dorso-ventral view; three stout proclades branched distally to encircle one large and two small laterally situated upper windows; a small apical ring; proclades broadened distally to encircle a median window; a continuation of opisthoclades, slightly more slender than proclades, also stout and branched distally to encircle three lower windows like an apical end.

An examination by scanning electron microscope revealed that the entire surface of the specimen is covered by small open cavities providing a rugged appearance for the margin of skeletal components (Pl. 13, Fig. 5).

Derivation of name:—The species is named after the Fletcher T-3 Ice Island where the analyzed sediment core was collected. The name also refers to Joe O. Fletcher, currently at the NOAA, honoring his contribution to Arctic climatology.

Remarks:—This new species shows some resemblance to *A. speciosum* Deflandre (1934, pp. 92-94, figs. 37, 38) reported from diatomites of Skive (Jutland), Denmark, and from submarine deposits of DSDP Site 277 (52°12.43'S; 116°11.48'E) of the southern Campbell Plateau of the subantarctic southeast Pacific (Perch-Nielsen, 1975b, p. 880, pl. 5, figs. 1, 2). This species is, however, distinctly different from them by: (a) the more ovoidal outline; (2) having only one median window instead of two, resulting in the absence of mesoclades; and (3) possessing two extra lateral small windows at the apical and antapical ends.

Measurements:—Length 28-36 μm ; width, 24-30 μm .

Types:—Holotype, USNM 392825; Isotype,

USNM 392826.

Ammodochium rectangulare (Schulz)

Pl. 11, Figs. 21-23.

Ebria antiqua var. *rectangularis* Schulz, 1928, p. 274, figs. 72 a-d.

Ammodochium rectangulare (Schulz), Deflandre, 1932, pp. 303-305, figs. 1-13; Ling, 1971, p. 694, pl. 2, figs. 6, 7.

Genus *Ebriopsis* Hovasse, 1932a

Ebriopsis cornuta Dumitrica and Perch-Nielsen

Pl. 11, Fig. 24; Pl. 13, Fig. 4.

Ebriopsis cornuta Dumitrica and Perch-Nielsen, in Perch-Nielsen, 1975b, p. 880, fig. 2, pl. 7, figs. 8, 9.

Remarks:—The present taxon seems to agree well with those observed by Perch-Nielsen from the subantarctic southwest Pacific (1975b) and the Norwegian Sea (1976b).

The surface microstructure on the skeletal components is shown in the scanning electron micrograph (pl. 13, Fig. 4). Note that the small cavities are scattered over the surface of the skeletons.

Genus *Pseudammodochium* Hovasse, 1932b

Pseudammodochium dictyoides Hovasse

Pl. 11, Figs. 25-27.

Pseudammodochium dictyoides Hovasse, 1932b, pl. 463, figs. 12-15.

Discussion

(A) Microfloral comparison and age assignments

Table 1 presents the geological occurrence of silicoflagellate and ebridian taxa observed from the core 422 sediments of the Alpha Ridge. These taxa are also illustrated in Plates 10-13. The uniqueness of the assemblage is apparent when a comparison is attempted with all the previously published records of this group of siliceous microfossils worldwide: (1) completely absent are the age diagnostic forms of either

Cretaceous or those of well-known forms of late Late Paleocene or younger age, and (2) a few siliceous microfossils show some resemblance only with those taxa reported previously from Paleocene outcrops of USSR.

The silicoflagellate composition of Late Cretaceous age has been well documented in detail (Hanna, 1928; Mandra, 1968; Ling, 1972), including the nearby FL-437 core from the Arctic (Ling *et al.*, 1973; Bukry, 1981a), and Sites 208, 216 and 275 of Legs 21, 22 and 29 respectively (Bukry, 1973, 1974, 1975b) of the Deep Sea Drilling Project from the southern hemisphere. None of these age diagnostic species were encountered from the core 422 materials.

On the other hand, the conspicuous complete absence of specimens belonging to the genera *Naviculopsis* and *Mesocena* from the core 422 is rather striking and warrants further discussion. Both of these two genera are characteristic and/or abundant for upper Upper Paleocene and younger sediments although Glezer (1966,

p. 163) reported *Mesocena* aff. *apiculata* (Schulz) from Early Paleocene of Ural (*e.g.*, Glezer, 1966; Bukry, 1981b; Ling, 1981).

Numerous articles have been published from both the northern and southern hemispheres including areas as far north as Russia (Glezer, 1966) and Denmark (Perch-Nielsen, 1976a) and as far south as the subantarctic regions (Busen and Wise, 1976; Ling, 1981). Consequently, noting the complete absence of these two genera from the core 422, it appears safe to conclude that: (1) their absence is probably not due to paleogeographic limitation, and (2) the age of the cored sediments is Early Paleogene, probably predates late Late Paleocene.

Once the above age assignment has been established, it is not surprising that the Late Cretaceous core FL-437 shows only normal polarity (Clark, 1971), because the majority of the Cretaceous Period has been known to have normal magnetic polarity (van Hinte, 1976). On the other hand, throughout the Early

Explanation of Plate 10

Scale bar = 10 μ m. Upper left bar for figures 1–6, 8–11; lower left bar for figures 7, 16–22. Location of specimen is indicated as: sample no., slide no., England Finder reading.

Figs. 1, 2. *Corbisema apiculata* (Lemmermann)

1. 21, L-2, U21/0; 2. 16, R-1, D15/0, abapical lateral view showing the nature of abapical accessory spines.

Figs. 3, 4. *Corbisema hastata hastata* (Lemmermann)

10, R-1, F20/3.

Figs. 5, 6. *Corbisema* sp. cf. *C. inermis minor* (Glezer)

5, L-2, 019/0.

Fig. 7. *Corbisema triacantha* (Ehrenberg)

20, L-2, T39/2.

Figs. 8–11. *Dictyochoa* sp.

8, 9. 18, R-1, U23/0, 10, 11. 19, R-1, V24/0.

Figs. 12–15. *Dictyochoa arctios* Ling, n. sp.

12, 13. 1, R-1, F15/0, Holotype U.S.N.M. No. 395821.

14, 15. 2, L-3, M21/0, Isotype U.S.N.M. No. 395822.

Figs. 16, 17. *Dictyochoa* sp. cf. *D. carentis incerta* (Glezer)

10, L-2, D17/3.

Figs. 18–21. *Dictyochoa curta* Ling, n. sp.

18, 19. 8, L-2, L41/0, Holotype U.S.N.M. No. 395823.

20, 21. 1, L-2, F10/0, Isotype U.S.N.M. No. 395824.

Fig. 22. *Dictyochoa deflandrei* Frenguelli ex Glezer

20, L-2, Q24/0.

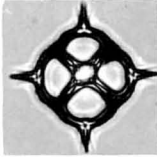
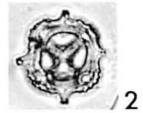
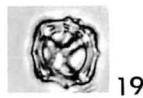
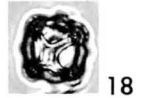
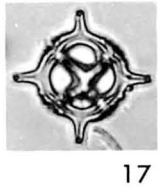
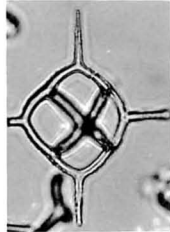
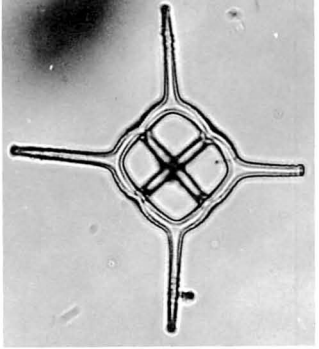
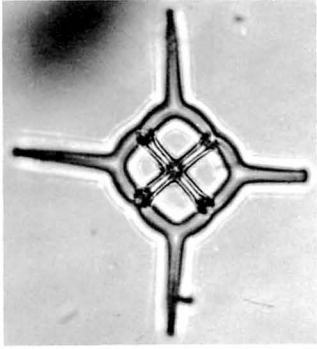
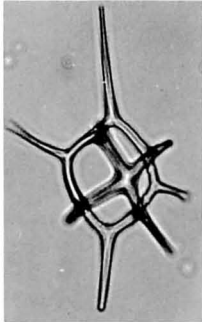
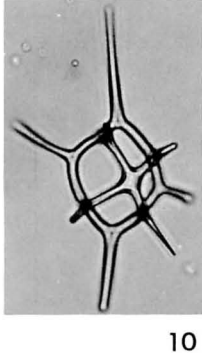
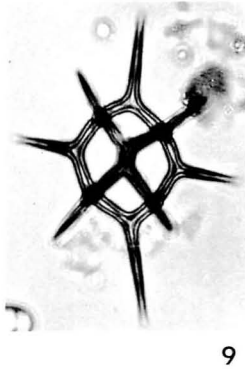
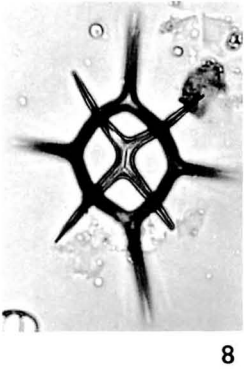
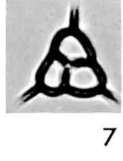
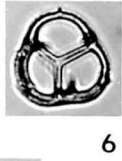
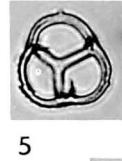
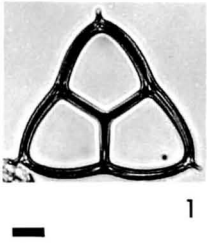


Table 1. Occurrence of silicoflagellates and ebridians (based on 300 specimen count) from FL-422 cored sediments of the Alpha Cordillera region of the Arctic Ocean, (P, single specimens; R, 2–5%; C, 6–25%; A, > 26%).

SAMPLE	TAXA
24	<i>Corbaisema apiculata</i>
23	<i>Corbaisema hirsuta</i> <i>hirsuta</i>
22	<i>Corbaisema</i> sp. cf. <i>C. inermis</i> <i>minor</i>
21	<i>Corbaisema tricantha</i>
20	<i>Diatyocha</i> sp.
19	<i>Diatyocha aretios</i> n. sp.
18	<i>Diatyocha</i> sp. cf. <i>D. carentis</i> <i>incerta</i>
17	<i>Diatyocha curta</i> n. sp.
16	<i>Diatyocha deflandrei</i>
15	<i>Diatyocha fibula</i>
14	<i>Diatyocha obliqua</i>
13	<i>Diatyocha</i> sp. cf. <i>D. rotundata</i>
12	<i>Diatyocha striatula</i>
11	<i>Diatyocha</i> sp.
10	<i>Diatyocha</i> sp.
9	<i>Diatyocha</i> sp.
8	<i>Diatyocha</i> sp.
7	<i>Diatyocha</i> sp.
6	<i>Diatyocha</i> sp.
5	<i>Diatyocha</i> sp.
4	<i>Diatyocha</i> sp.
3	<i>Diatyocha</i> sp.
2	<i>Diatyocha</i> sp.
1	<i>Diatyocha</i> sp.

Paleogene interval, the magnetic polarity of the normal-reversed combination has been repeated several times (Hardenbol and Berggren, 1978). Therefore it is plausible that the Paleocene FL-422 core contains a short normal-reversed normal polarity record within the core (Clark, 1974). Exactly to which normal-reversed combination the core 422 under discussion will correlate cannot be determined at this time.

Before leaving the subject of the geological occurrence and age determination of the FL-422 assemblage, a short discussion should be added

here. Some perplexing problems are posed by occurrences of several species in the Alpha Ridge sediments whose geological ranges have been reported only from Late Eocene and Oligocene from the Soviet Union. It is possible that these silicoflagellates and ebridians are reworked or contaminated; nevertheless, the complete absence of *Mesocena* and *Naviculopsis* species in the present assemblage seems to refute such a possibility. Thus the only plausible explanation, at least for the time being, is that the assemblage recovered from the FL-422 is genuine and that these taxa recovered actually made their initial geological appearance as early as during Early Paleogene time in this part of the world.

(B) Significance to tectonic history of Arctic Ocean

In spite of their characteristic microfloral compositions and their occurrences from the Arctic Ocean, it has been difficult to conceive that these Late Mesozoic (FL-437) and Early Cenozoic (FL-422) cored sediments were sandwiched both above and below by foraminifera-bearing Pleistocene deposits. Therefore, unless additional occurrence of these sediments on the Alpha Ridge or geophysical data of the area can be substantiated, the positive confirmation as to the source of the sediments from the Alpha Ridge would remain mere speculation.

The results of the seismic profile of the area obtained from the Ice-Island reveal that the Alpha Ridge is one of the largest submarine features in the Arctic Ocean (Hall, 1970, 1979). Instead of jagged arcuate zones, which typify the well-known mid-oceanic ridges, it is rather a flat-top feature dipping toward the south. The Cretaceous FL-437 core was recovered on the flank of a faulted graben-like structure immediately north of the northern end of the Alpha Ridge's highest edge (Text-fig. 2). There is no discernible sediment cover over this graben structure, suggesting that it was formed comparatively recently, probably in the Late Pleistocene at the same time that the material in core 437 was slumped. On the other hand, the Late Paleogene core 422 was raised from the southern foothill of the Ridge (Hall, 1979), the likely

place where such slumping would take place (Text-fig. 2). Thus, although these two cores are slumped materials, it is highly likely that their source can be traced back to the nearby crestral area of Alpha Ridge.

Perhaps it is a lucky coincidence that these two cores are located on the opposite flanks of the Alpha Ridge, but the location of the Early Paleogene core is farther away from the "Apparent axis" of the (Alpha) Ridge than that of Cretaceous age. While it is rather tempting to apply the age versus distance relationship to verify the sea-floor spreading hypothesis for the area, this author believes that this judgement is still premature because it relies on merely two cores of different ages to evaluate whether Alpha Ridge was the dormant axis of early Cenozoic spreading center in the Arctic (Vogt and Ostenso, 1970, Hall, 1970, 1979) or not (Vogt *et al.*, 1979).

(C) Significance to paleoceanography of Arctic Ocean

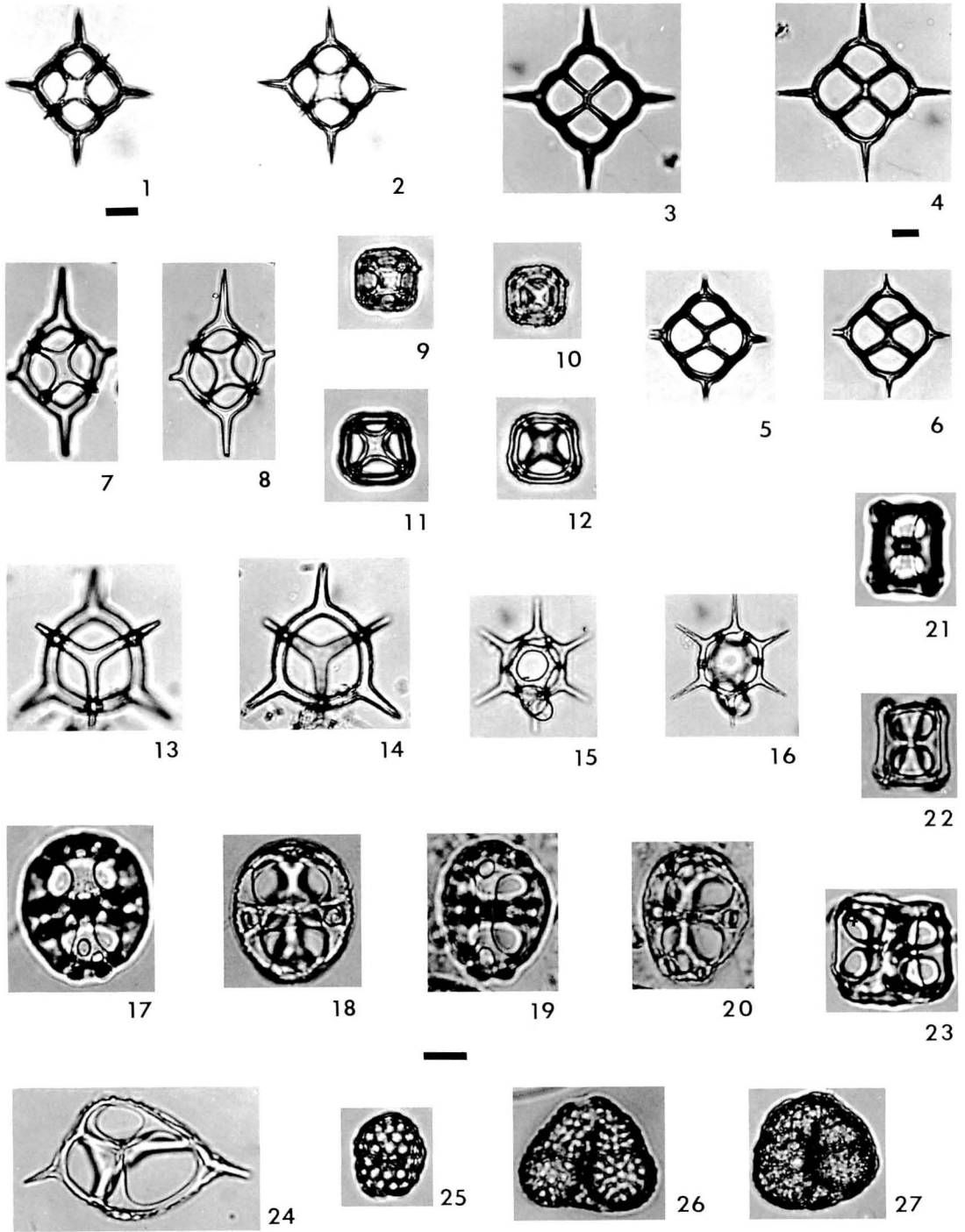
The finding of siliceous microfossils from cores FL-422 and -437 is significant to the consideration of paleoceanography of the Arctic Ocean. Silicoflagellates are widely recognized as a group of phytoplankton of the normal marine habitat (*e.g.*, Marshall, 1934, Gemeinhardt, 1930), and such interpretation has been substantiated by laboratory experiment (Van Valkenburg and Norris, 1970). Thus it is safe to assume that the submarine deposits containing abundant silicoflagellate specimens were deposited during the normal marine environment. The ages of two pre-Pliocene cores from the Arctic Basin are fortunately identified as one from the Latest Cretaceous and the other Early Paleogene; that is, from both above and below the Cretaceous-Tertiary boundary.

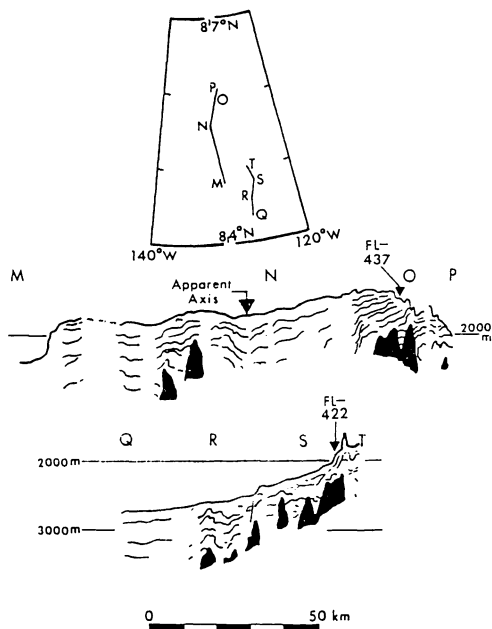
The massive extinction of the organic world at the end of the Mesozoic has been well known to earth scientists and numerous hypotheses have been brought forward attempting to account for this unusual event (see Alvarez *et al.*, 1980). One

Explanation of Plate 11

Scale bar = 10 μ m. Upper left bar for figures, 1, 2, 9-12, 25, 26; upper right bar for figures 3-8, 13-16; bottom bar for figures 17-24.

- Figs. 1, 2. *Dictyocha deflandrei* Frenguelli
22, R-1, N24/0.
- Figs. 3-6. *Dictyocha fibula* Ehrenberg
3, 4. 4, R-1, H28/0; 5, 6. 8, R-1, P34/1.
- Figs. 7, 8. *Dictyocha obliqua* Glezer
16, L-2, L39/1.
- Figs. 9-12. *Dictyocha* sp. cf. *D. rotundata* Jousé
9, 10. 9, L-2, J18/1; 11, 12. 23, L-2, 027/0.
- Figs. 13, 14. *Dictyocha spinosa* Deflandre
22, R-1, N23/4.
- Figs. 15, 16. *Distephanus speculum* (Ehrenberg)
9, L-2, N25/3.
- Figs. 17-20. *Ammodoichium fletcheri* Ling, n. sp.
17, 18. 3, L-2, T17/0; Holotype U.S.N.M. No. 395825.
19, 20. 21, L-3, U40/0; Isotype U.S.N.M. No. 395826.
- Figs. 21-23. *Ammodoichium rectangulare* (Schulz)
21, 22. 17, L-2, E14/4; 23. 16, L-2, C26/3.
- Fig. 24. *Ebriopsis cornuta* Dumitrica and Perch-Nielsen
8, R-1, E26/4.
- Figs. 25-27. *Pseudammodoichium dictyoides* Hovasse
25, 26. 22, L-2, R23/4; 27. 22, L-2, W29/2.





Text-fig. 2. Seismic reflection profiles of Alpha Cordillera in the vicinity of pre-Miocene cores FL-422 and FL-437 (after Hall, 1970, 1979). The position of the "apparent axis" (Hall, 1970) is marked by an inverted triangle.

of the most interesting and recent views has been expressed by Gartner and Keany (1978), Thierstein and Berger (1978) and Bukry (1981a). They suggest that the presence of low salinity surface water in the Arctic Ocean for a very short time — approximately 10,000 years — was responsible for the "terminal event." This view was already commented upon by Clark and Kitchell (1979) and Kitchell and Clark (1982).

The resolution of silicoflagellate zonation is not precise enough at the present time to date the effect of such a short geological phenomenon. However, the continuous occurrence of Cretaceous silicoflagellates in the Early Paleogene has been reported from Russia (Glezer, 1966), from the Tasman Sea (DSDP Site 208) and the Indian Ocean (Sites 214 and 216) (Bukry, 1973, 1981b). This implies that at least some Cretaceous silicoflagellate taxa did successfully survive through the boundary crisis and that a normal marine paleoenvironment was present at least during these times in these areas. The finding of

the present two silicoflagellate-bearing cored sediments from both sides of the boundary further substantiates the existence of normal marine conditions in the Arctic Ocean during these intervals.

According to Thierstein and Okada (1979), based on the analyses of closely spaced samples of every two cm interval across the boundary at DSDP Site 384 in the western North Atlantic, the Mesozoic calcareous nannofossil taxa are gradually replaced by Tertiary forms in the "apparent" continuous deep-sea sediments.

On the other hand, a sharp drop of both $\delta^{18}\text{O}$ and $\delta^{13}\text{C}$ values at the terminal event has been observed in samples from the DSDP Site 356 of the western South Atlantic (Thierstein and Berger, 1978). They consider the "repeated isolation and opening of the Arctic which led to repeated injection of freshwater" as one of the mechanisms accounting for the rapid fluctuations in isotopic value.

It is neither within the scope of this paper nor the intention of this author to become involved further in this intriguing and important boundary problem. Whatever the concluding hypothesis will be, in order for any one interpretation to prevail, even for a short duration, it should be able to accommodate or explain all the conceivable questions of geologic phenomena. In case of silicoflagellates and ebridians, it must be able to explain at least (1) how marine conditions were reestablished after the sudden, rapid extinction of some biota, and at the same time (2) the continuous survival of some Cretaceous forms in various parts of the world.

Acknowledgments

The core sediments upon which the present investigation was based were collected originally by Arthur Lachenbruch and Vaughn Marchall, U.S. Geological Survey (Menlo Park), and were later provided by David L. Clark, University of Wisconsin-Madison. As in the previous investigation of Core FL-437, the documentation of pre-Pliocene silicoflagellates and ebridians from the Arctic Ocean bottom could never have taken place without their kind assistance.

The critical review by Drs. Katharina Perch-Nielsen (Switzerland) and John F. Sweeney (Canada) greatly facilitated the final preparation of the manuscript. This research was supported in part by NSF grant (DPP 79-11304).

References

- Alvarez, L. W., Alvarez, W., Asaro, F. and Michel, H.V. (1980): Extraterrestrial cause for the Cretaceous-Tertiary extinction. *Science*, vol. 208, no. 4448, p. 1095–1108.
- Bukry, D. (1973): Coccolith and silicoflagellate stratigraphy, Tasman Sea and southwestern Pacific Ocean, Deep Sea Drilling Project Leg 21. *In*: Burns, R.E., Andrews, J.E., *et al.*, Initial Reports of the Deep Sea Drilling Project, vol. 21, p. 885–893. U.S. Government Printing Office.
- (1974): Coccolith and silicoflagellate stratigraphy, Eastern Indian Ocean, Deep Sea Drilling Project Leg 22. *In*: von der Borch, C. C., Sclator, J. G., *et al.*, *ibid.*, vol. 22, p. 521–605.
- (1975a): Coccolith and silicoflagellate stratigraphy near Antarctica, Deep Sea Drilling Project, Leg 28. *In*: Hayes, D.E., Frakes, L.A., *et al.*, *ibid.*, vol. 28, p. 709–723.
- (1975b): Silicoflagellate and coccolith stratigraphy, Deep Sea Drilling Project Leg 29. *In*: Kennett, J.P., Houtz, R.E., *et al.*, *ibid.*, vol. 29, p. 845–872.
- (1976a): Cenozoic silicoflagellate and coccolith stratigraphy, South Atlantic Ocean, Deep Sea Drilling Project Leg 36. *In*: Hollister, C.D., Craddock, C., *et al.*, *ibid.*, vol. 35, p. 885–917.
- (1976b): Silicoflagellate and coccolith stratigraphy, Norwegian-Greenland Sea, Deep Sea Drilling Project Leg 38. *In*: Talwani, M., Udintsev, G., *et al.*, *ibid.*, vol. 38, p. 843–855.
- (1977): Cenozoic coccolith and silicoflagellate stratigraphy, offshore northwest Africa, Deep Sea Drilling Project Leg 41. *In*: Lancelot, Y., Seibold, E., *et al.*, *ibid.*, vol. 41, p. 689–707.
- (1981a): Cretaceous Arctic silicoflagellates. *Geo-Marine Lett.*, vol. 1, p. 57–63.
- (1981b): Synthesis of silicoflagellate stratigraphy for Maestrichtian to Quaternary marine sediment. *In*: Warme, J. E. *et al.* (eds.), "The Deep Sea Drilling Project: a decade of progress." *Soc. Econ. Paleont. Mineral., Spec. Publ.*, no. 32, p. 433–444.
- (1984): Paleogene paleoceanography of the Arctic Ocean is constrained by the middle or late Eocene age of USGS Core FI-422: Evidence from silicoflagellates. *Geology*, vol. 12, no. 4, p. 199–201.
- Busen, K.E. and Wise, S.W. Jr. (1977): Silicoflagellate stratigraphy, Deep Sea Drilling Project, Leg 36. *In*: Barker, P.F., Dalziel, I.W.D., *et al.*, *ibid.*, vol. 36, p. 687–743.
- Clark, D. L. (1971): Arctic Ocean ice cover and its late Cenozoic history. *Geol. Soc. Amer., Bull.*, vol. 82, no. 12, p. 3313–3324.
- (1974): Late Mesozoic and early Cenozoic sediment cores from the Arctic Ocean. *Geology*, vol. 2, no. 1, p. 41–44.
- and Kitchell, J.A. (1977): Comment on "The terminal Cretaceous event: a geologic problem with an oceanographic solution." *Ibid.*, vol. 7, no. 5, p. 228.
- Deflandre, G. (1932): Remarques sur quelques

Explanation of Plate 12

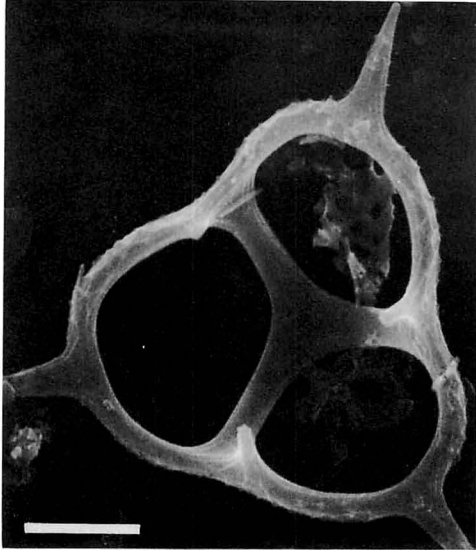
All the illustrations were photographed with a scanning electron microscope. Scale bar = 5 μ m.

Fig. 1. *Corbisema triacantha* (Ehrenberg)

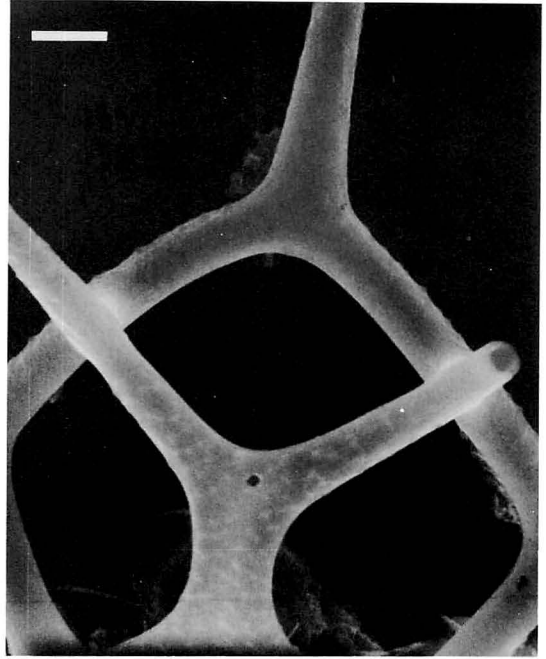
Abapical view showing the nature of basal accessory spines and surface microstructure on the basal body ring. Note here that the surface microstructure is also on the abapical side.

Figs. 2–4. *Dictyocha* sp.

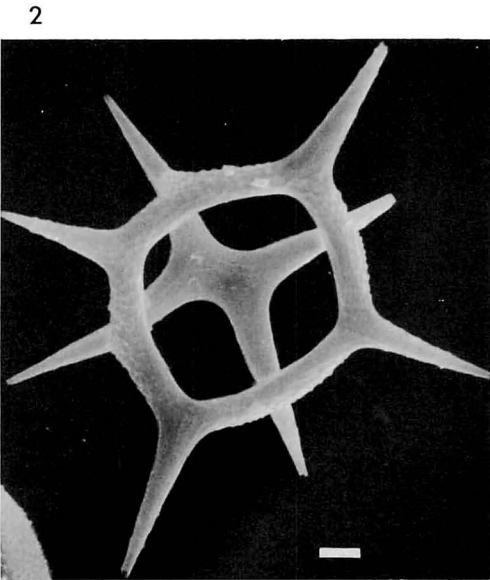
2. Abapical view showing surface microstructure on all the skeletal components.
3. A part of a specimen of figure 2 showing the details of surface microstructure of basal body ring and a radial spine.
4. Apical view showing surface microstructure on an apical bar and lateral rods.



1

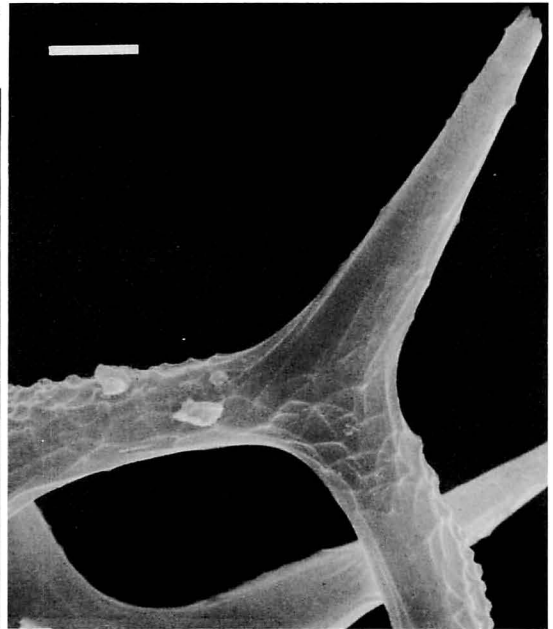


4



2

3



- Ébriacées. *Soc. Zool. France, Bull.*, vol. 57, no. 4, p. 302–315.
- (1934): Nomenclature du squelette des Ébriacées et description de quelques formes nouvelles. *Annal. Protistol.*, vol. 4, p. 75–96.
- (1950): Contribution a l'étude des Silicoflagellidés actuels et fossiles. *Microscopie*, vol. 2, p. 1–82.
- (1951): Recherches sur les Ébriédiens. Paléobiologie. Evolution. Systématique. *Biol. France, Belg., Bull.*, vol. 45, no. 1, p. 1–84.
- Ehrenberg, C.G. (1838): Über die Bildung der Kreidefelsen und des Kreidemergels durch unsichtbare Organismen. *K. Akad. Wiss. Berlin, Jahrg. 1838. Abh.*, p. 59–147.
- (1844): Ueber 2 neue Lager von Gebirgsmassen aus Infusorien. *Verh. K. preuss. Akad. Wiss. Berlin, Jahrg. 1844, Ber.*, p. 57–97.
- (1854): Mikrogeologie. 374 pp. Leipzig, Leopold Voss.
- Frenquelli, J. (1940): Consideraciones sobre les Silicoflagelados Fósiles. *Rev. Mus. La Plata, N.S.*, vol. 7, no. 7 (Paleont.), p. 37–112.
- Gartner, S. and Keany, J. (1978): The terminal Cretaceous event: A geologic problem with an oceanographic solution. *Geology*, vol. 6, no. 12, p. 708–712.
- Gmeinhardt, K. (1930): Silicoflagellatae. In: Rabenhorst, L., Kryptogamen-Flora von Deutschland, Österreich und der Schweiz., vol. 10, no. 2, p. 1–87.
- Glezer, S.I. (1964): Novye kremnevye zhgutikovye vodorosli Paleogene SSSR, Silicoflagellatae fossiles novae URSS: Akad. Nauk SSSR, Novisti sistematiki nizshikh rasteniy otdel. ottisk, p. 46–58.
- (1966): Kremnevye zhgutikovye vodorosli (Silicoflagellaty). Silicoflagellatophyceae: Flora Sporovykh Rasteniy SSSR, Flora Platarum Cryptogamarum URSS. Akad. Nauk SSSR, Botanicheskiy Institut V. L. Komarova, Moscow, vol. 7, 330 p.
- Haeckel, E. (1887): Report on the Radiolaria collected by H.M.S. Challenger during the years 1873–76. *Rept. Voy. Challenger, Zool.*, vol. 18, 1803 p.
- Hall, J.K. (1970): Arctic Ocean geophysical studies: The Alpha Cordillera and Mendeleyev Ridge. *Columbia Univ., Lamont-Doherty Geol. Obs., Tech. Rept.*, no. 2, 125 p.
- (1979): Sediment waves and other evidence of paleobottom currents at two locations in the deep Arctic Ocean. *Sediment. Geol.*, vol. 23, nos. 1–4, p. 269–299.
- Hanna, G.D. (1928): Silicoflagellates from the Cretaceous of California. *Jour. Paleont.*, vol. 1, no. 4, p. 259–264.
- (1931): Diatoms and silicoflagellates of the Kreyenhagen Shale. *State of Calif., Dept. Natur. Res., Div. Mines, Mining in Geology*, vol. 27, no. 2, p. 187–201.
- Hardenbol, J. and Berggren, W.A. (1978): A new Paleogene numerical time scale. In: Cohee, G.V., Glaessner, M.F., and Hedberg, H.D. (eds.), Contributions to the geologic time scale. *Amer. Assoc. Petrol. Geol., Studies in Geol.*, no. 6, p. 213–234.
- Herron, E.M., Dewey, J.F. and Pitman, W.C. III. (1974): Plate tectonics model for the evolution of the Arctic. *Geology*, vol. 2, no. 8, p. 377–380.
- Hovasse, R. (1932a): Note Préliminaire sur les Ébriacées. *Soc. Zool. France, Bull.*, vol. 57, no. 2, p. 118–131.
- (1932b): Troisième note sur les Ébriacées. *Ibid.*, p. 457–476.
- Johnson, G.L., Taylor, P.T., Vogt, P.R. and Sweeney, J.F. (1978): Arctic Basin morphology. *Polarforsch.*, vol. 48, nos. 1–2, p. 20–30.
- Kitchell, J.A. and Clark, D.L. (1982): Late Cretaceous-Paleogene paleogeography and paleocirculation: Evidence of north polar upwelling. *Paleogeogr., -climatol., -ecol.*, vol. 40, nos. 1–3, p. 135–165.
- Lemmermann, E. (1901a): Beiträge zur Kenntniss der Planktonalgen. *Deutsch. Bot. Ges., Ber.*, vol. 19, p. 85–95.
- (1901b): Silicoflagellatae. *Ibid.*, p. 247–271.
- (1903): Klasse Silicoflagellatae. In: Brandt, K. and Apstein, C. (eds.), *Nordisches Plankton, Bot.*, no. 21, p. 25–32.
- Ling, H.Y. (1970): Silicoflagellates from central North Pacific core sediments. *Amer. Paleont., Bull.*, vol. 58, no. 259, p. 85–129.
- (1971): Silicoflagellates and ebridians from the Shinzan diatomaceous mudstone Member of the Onnagawa Formation, (Miocene), Northeast Japan. In: Farinacci, A. (ed.), Proceedings of the II Planktonic Conference, Roma, 1970, vol. 2, p. 689–703. Edizioni Tecnoscienza.

- (1972): Upper Cretaceous and Cenozoic silicoflagellates and ebridians. *Amer. Paleont., Bull.*, vol. 62, no. 273, p. 135–229.
- (1973): Silicoflagellates and ebridians from Leg 19. In: Creager, J.S., Scholl, D.W., *et al.*, Initial Reports of the Deep Sea Drilling Project, vol. 19, p. 751–775. U.S. Government Printing Office.
- (1975): Silicoflagellates and ebridians from Leg 31. In: Karing, D.E., Ingle, J.C. Jr., *et al.*, *ibid.*, vol. 31, p. 763–777.
- (1977): Late Cenozoic silicoflagellates and ebridians from the eastern North Pacific Region. In: Saito, T. and Ujiie, H. (*eds.*), Proceedings of the First International Congress on Pacific Neogene Stratigraphy. Tokyo, 1976: p. 205–233. Science Council of Japan-Geological Society of Japan.
- (1981): *Crassicorbisema*, a new silicoflagellate genus from the southern oceans and Paleocene silicoflagellate zonation. *Palaeont. Soc. Japan, Trans. Proc.*, N.S., no. 121, p. 1–13.
- , McPherson, L.M. and Clark, D.L. (1973): Late Cretaceous (Maestrichtian?) silicoflagellates from the Alpha Cordillera of the Arctic Ocean. *Science*, vol. 180, no. 4093, p. 1360–1361.
- Locker, S. (1974): Revision der Silicoflagellaten aus der Mikrogeologischen Sammlung von C.G. Ehrenberg. *Ecol. Geol. Helv.*, vol. 67, no. 3, p. 631–646.
- Loeblich, A.R. III, Loeblich, L.A., Tappan, H. and Loeblich, A.R., Jr. (1968): Annotated index of fossil and Recent silicoflagellates and ebridians with descriptions and illustrations of validity proposed taxa. *Geol. Soc. Amer., Memoir* 106, 319 p.
- Mandra, Y.T. (1968): Silicoflagellates from the Cretaceous, Eocene, and Miocene of California, U.S.A. *Calif. Acad. Sci. Proc.*, vol. 36, no. 9, p. 231–277.
- Marshall, S.M. (1934): The Silicoflagellata and Tintinninea. *Sci. Rept. Great Barrier Reef Exped.*, vol. 4, no. 15, p. 623–662.
- Martini, E. and Müller, C. (1976): Eocene to Pleistocene silicoflagellates from the Norwegian-Greenland Sea (DSDP Leg 38). In: Talwani, M., Udintsev, G., *et al.*, Initial Reports of the Deep Sea Drilling Project, vol. 38, p. 857–895. U.S. Government Printing Office.
- Perch-Nielsen, K. (1975a): Late Cretaceous to Pleistocene silicoflagellates from the Southwest Pacific, Deep Sea Drilling Project, Leg 29. In: Kennett, J.P., Houtz, R.E. *et al.*, *ibid.*, vol. 29, p. 677–721.
- (1975b): Late Cretaceous to Pleistocene aracheomonads, ebridians, endoskeletal dinoflagellates, and other siliceous microfossils from the subantarctic Southwest Pacific, DSDP, Leg 29. *Ibid.*, vol. 29, p. 873–907.
- (1976a): New silicoflagellates and a silicoflagellate zonation in north European Palaeocene and Eocene diatomites. *Geol. Soc. Denmark, Bull.*, vol. 25, nos. 1–2, p. 27–40.
- (1976b): Eocene to Pliocene aracheomonads, ebridians and endoskeletal dinoflagellates from the Norwegian Sea, DSDP Leg 38. In: Talwani, M., Udintsev, G. *et al.*, Initial reports of the Deep Sea Drilling Project, vol. 38 (Supplement), p. 147–175. U.S. Government Printing Office.
- Schulz, P. (1928): Beiträge zur Kenntnis fossiler und rezenter Silicoflagellaten. *Bot. Archiv*, vol. 21, no. 2, p. 225–292.
- Stöhr, E. (1880): Die Radiolarienfauna der

Explanation of Plate 13

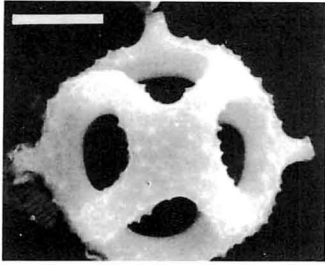
All the illustrations were photographed with a scanning electron microscope. Scale bar = 5 μm for figures 1, 2, 4, 5; = 2 μm for figure 3.

Figs. 1–3. *Dictyocha* sp. cf. *D. carentis incerta* (Glezer)

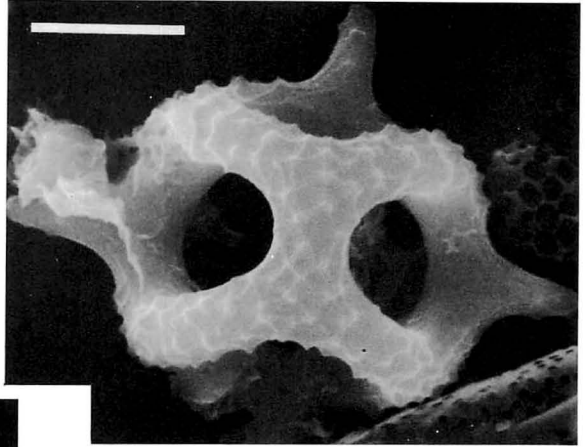
1. An apical view showing the microstructure of the skeletal components.
2. An apical view showing microstructure of skeletal components.
3. The detail of surface microstructure of lateral rods and an apical bar.

Fig. 4. *Ebriopsis cornuta* Dumitrica and Perch-Nielsen

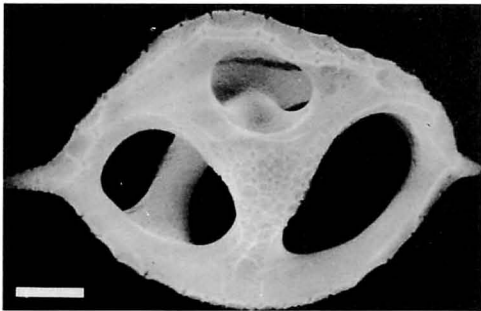
Fig. 5. *Ammodochium fletcheri* Ling, n. sp.



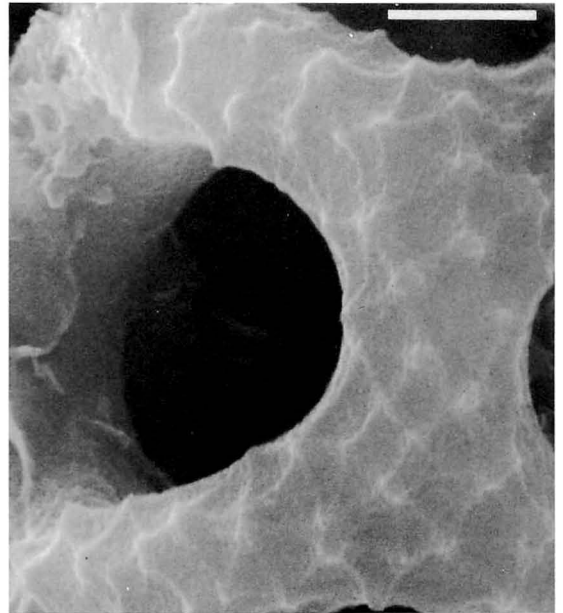
1



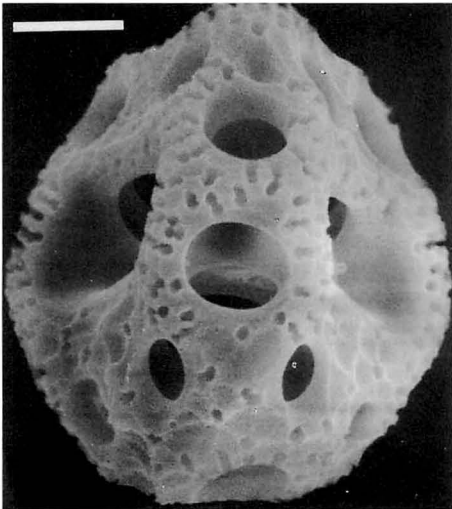
2



4



3



5

- Tripoli von Grotte Provinz Girgenti in Sicilien. *Palaeontographica*, vol. 26, p. 69—124.
- Thierstein, H.R. and Berger, W.H. (1978): Injection events in ocean history. *Nature*, vol. 276, no. 5687, p. 461—466.
- and Okada, H. (1979): The Cretaceous/Tertiary boundary event in the North Atlantic. In: Tucholke, B. E., Vogt, P.R., et al., Initial reports of the Deep Sea Drilling Project, vol. 43, p. 601—616. U.S. Government Printing Office.
- Van Hinte, J.E. (1976): A Cretaceous time scale. *Amer. Assoc. Petrol. Geol., Bull.*, vol. 60, no. 4, p. 498—516.
- Van Valkenburg, S.D. and Norris, R.E. (1970): The growth and morphology of the silicoflagellate *Dictyocha fibula* Ehrenberg in culture. *Jour. Phycol.*, vol. 6, no. 1, p. 48—54.
- Vogt, P.R. and Avery, O.E. (1974): Tectonic history of the Arctic Basins: Partial solutions and unsolved mysteries. In: Herman, Y. (ed.), *Marine geology and oceanography of the Arctic Seas*: p. 83—117. Springer-Verlag, Inc.
- and Ostenso, N.A. (1970): Magnetic and gravity profiles across the Alpha Cordillera and their relations to Arctic sea-floor spreading. *Jour. Geophys. Res.*, vol. 75, no. 26, p. 4925—4937.
- , Taylor, P.T., Kovacs, L.C. and Johnson, G.L. (1979): Detailed aeromagnetic investigation of the Arctic Basin. *Ibid.*, vol. 84, no. B3, p. 1071—1089.
- Zanon, V. (1934): Silicoflagellate fossili italiane. *Acta Pont. Acad. Sci. Nov. Lincei*, vol. 87, p. 40—82.

北極海底より見出された古第三紀早期珪質鞭毛藻とエブリア類群集：北極海のアルファ海嶺地域で流水島 (T-3) より採取したコア (FL-422) は、珪質鞭毛藻とエブリア類に富む珪質軟泥を含んでおり、構成する微化石群集より、その時代を古第三紀の早期と考えるのが妥当と思われる。そしてこの海底堆積物は、既に報告された後期白亜紀のコア (FL-327) 堆積物と共に、北極海底にも中新世以前の海成堆積物が存在する事実を確証するのみならず、北極海全体の形成史、ひいては白亜紀—第三紀 (K-T) の境界問題を考える上での貴重な資料である。併せて *Dictyocha arctios*, *D. curta*, *Ammodoichium fletcheri* の3種を新しく記載報告した。

林 信一

796. A MIDDLE DEVONIAN TRILOBITE FAUNA
FROM THE KITAKAMI MOUNTAINS, NORTHEAST JAPAN
— II. THE CALYMENIDAE*

ATSUSHI KANEKO

15-7, Fukae-honmachi 1-chome, Higashinada-ku, Kobe 658, Japan

Abstract. This is part 2 of serial papers of the Middle Devonian (probably Eifelian) trilobite fauna from the Nakazato Formation in Northeast Honshu, Japan.

A calymenid genus *Nipponocalymene*, gen. nov. and its type-species *Nipponocalymene hamadai*, gen. et sp. nov. are proposed in this part.

Introduction

A newly discovered calymenid from the present trilobite fauna clearly demonstrates the papillate butress structure at the 2p lateral glabellar lobe on the cranidium, a character diagnostic of the subfamily Calymeninae in the restricted sense of Siveter (1977). At first glance, the dorsal exoskeleton of the Japanese form appears to fall into the genus *Calymene* Brongniart, 1822, but the hypostome of the holotype specimen (Pl. 14, Figs. 1f-l) shows completely exclusive characters, the main one being a pair of protuberances on the median body. It was necessary to determine whether or not they are original in nature. Fortunately the author has obtained very kind co-operation from Yoshiaki Okamura of the Sekishin-kan Museum, Kusatsu City, Shiga Prefecture and radiographically searched for hypostomes in the available samples retaining the cephalic regions. As a result, we have succeeded in discovering an additional hypostome lodged directly below

the glabella of the paratype B cephalo-thorax (Pl. 16, Figs. 1a-c) in the same slab as the paratype pygidium of *Nipponarges mediosulcatus* (Part 1, pl. 87, figs. 2a-d) and to excavate for the taking of a cast from the external mould.

The author is now convinced that the aberrant characters seen on the hypostomes of the new Japanese calymenid are original in nature and never attributable to a particular state of preservation.

These are chiefly used to separate *Nipponocalymene* from *Calymene* at the generic level.

Systematic palaeontology

Family Calymenidae Burmeister, 1843

Subfamily Calymeninae Burmeister, 1843

Genus *Nipponocalymene* Kaneko, gen. nov.

Derivation of name:—*Nippon*, Japan + typical genus *Calymene* Brongniart, 1822.

Type-species:—*Nipponocalymene hamadai* Kaneko, gen. et sp. nov. from the Middle Devonian (probably Eifelian) Nakazato Formation in the southern part of the Kitakami Mountains, northeastern Japan.

Species assigned:—Presently only the type-

*Received March 31, 1984.

*J.T.A.F. (Studies on Japanese Trilobites and Associated Fossils) contrib. no. 38.

species is known.

Generic diagnosis:—Papillate-butressed calymenid with unusual hypostome characterized by median body with no distinct median furrow, anteriorly very strongly inflated main part of median body homologous with anterior lobe of usual calymenid pattern with a pair of protuberances directed ventro-laterally and anteriorly from ventro-lateral sides of its most raised portion and symmetrically arranged with regard to sagittal line, by considerably shortened (sag. and exsag.) crescentic-shaped remainder of median body homologous with posterior lobe sloping away steeply posteriorly and by prominent, somewhat pointed macula situated near posterolateral corner of median body. Glabella bell-shaped in outline, with three pairs of lateral glabellar lobes. Anterior border rolled, convex. Preglabellar furrow relatively short (sag. and exsag.). Palpebral lobe opposite 2p lateral glabellar lobe.

Thorax of thirteen segments:

Pygidial axis almost reaching pygidial extremity. Pleural furrow deeply incised, running on to border roll; no modification of fifth pleural furrow. Interpleural furrow absent. Ventral portion of pygidial border roll narrow (sag. and trans.). Very large, elongate oval, somewhat blister-like tubercles on posterior-most face of glabella along occipital furrow; posterior cephalic border, occipital ring, thorax and pygidium except its granulate ventral face with scattered pits; hypostome apparently smooth; rest of body tuberculate and/or granulate.

Distribution:—Confined to the Nakazato Formation in Northeast Honshu, Japan.

Discussion:—Whittington (1956, pp. 170–171) pointed out four subtypes of the hypostomes to form one of the main bases of four corresponding subfamilies in the family Odontopleuridae.

As for the Calymenidae, Whittington (1971b, p. 455) suggested that “certain taxonomic characters such as the outline and the presence or absence of the raised area on the median body of the hypostome may prove to be of value in generic and in higher subdivisions such

as Shirley’s groups A and B”.

Siveter (1977, p. 353) proposed the subfamily Calymeninae to be limited to Shirley’s group B, characterized by the presence of the papillate butress structure and a new subfamily name Flexicalymeninae for Shirley’s group A characterized by the absence of the papillate butress structure, and noted that “In the present state of knowledge the hypostome also separates these two subfamilies. Contrary to that of the generally later calymenines, all known flexicalymenine hypostomes do not have a discrete raised area or protuberance on the anterior lobe”. But he suggested *Metacalymene* may be an exception to this rule. Later he (Siveter, 1979) described and illustrated isolated calymenid hypostomes with raised area from the Silurian Kopanina Formation at Kosovo in Bohemia as *?Metacalymene baylei* (Barrande, 1846) rather than as *Calymene tenera* Barrande, 1852 which co-occurs with it and has the papillate butress structure and suggested that his subfamilial diagnosis would require appropriate amendment if the assignment of the hypostomes to the papillate-butress-free genus *Metacalymene* was proved.

Recently Price (1982) indicated that the hypostomal protuberances are not restricted to the papillate-butressed genera of the subfamily Calymeninae because isolated hypostomes assigned to *Gravicalymene quadrata* (King, 1923) and *Gravicalymene arcuata* Price, 1982 from the Ashgillian of North Wales, Great Britain have distinct protuberances.

In addition the anterior lobe of the median body of the hypostome is never flattened centrally in such species without papillate butress structures as *Flexicalymene (F.)* sp. ex. aff. *onniensis* described by Haas (1968, text-fig. 17c, pl. 29, fig. 3) from the upper Llandoveryan to lower Wenlockian of Northwest Turkey, *Gravicalymene quadrilobata* Chatterton, 1971 (pl. 19, figs. 11A, B, pl. 20, figs. 2A, B, 3A, B) from the Emsian of Australia, *Apocalymene coppinsensis* Chatterton & Campbell, 1980 (pl. 8, figs. 3, 5, 13) from the Wenlockian of Australia and *Gravicalymene eunoa* Haas, 1968

(text-fig. 18c, pl. 29, figs. 13–14) from the lower Emsian of Northwest Turkey; the former three show indistinct, gentle axial ridges and the last one shows an indistinct, flat cone-shaped central swelling. Chatterton and Campbell (1980) have regarded the species *quadrilobata* and *eunoa* to be congeneric with their new species *Apocalymene coppinsensis*, the type-species of their new genus *Apocalymene*, which they have considered to have a style of enrollment in common with *Calymene* with discrete, prominent protuberance on the anterior lobe of the median body of the hypostome.

In the family Calymenidae all known discrete protuberances and indistinct ridges or swellings on the anterior lobes of the median bodies of the hypostomes are single and situated on the sagittal line [see *Calymene blumenbachii* Brongniart, 1822 (Whittington in Moore (ed.) 1959, fig. 359, 1c) from the Wenlockian of Britain; *Calymene lawsoni* Shirley, 1962 (Haas, 1968, text-fig. 16f, Siveter, 1983, pl. 7, figs. 12–13, 16) from the Ludlovian of Britain; *Calymene puellaris* Reed, 1920 (Siveter, 1983, pl. 10, fig. 12) and *C. cf. puellaris* Reed, 1920 (*ibid.*, pl. 10, fig. 17) from the Ludlovian of Britain; *Calymene pompeckji* Kummerow, 1928 (Schränk, 1970, pl. 2, fig. 7) from the Silurian erratics of north Germany; *Calymene neointermedia* R. & E. Richter, 1956 (Lindström, 1901, pl. 3, figs. 6–7, Haas, 1968, text-fig. 16d) from the Ludlovian of Gotland (see Siveter, 1983, pp. 75–78); *Calymene interject vaneki* Pillet, 1968 (pl. D, fig. 4) from the Lower Devonian of Bohemia; *Calymene arotia* Haas, 1968 (text-fig. 16b, pl. 29, figs. 6–7) from the upper Ludlovian of Northwest Turkey; *Calymene antigonishensis* McLearn, 1924 (pl. 26, figs. 7–8) from the Wenlockian and Downtonian of Nova Scotia; *Calymene platys* Green, 1832 (Hall and Clarke, 1888, pl. 1, figs. 7–8) from the Emsian (Schoharie Formation) of New York, U.S.A., *Calymene clavicular* Campbell, 1967 (pl. 10, figs. 1–7, 13–15) from the upper Wenlockian to lower Ludlovian of Oklahoma, U.S.A.; *Calymene* (s.l.) *subdiademata* McCoy, 1851 (McNamara, 1979, pl. 9, fig. 16) from the Ashgillian of Britain; *Calymene* (s.l.) cf.

marginata (Shirley, 1936) (Ingham, 1977, pl. 21, fig. 22) from the Ashgillian of Britain; *Tapinocalymene nodulosa* (Shirley, 1933) (Siveter, 1980, pl. 97, fig. 6) from the upper Wenlockian of Britain; *Tapinocalymene vulpecula* Siveter, 1980 (pl. 100, fig. 15) from the upper Wenlockian of Britain; *Tapinocalymene volsoriforma* Siveter, 1980 (pl. 99, fig. 8) from the lower Wenlockian of Britain; hypostomes illustrated as *Calymene tuberculata* Brännich, 1781 (see Shirley, 1933, pp. 52–53, 62) by Angelin (1854, pl. 19, figs. 5b, c), by Lindström (1901, pl. 3, figs. 8–9) and by Fr. Schmidt (1907, pl. 3, fig. 1a)].

So it is quite unexpected that the hypostome attached to the dorsal exoskeleton which remains analogous to that of the genus *Calymene* Brongniart, 1822 bears a pair of protuberances arranged symmetrically with regard to the sagittal line on the main part of the median body homologous with anterior lobe of usual calymenid pattern.

Most calymenid genera have been defined mainly on such characters of the dorsal exoskeleton as the presence or absence of the fixigenal buttresses, the shape of the glabella and the form of the anterior border, but never on the characters of the sternites except the rostral plate, of which border sector tends to be modified according to the anterior border, for example, in *Spathacalymene* Tillman, 1960.

The hypostome is a sternite preoral in position and may have formed a part of feeding mechanism and served as an anchor and a protection for the soft parts consisting of such digestive organs as the esophagus and stomach or proventriculum lodged below the anterior part of the glabella (see Whittington, 1941, p. 521). Thus this sternite should be considered of no less significance than the cephalon, especially the glabella lying vertically above it as an integumental organ.

In papillate-butressed genera of the subfamily Calymeninae significant differences have not previously been recognized among known hypostomes (see Whittington, 1971b, pp. 458, 463). This may possibly be a reflection of

conservatism in feeding habit of this trilobite group.

Therefore, the presence of completely exclusive characters of such a vital organ in a member of the subfamily Calymeninae should be given more weight in classification than such modifications of the anterior border as "ridging" and a spatulate process, which are used essentially as single characters of generic importance to distinguish *Diacalymene* (Middle Ordovician to Middle Silurian) and *Spathacalymene* Tillman, 1960 (Upper Silurian) from *Calymene* respectively, but are now generally considered to be primarily adaptive in nature (see Whittington, 1981b, p. 459). Temple (1975) has questioned the taxonomic importance of the "ridging" of the anterior border in the family Calymenidae. Ingham (1977) and McNamara (1980) have accepted his view, but Siveter (1980) and Holloway (1980) have not. Siveter (1980, p. 796) pointed out the evolution on the preglabellar area of *Spathacalymene* from that of "*Calymene*" *vogdesi* Foerste, which has been regarded as a *Diacalymene* species by Holloway (1980, p. 58), or similar species would require only the lengthening of the anterior border and this morphological change to be much less than that within his new genus *Tapinocalymene*, in which the form of the anterior border was used only for specific discrimination. In *Papillicalymene* Shirley, 1936 (the upper Silurian) the anterior border, which is strongly upcurved (Whittington, 1971a, p. 131, figs. 1e-g, 1971b, pp. 463-470, pls. 85-86), is not essentially different from that in *Calymene*. Judging by the position of the papillate 3p and frontal glabellar lobes and corresponding genal buttresses, characters diagnostic of *Papillicalymene*, it seems likely that they are more closely related to the ventral appendages than the digestive organs, but there seems to be no reason to draw a distinction of taxonomic value between characters shown on the dorsal and ventral integuments covering the anterior part of the cephalic region.

Schrank (1970, pp. 115-116, 138-141) has not used the form of the anterior border to

define the genus *Calymene* because of the considerable variation of this feature within that genus itself, but has used mainly this feature to classify that genus into six species groups.

The cephalon of *Nipponocalymene hamadai* is very closely comparable to those of the representatives of Schrank's third species group, the *tentaculata* group, in the form of the anterior border and in the shape of the glabella. The former differs from the latter by somewhat shorter (sag. and exsag.) preglabellar furrow and by rather more coarse tubercles on the glabella. The *tentaculata* group of the genus *Calymene* consists of the following species; *Calymene tentaculata* (Schlotheim, 1820) (= *C. beyeri* R. & E. Richter, 1956) from the Köbbinghäuser Formation of Middle Ludlovian age in Ebbe-Sattels in Rheinland, Germany and from a glacial boulder of equivalent "Beyrichienkalk"; *C. antigonishensis* McLearn, 1924 from the Moydart and Stonehouse Formations of Wenlock and Downton (Pridoli) age at Arisaig, Nova Scotia; *C. planicurvata* Shirley, 1936 from the Upper (Shirley, 1936, p. 412) or ?Middle (Temple, 1975, p. 139) Llandoveryan at Bog Mine in Shelve in Shropshire, Britain; *C. ohhesaarensis* Fr. Schmidt, 1894 (= *C. conspiqua* Fr. Schmidt, 1894?, see Schrank, 1970, p. 140) from the Silurian (K stage) at Ohhesaarepank in Ösel, Estonia; *C. weberi* Maximova, 1968 from the Upper Silurian (S₂) Kockbaital and Lower Devonian (D₁¹) Pribalkhas horizons in central Kazakhstan; *C. aff. weberi* Maximova, 1968 from the Kockbaital horizon; *C. kockbaitalensis* Maximova, 1968 from the Pribalkhas horizon; *Calymene* sp. by Maximova (1968) from the Kockbaital horizon; *C. killarensis* Gill, 1945 from the Lower Devonian Yeringian Series at Killara in Victoria, Australia.

Hypostomes of the species within the *tentaculata* group have never known except for that of *Calymene antigonishensis*, which was suggested to be possibly conspecific with typical species *C. tentaculata* by Schrank (1970, pp. 139-140). Through the kindness of Dr. M. J. Copeland of Geological Survey of Canada the author obtained a rubber cast and mould of the

paratype hypostome (GSC No. 5590) of *C. antigonishensis*, which had been illustrated on figure 7 of McLearn's (1924) plate 26, and has been able to make a comparison between those of these calymenid species whose caphala are comparable with each other.

The hypostome of *Calymene antigonishensis*, which is figured here for comparison (Pl. 14, Figs. 5a-c), is of usual calymenid pattern showing the following features: the median body is moderately inflated and is divided by the median furrow into two lobes; the anterior lobe bears a single, central protuberance directed only ventrally (though the specimen figured here shows only its stump) and is somewhat wider (trans.), much longer (sag. and exsag.), more convex than the posterior lobe; the posterior lobe is somewhat shorter (sag. and exsag.) than those on most of the other known hypostomes of *Calymene* species; the median furrow is weakly incised through its whole course and runs postero-axially from the lateral border furrow to the maculae, around which it is represented by maculate furrows and between which represented by a somewhat broad (sag.) depression; the macula is slightly convex and situated more anteriorly than the posterior wing.

As opposed to this, the hypostome of *Nipponocalymene hamadai* shows the following features unusual for calymenids: the median body is much more strongly expanded anteriorly and divided by no distinct median furrow; the main part of the median body homologous with the anterior lobe of usual calymenid pattern is much longer (sag. and exsag.) and more convex (sag. and trans.) than the anterior lobe of the median body of the former and is very strongly inflated anteriorly and bears a pair of symmetrically arranged protuberances directed ventrolaterally and anteriorly from the ventrolateral sides of its most raised portion; the macula is situated near the posterolateral corner of the median body and further backward than the posterior wing, so that the remainder, homologous with the posterior lobe of usual calymenid pattern, is considerably reduced; the macula

is not defined by a maculate furrow but prominent and somewhat pointed.

The comparison between the above-mentioned two hypostomes seems to indicate clearly that the extreme development of the anterior lobe of the median body brought about such changes in morphology from *Calymene* to *Nipponocalymene* as the bifurcation of the raised area (= protuberance) not to prevent the animal from enrolling as fully as possible but to preserve a balance, the effacement of the median (maculate) furrow and the considerable backward transfer of the maculate. The excessive development of the anterior lobe of the median body still appears to influence the style of enrollment despite the bifurcation of the raised area.

According to Chatterton and Campbell (1980, pp. 94-96), *Calymene* has a capacity of enrolling the posterior part of the thorax to a great degree and such correlative features with this as a tendency to keep the pygidial extremity undeflected, a weak cincture at which the pleural furrow are modified to fit against the cephalic doublure during enrollment, a postaxial projection which is sharply delineated laterally by an expanded furrow resulting from the modification of the fifth (or sixth) pleural furrow and the adjacent interpleural furrow and which fits into the deep narrow curvature of the posterior edge of the rostral plate. Also in *Calymene antigonishensis* these characters can be seen (see McLearn, 1924, pl. 26, figs. 5, 10).

By contrast, in *Nipponocalymene*, despite having a capacity to enroll the posterior part of the thorax as great as that of *Calymene* (Pl. 14, Fig. 1b, Pl. 15, Fig. 10), no cincture can be observed on the pygidial pleurae and the posterior end of the terminal piece of the axis almost reaches the upwardly deflected pygidial extremity and the fifth pleural furrow and rib are never modified. These indicate that the outer part of the dorsal exoskeleton of the pygidium are never tucked inside the cephalic doublure including the doublure sector of the rostral plate, but the ventral part of the pygidial

border roll lies against the ventral part of the cephalic border roll. In addition, the ventral part of the pygidial border roll (Pl. 15, Fig. 1p) is much narrower (trans. and sag.) than that of such species with a single but prominent protuberance as *Calymene clavica* Campbell, 1967 (pl. 9, fig. 1, pl. 10, figs. 12–15). This allows the animal to insert the raised area of extreme width (trans.) resulting from the prominent bifurcation on the median body of the hypostome into the medial embayment in the pygidial doublure.

Of the other species of the *tentaculata* group of the genus *Calymene* in which the pygidia are known, *C. weberi* can be considered to have a hypostome of ordinary type for that genus because of the similarity to *C. antigonishensis* in the pygidial morphology (see Maximova, 1968, pl. 9, figs. 5–6). In *C. tentaculata*, *C. kokbaitalensis* and *C. killarensis* the postaxial projection of the pygidium is relatively short (sag.), but appears to be delineated laterally by a modified fifth pleural furrow, so that there is little possibility of their hypostomes being similar to that of *Nipponocalymene hamadai* (see Schrank, 1970, pl. 10, figs. 2, 3, 7, pl. 11, fig. 7, pl. 12, fig. 4; R. and E. Richter, 1956, pl. 2, figs. 18a, d, 23a, b, text-fig. 7; Maximova, 1968, pl. 8, figs. 2–4, 6–7; Gill, 1945, pl. 7, figs. 3–4).

Another characteristic feature of *Nipponocalymene* is a surface ornamentation on the occipital ring, posterior cephalic border, thorax, and pygidium which consists mainly of scattered pits. In *Calymene* species in which the whole of the dorsal exoskeleton is known such as *C. platys* Green, 1832 described and illustrated by Hall and Clarke (1888, p. 3, pl. 1, figs. 1–6, 8–9, pl. 25, figs. 1–2) and *C. allportiana* Salter, 1865 described and illustrated by Shirley (1936, p. 58, pl. 1, figs. 12–14) from the Wenlockian of Britain the dorsal surface of thorax and pygidium, and also of the occipital ring in *C. platys*, is smooth, but never pitted. Of species of the *tentaculata* group, *C. weberi* also shows the pygidial surface to be smooth but to be never pitted. In addition the surface ornamenta-

tion of the posterior-most face of the glabella along the occipital furrow which consists of considerably large, elongate oval, somewhat blister-like tubercles is also exclusively characteristic.

The lack of interpleural furrows on the pygidium separates *Nipponocalymene hamadai* from the representatives of the *tentaculata* group, which show better defined interpleural furrows as most of the other species of *Calymene* do (see Siverter, 1980, p. 784).

The author comes to conclusion that *Nipponocalymene* gen. nov., which is one of the last survivors in the family Calymenidae, was derived from *Calymene* through species of Schrank's (1970) *tentaculata* group, especially through the Kazakhstan species.

Nipponocalymene hamadai Kaneko,
gen. et sp. nov.

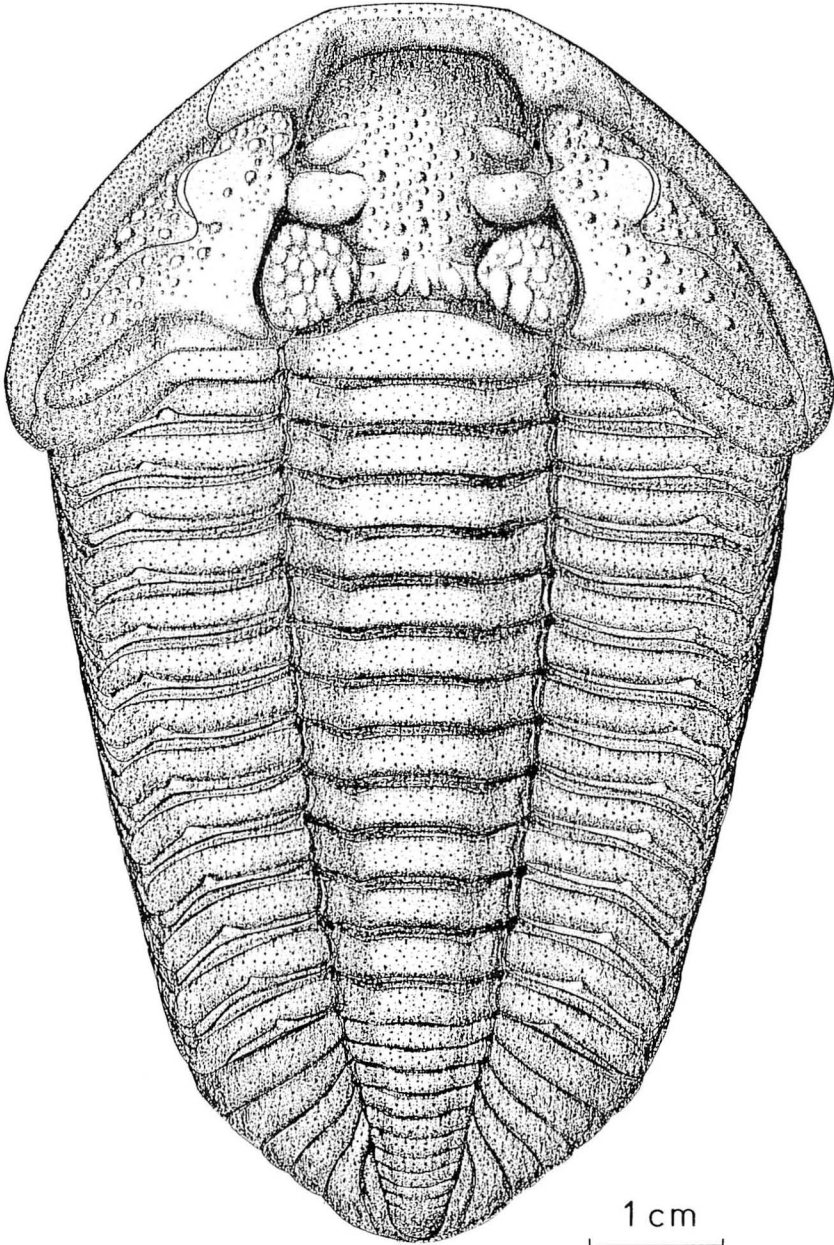
Pl. 14, Figs. 1a–4b; Pl. 15, Figs. 1a–2c;
Pl. 16, Figs. 1a–12; Text-figs. 1a–b.

Derivation of name:—Patronym in honor of Professor Dr. Takashi Hamada of the University of Tokyo.

Holotype:—Incomplete individual, KAC-D-T-0111 [PA 17144] (Pl. 14, Figs. 1a–1), coll. A. Kaneko, 1980.

Specific diagnosis:—As for the genus.

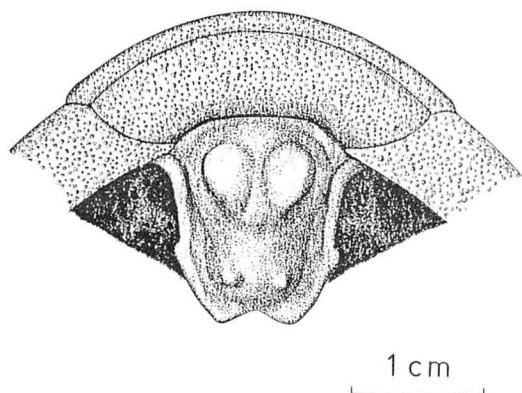
Description:—Cephalon more than two times as wide as long; anterior outline nearly straight in front, evenly rounded laterally; posterior outline nearly straight between fulcrum, at which it deflects gently backward and then curves forward again distally. Glabella with bell-shaped outline resulting from well-developed 1p lateral glabellar lobe, not so strongly inflated for calymenids; in lateral view, its frontal slope from preglabellar furrow nearly vertical, becoming progressively gentler posteriorly; 1p lateral glabellar furrow deeply incised, directed diagonally as far as not so markedly projecting intermediate lobe, which divides it into two branches; anterior branch weak, curving forward and inward; posterior branch strong, curving back-



Text-fig. 1a. Restoration of *Nipponocalymene hamadai* Kaneko, gen. et sp. nov. (Dorsal exoskeleton).

ward and inward, then turning to run transversely, extending so far adaxially that the narrowest (trans.) part of glabella at its adaxial extremity is much less than one third of the

widest part slightly anterior to postero-lateral corner of 1p lateral glabellar lobe; 2p lateral glabellar furrow directed inward and slightly backward; 3p lateral glabellar furrow weakly



Text-fig. 1b. Restoration of *Nipponocalymene hamadai* Kaneko, gen. et sp. nov. (Part of ventral side of cephalic region).

incised, directed inward and slightly forward; 1p lateral glabellar lobe about one third as wide (trans.) as glabella, more or less depressed, with roundly quadrilateral outline, separated from frontomedian glabellar lobe by a moderate depression; 2p lateral glabellar lobe papillate, elongate (trans.), jointed to fixigenal butress, separated from frontomedian glabellar lobe by a weak depression; 3p lateral glabellar lobe small, elongate (trans.). Anterior border rolled, convex; in dorsal view shortest (sag.) medially, widening rapidly in front of antero-lateral corner of frontal glabellar lobe, attaining maximum length (exsag.) opposite axial furrow, and then slightly shortening before widening distally; in lateral view rising in a gentle slope upward and forward from base of preglabellar furrow to rounded crest, at which it curves over to become inclined downward and backward to rostral suture; in anterior view weakly arched dorsally or nearly straight in front of glabella. Preglabellar furrow short (sag. and exsag.), moderately deep, U- to V-shaped. Occipital ring about one-fifth as long (sag.) as wide, slightly wider than glabella across lateral glabellar lobe 1p, longest (sag.) medially, then becoming progressively shorter (exsag.) laterally and slightly curving distally. Occipital furrow shallowest medially, deepening progressively laterally, curving backwards and narrowing (exsag.) behind adaxial part of 1p lateral glabellar lobe, finally turning slightly forward. Axial

furrow sigmoidal, steep-sided, more or less overhung by adaxial side of fixigena, shallowest at distal end of occipital ring, moderately deep and considerably narrow (trans.) beside 1p lateral glabellar lobe, bridged by fixigenal butress at 2p lateral glabellar lobe, moderately wide (trans.) at 3p lateral glabellar lobe, deepening abruptly into anterior pit which is situated just anterior to 3p lateral glabellar lobe, then expanding and becoming slightly shallower at junction of preglabellar and anterior border furrows. Anterior pit represented ventrally by a boss, on inner anterior slope of which there are excavations for anterior wing process of hypostome. Facial suture gonatoparian; converging gently from ω in genal angle to junction of posterior and lateral border furrows, converging less gently and then curving to nearly transversely from there to ϵ , curving gently outward around palpebral lobe from ϵ to ν , converging gently from ν to marginal border furrow, diverging gently for a short distance from there to β in marginal border, curving rapidly inward from β to α . Fixigena convex, attaining maximum height in region of palpebral lobe; in lateral view from there sloping down steeply anteriorly to anterior border furrow and gently posteriorly to posterior border furrow; in anterior view sloping down evenly laterally in a moderate curve. Palpebral lobe almost flat abaxially, sloping down very gently adaxially to fixigenal butress; its mid-line at level of anterior margin of 2p lateral glabellar lobe. Librigena subtriangular in outline, with narrow (exsag. and trans.) eye socle; genal field narrow (trans.), descending to lateral border furrow in a steep slope. Lateral border furrow shallow, broadly (trans.) round-bottomed. Lateral border wide (trans.), well rolled; its posterior-most portion flexed backward and inward to form rounded angle. Posterior border short (exsag.), sloping slightly upward from axial furrow to fulcrum, at which it curves downward postero-laterally and progressively lengthens (exsag.) before becoming nearly parallel-sided near genal angle. Posterior border furrow shortest (exsag.) most adaxially, lengthening rapidly laterally to near

fulcrum, from which it becomes parallel-sided and then progressively slightly narrower before ending near facial suture; its anterior slope gentle; its posterior slope nearly vertical between axial furrow and fulcrum, beyond which it becomes progressively gentler.

Rostral plate usual for calymenids; border sector about one fourth as long as wide, more or less longer (sag.) medially than laterally; connective suture gently convex outward, converging sharply postero-ventrally to join abaxial extremity of inner arc of border sector; inner arc of border sector subparallel to rostral suture, marked by a sharp ridge; doublure sector only poorly known.

Hypostome unusual for calymenids; anterior margin gently convex forward; anterior border flexed ventrally, but details unknown; anterior wing unknown; median body pear-shaped in outline, divided by no distinct median furrow; main part of median body homologous with anterior lobe of usual calymenid pattern, with strongly convex (sag. and trans.) anterior raised portion, whose top is bifurcate due to development of a pair of stout, spur-like protuberances which are symmetrically arranged with regard to sagittal line and directed ventrolaterally and anteriorly; rest of median body behind macula homologous with posterior lobe of usual calymenid pattern, crescentic in shape, considerably short (sag. and exsag.), rapidly sloping away posteriorly; macula prominent, ovate, somewhat pointed, situated at postero-lateral corner of median body and much more posteriorly than posterior wing; lateral border furrow most distinct opposite (trans.) protuberances of anterior raised portion of main part of median body, somewhat convergent and narrowing (trans.) posteriorly; posterior border almost flat, projecting into two broad (trans.) but short (exsag.) spines; posterior border furrow represented by abrupt change of slope, sometimes broken off medially.

Thorax of thirteen segments; Axial ring highly arched, flexed forward and expanded slightly abaxially; articulating furrow moderately deep, round-bottomed, with steep anterior

slope and slightly gentler posterior slope, more sharply incised laterally than medially; articulating half ring only slightly higher than bottom of articulating furrow, with clearly defined posterior margin. Inner part of pleurae tending to be inclined slightly posteriorly in dorsal view and to slope slightly upward abaxially in transverse section; outer part of pleurae sloping down nearly vertically from fulcrum; posterior band of pleura well rounded in exsagittal section, flexed slightly forward adaxially, continued laterally to form bounding ridge around margin of articulating facet; anterior band of pleura lower and shorter (exsag.) than posterior band, rounded in exsagittal section; pleural furrow moderately deep, round-bottomed, diminishing adaxially.

Pygidium subrhombic in outline. Axis gently arched, comprising an articulating half-ring, eight distinct and two indistinct axial rings and a terminal piece; ring furrows tending to shallow medially; first ring furrow deepest and longest (sag. and exsag.); subsequent ring furrows becoming progressively shallower and shorter (sag. and exsag.), thus ninth and tenth furrows failing to reach axial furrow and tenth furrow lacking also its medial part near sagittal line; terminal piece almost reaching pygidial extremity which is deflected upward medially. Axial furrow not so deep, broken off by junction first three ring and pleural furrows. Pleural region defined articulating half-rib (anterior pleural band of first segment) and five ribs by five pleural furrows; first pleural furrow deepest, nearly straight, cutting into broad (exsag. and trans.) pleural facet; subsequent furrows becoming progressively slightly shallower posteriorly, extending onto border roll, then shallowing rapidly and flexed anteriorly to carry across its ventral surface to doublure; fifth pleural furrow never modified to form postaxial sector. Pleural ribs highly vaulted in lateral view, tending to be flat-topped, with no interpleural furrows. Border roll strongly rounded; its ventral portion relatively narrow (trans. and sag.), widest in front. Doublure narrow, rolled in.

Surface ornamentation.—Moderately spaced,

small to medium sized tubercles on frontomedian glabellar lobe except its posterior-most face along occipital furrow, with which posterior portion of 1p lateral glabellar lobe shares extremely large, elongate-oval, somewhat blister-like tubercles; closely spaced, small to moderately large sized tubercles on anterior portion of 1p lateral glabellar lobe and outer slope of genal area inside anterior and lateral border furrows; fine granules scattered between these tubercles; occasional small to medium sized tubercles and moderately scattered granules on outer part of inner raised portion of genal area inside border furrows except palpebral lobe, but decreasing in number toward postero-axial corner of inner raised portion opposite 1p lateral glabellar lobe (tans.), which is apparently smooth; fine granules of various sizes moderately scattered on inner part of border roll, but progressively more closely spaced outward, densest on outer part below the level of rostral suture including border sector of rostral plate; 2p and 3p lateral glabellar lobe and palpebral lobe very weakly granulated; doublure of librigena, doublure sector of rostral plate and hypostome apparently smooth; occipital ring, crest of posterior cephalic border, thoracic and pygidial segments except near axial furrow finely pitted scatteredly; granules on ventral portion of pygidial border roll similar to that on the ventral portion of cephalic border roll below level of rostral suture; weak, fine granules discernible near lateral pygidial margin; pygidial doublure apparently smooth; at least some of tubercles on dorsal surface of frontomedian glabellar lobe perforated. Raised surface of internal mould of cephalon covered all over with closely spaced, fine pits of various sizes each of which has a central swelling surrounded by raised rim, which are impressions of canal openings.

Observation:—In the holotype specimen (Pl. 14, Figs. 1a–1) the anterior border is cracked by longitudinal compression so that it looks as if it had a sharp crest in lateral view (Pl. 14, Fig. 1b). While the paratype A (Pl. 15, Figs. 1a–q) specimen is much larger than the holotype specimen, the anterior border in the former is much lower

than that in the latter. This difference is intra-specific and partly attributable to growth change (see Holloway, 1980, p. 56). In a fragment of a large cranidium (Pl. 16, Fig. 2) the preglabellar furrow is longer (exsag.) than those in the holotype and paratype A specimens. However another large, damaged cranidium (Pl. 16, Fig. 4) of similar size, though preserved as an internal mould, shows not so long (exsag.) preglabellar furrow. The hypostome in the holotype (Pl. 14, Figs. 1f–l) differs from that of the paratype B (Pl. 14, Figs. 3a–d, Pl. 16, Figs. 1b–c) in the convexity of the median body, especially its anterior raised portion, in the relative sizes and shapes of the protuberances and in the degrees of the angle between the protuberances. In the holotype the anterior raised portion of the median body is more developed so that the protuberances are more elongate (exsag.) and less gently divergent ventrally. Nevertheless the author considers that the associated calymenid remains from the present horizon are undoubtedly conspecific with each other and that these differences may be intraspecific and in part ontogenetic. The precise nature of the ornamentation on the thorax and pygidium except pitting is not clear because of a layer of granular silica over the external mould which is difficult to remove, but their surface may be weakly granulated. The surface of the internal mould of the hypostome of the paratype C (Pl. 14, Figs. 2a–b) is covered with a layer of granular silica, which never represents a surface ornamentation. The radiographs (Pl. 16, Figs. 1b–c) show that the bifurcated raised area of the hypostome is never attributable to an artefact of preparation. Judging by the size of the fragment of the largest pygidium (Pl. 16, Fig. 9), the animal may have attained about 20 cm in length.

Discussion:—With the Upper Silurian form *Calymene* aff. *weberi* Maximova, 1968 and Lower Devonian form *C. kokbaitalensis* Maximova, 1968, *Nipponocalymene hamadai* shares very similarly shaped glabellae and 1p lateral glabellar lobes, but differs from the Kazakhstan forms in the nature of the preglabellar area. *C. aff. weberi* has a more or less longer (sag. and

exsag.) preglabellar furrow meeting slightly shorter (sag. and exsag.) anterior border at angular break in slope. *C. kokbaitalensis* has as elongate (sag. and exsag.) preglabellar area as has been not only compared with *C. macrocephala* Prouty, 1923 (pl. 34, figs. 10–13, 18) from the Silurian of North America by Maximova (1968, p. 53) but also suggested to be a possible representative of *Diacalymene* by Whittington (1971, p. 458). Maximova (1978, p. 103, pl. 3, figs. 11–12, text-fig. 1/2a–6) proposed a new subgenus *Calymene* (*Limbocalymene*) on the basis of that form. An Upper Silurian to Lower Devonian form *C. weberi* Maximova, 1968 from Kazakhstan was considered to be conspecific with *C. aff. weberi* by Schrank (1970, p. 116, 140) probably because of an impressional similarity in morphology of the preglabellar area, but differs from the latter in a less developed 1p lateral glabellar lobe according to Maximova (1968, p. 51). Of these Kazakhstan forms, thus, *C. aff. weberi* seems to be most closely related to *Nipponocalymene hamadai*.

The Japanese species is slightly less similar to the Upper Silurian form *C. tentaculata* (Schlotheim, 1820) from Germany, the typical species of Schrank's (1970) species group 3 than to the Kazakhstan forms except *C. weberi* in glabellar morphology. The German species has a relatively well-developed 2p and slightly less depressed 1p lateral glabellar lobes. The preglabellar area of the Schrank's (1970, p. 139) intraspecific variation type 3 in *C. tentaculata*, although a juvenile specimen, shows a rounded anterior border and relatively shorter (sag. and exsag.) preglabellar furrow, but the anterior border is relatively longer (sag. and exsag.). According to R. and E. Richter (1956, pp. 18–19) *C. beyeri* R. & E. Richter, 1956 conspecific with *C. tentaculata* has eight pygidial axial rings and one or two additional ones as *Nipponocalymene hamadai* does. The Middle to Upper Silurian form *C. antigonishensis* McLearn, 1924 from Nova Scotia, Canada may possibly fall within a range of variation of the morphology of *C. tentaculata* as was pointed out by Schrank

Explanation of Plate 14

Figs. 1a–4b. *Nipponocalymene hamadai* Kaneko, gen. et sp. nov.

Figs. 1a–l. Holotype, KAC-DT-0111 [PA 17144]. Incomplete individual with somewhat displaced rostral plate and hypostome. a–k, rubber casts from external moulds; a–b, dorsal stereo pair, $\times 1$. c, left lateral view, $\times 1$. d, anterior view, $\times 1$. e, enlargement of part of cranidium to show very large, elongate oval, somewhat blister-like tubercles on posterior-most face of glabella and pitting on occipital ring, dorsal view, $\times 2$. f–g, ventral stereo pair of cephalic region, $\times 1$. h–i, ventral stereo pair of hypostome, $\times 2$. j, left lateral view of hypostome, $\times 2$. k, posterior view of ventral side of cephalic region, $\times 2$. l, ventral view of damaged internal mould of hypostome, $\times 2$.

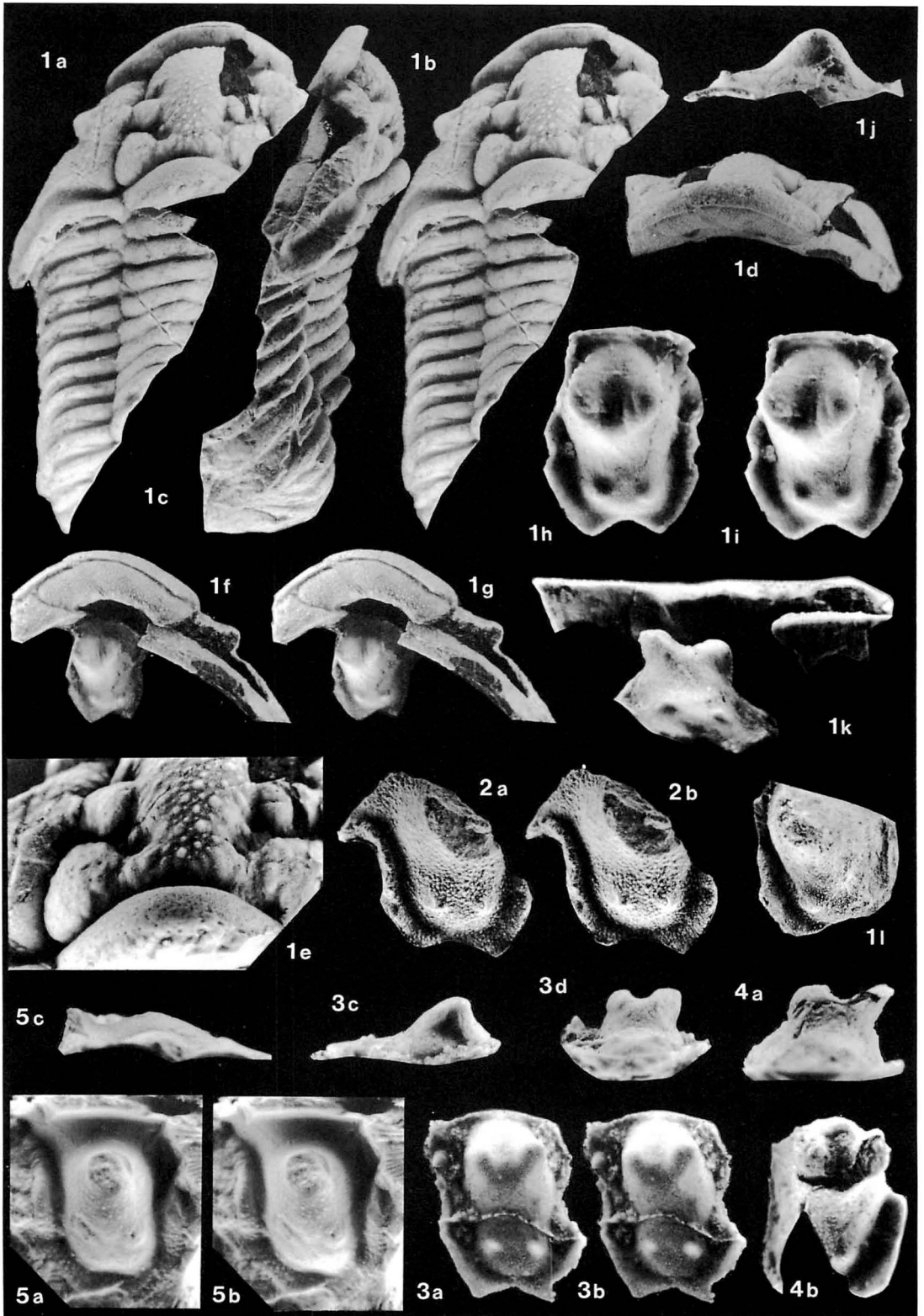
Figs. 2a–b. Internal moulds of incomplete hypostome lacking protuberances of paratype C, Sasaki-Koizumi coll. [PA 17145] shown in Figures 5a–b of Plate 16, ventral stereo pair, $\times 2$.

Figs. 3a–d. Rubber casts from external moulds of hypostome of paratype B, KAC-DT-0113 [PA 17146] shown in Figures 1a–c of Plate 16. a–b, ventral stereo pair, $\times 2$. c, left lateral view, $\times 2$. d, posterior view, $\times 2$.

Figs. 4a–b. Rubber casts from external moulds of damaged hypostome of paratype D, Sasaki-Koizumi coll. [PA 17147] shown in Figures 6a–b of Plate 16. a, posterior view, $\times 2$. b, ventral view, $\times 2$.

Fig. 5. *Calymene antigonishensis* McLearn, 1924.

Figs. 5a–c. Rubber casts from external moulds of hypostome of paratype, G.S.C. No. 5590, for comparison with those of *Nipponocalymene hamadai*, gen. et sp. nov.; a–b, ventral stereo pair, $\times 2$. c, right lateral view, $\times 2$.



(1970, pp. 139–141).

In so far as the morphological information known from the internal mould is concerned, the Lower Devonian form *C. killarensis* Gill, 1945 from Australia is similar to *Nipponocalymene hamadai* in the nature of cranidium, especially in the lateral profile (see Gill, 1945, fig. 1B) and in the nature of the preglabellar area, but differs from the Japanese species in having more or less distinct 4p lateral glabellar lobe.

The Silurian form *C. conspicua* Schmidt, 1894 from Estonia was considered to be a possible synonym of *C. ohnesaarensis* Schmidt, 1984 by Schrank (1970, p. 116, 140). Schmidt's 1894 paper in which the original descriptions of these Estonian species are presented is not available to the author, but his paper (1907) in which the former is re-illustrated is available. *C. conspicua* appears to have in common a most similar preglabellar area with *Nipponocalymene hamadai*, but differs from the Japanese form in having distinct 4p lateral glabellar lobe, in having laterally well expanded antero-lateral corner of the glabella, in having somewhat slender glabella and in having wider (trans.) fixigena.

The above-mentioned comparisons demonstrate the closest relationship between the Kazakhstan and Japanese species. Thus, also another calymenid remains distributed from Kazakhstan to Primorie become a subject of discussion. However available information is too unsatisfactory for detailed comparisons to be made as shown below.

An incomplete cranidium illustrated as *Calymene* sp. indet. by Weber (1932, pl. 1, fig. 2) from the Middle Devonian strata of the Khodjent district in Turkestan is too strongly damaged by weathering for us to say whether or not it is a papillate-butressed form, but it is possible to say that its frontal glabellar lobe appears to be somewhat wider (trans.) than those of *Calymene* species of the *tentaculata* group and the Japanese species.

Incomplete specimens described and illustrated as *Calymene* ex. gr. *blumenbachii* by

Maximova (1960, pl. 7, figs. 1–3) from the lower Middle Devonian (D_2^1) of the Rudny Altai also do not allow us to grasp characters useful for generic and subfamilial discrimination precisely. However, Maximova's figure 1 of plate 7 may possibly indicate the fixigenal buttress opposite (trans.) the 2p lateral glabellar lobe. If this is a papillate-butressed form, its glabellar shape shown in figure 1 may suggest some relationship to those of *Calymene* species of the *tentaculata* group, but figure 2 shows, if not deformed, a more slender glabella as in the cranidium shown in figure 14 of Balashova's (1960) plate 1 of *C. taimyrica* Balashova, 1960 from the Llandovery of the Taimyr Peninsula.

Of the specimens described and illustrated as *Calymene* spp. α and β by Maximova (1962, pl. 10, figs. 4–6) from the Llandoveryan to Wenlockian strata of the Siberian platform, two cranidia called *Calymene* sp. α seems to fall within the concept of the genus *Calymene* and to show relatively broad furrows surrounding the glabella as species of the *tentaculata* group do, but they differ from the latter and the Japanese species in having much more rounded lateral glabellar lobes. The pygidium called *Calymene* sp. β shows a modified postaxial sector of usual calymenid pattern.

In the Amur region, Modzalevskaya (1967, p. 546) recorded only the generic name *Calymene* without any further descriptions and figures from the lower part of the Eifelian Jmatchinskaya Suite. According to her the "*Calymene*"-bearing fauna in this region is characterized by the pronounced Appalachian affinities as in Kazakhstan.

In West Primorie, *Calymene* ex. gr. *blumenbachii* and *Calymene* sp. were reported from the Grodekov district by Maximova and Organova (1959). The former represented by a fairly compressed, partial pygidium (fig. 1a) was compared with *C. macrocephala*, n. sp. from the Lower Devonian (D_1^1) of northeastern Pribalkhas in Kazakhstan, which was figured there for comparison (fig. 1 δ = fig. 3 of Maximova's (1968) plate 8 of *C. kokbaitalensis* Maximova, 1968?, non *C. macrocephala* Prouty, 1923). On the

other hand, the latter, represented by a largely damaged cephalo-thorax (fig. B), was discussed as allied to *C. platys* Green, 1832 described and illustrated by Hall and Clarke (1888) from the Lower to Middle Devonian of New York State, U.S.A. However the illustrations of these calymenid remains are too poor for us to assign them precisely generically. It is safe to say that at least the pygidium (fig. 1a) may possibly be a Kazakhstan affinity and have some relationship to that of the Japanese species judging by the possession of considerably reduced postaxial sector.

Acknowledgments

The author is extremely grateful to Dr. Allen R. Ormiston of Amoco Production Company, Tulsa, Oklahoma, for linguistic improvement of the present manuscript, invaluable suggestions, useful literature and very kind encouragement; to Dr. Derek J. Siveter of the University of Hull, for instructive advices and discussions on many aspects of the present calymenid material. The author is deeply indebted to Professor Dr. Takashi Hamada of the

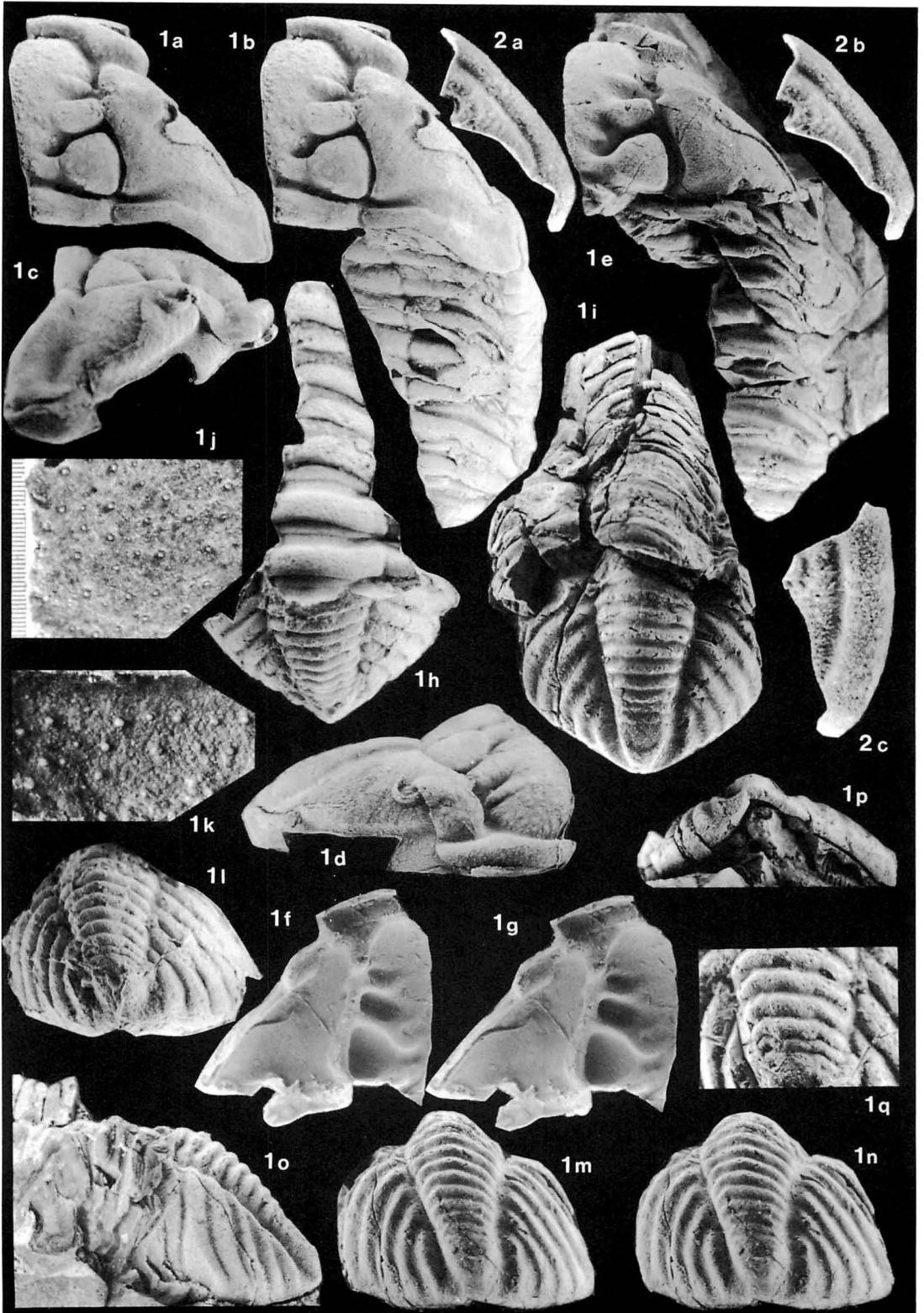
University of Tokyo for reading over the manuscript, very kind instruction and encouragement; to former Curator Dr. Eiji Matsumoto of National Science Museum, Tokyo, for helpful criticism on earlier drafts of the manuscript and constant encouragement; to Professor Dr. Harry B. Whittington of the University of Cambridge, for his critical comment on the present calymenid material. He expresses his sincere gratitude to M.D. Yoshiaki Okamura of the Sekishin-kan Museum, Kusatsu City, for his kind care in preparing the radiographs used in the plate; to Dr. M. J. Copeland of Geological Survey of Canada, Ottawa, for supplying rubber casts from the GSC collection and copies of useful literature; to Dr. I. A. Dubrovo of Palaeontological Institute, Moscow, for her kind care in filming many useful Russian literature; to Mr. Ko-ichi Nakamura of Geological Survey of Japan and Miss Eleanor A. Gossen of New York State Museum and Science Service, Albany, for supplying copies of many useful literature. Deep appreciation is also expressed to Mr. Hitoshi Koizumi of Kesen Chishitsu Kenkyūsho (K.K.), for many helpful informations and useful literature; to Mr. Teruo Ono and Mr. Kazuhiro

Explanation of Plate 15

Figs. 1a–2c. *Nipponocalymene hamadai* Kaneko, gen. et sp. nov.

Figs. 1a–q. Paratype A, KAC-DT-0112 [PA 17148]. Incomplete individual. a–d, rubber casts from external moulds of cephalon and thorax; a–b, dorsal stereo pair of cephalon and disarticulated ten incomplete thoracic segments (b), $\times 1$. c, right lateral view of cephalon, $\times 1$. d, oblique antero-lateral view of cephalon to show displaced incomplete librigena, $\times 1$. e, internal mould of cephalon and thorax, dorsal view, $\times 1$. f–g, rubber casts from internal moulds of cephalon shown in e, ventral stereo pair, $\times 1$. j, enlargement of internal mould of median portion of glabella shown in e, details showing impressions of canal openings, $\times 7$ (an interval of 0.1 mm between scale lines). k, enlargement of external mould of most posterior thoracic segment shown in h, details showing scattered spines which are impressions of pits, $\times 8$. h, l, q, rubber casts from external moulds of pygidium and thorax; h, dorsal view of pygidium and disarticulated seven incomplete thoracic axial rings, $\times 1$. l, posterior view of pygidium, $\times 1$. q, enlargement of dorsal surface of part of pygidium to show pitting, dorso-posterior view, $\times 1.55$. i, m–p, internal mould of pygidium and thorax; i, dorso-posterior view of pygidium and thorax, $\times 1$. m, n, posterior stereo pair of pygidium, $\times 1$. o, left lateral view of pygidium and thorax, $\times 1$. p, postero-ventral view of pygidium, $\times 1$.

Figs. 2a–c. Rubber casts from external moulds of librigena, KAC-DT-0114 [PA 17149]. a–b, dorsal stereo pair, $\times 1$. c, oblique antero-lateral view, $\times 1$.



Sasaki, for their kind cooperation and lending of the specimens used in the plates; to Mr. Kazuo Kitagawa, for his kind cooperation. Finally, special thanks are due to Mr. Ken Kawanami, the landowner of the present locality, for giving his consent to the author's fossil hunting, Mis Toshiko Imai and Mis Tamiko Nasu of the library of Department of Geology and Mineralogy, Faculty of Science, Kyoto University, for providing facilities to search the literature.

Repository of material:—University Museum, University of Tokyo ([PA]). Kaneko Collection (KAC-DT); 15-7 Fukae-honmachi 1-chome, Higashinada-ku, Kobe, 658, Japan.

References

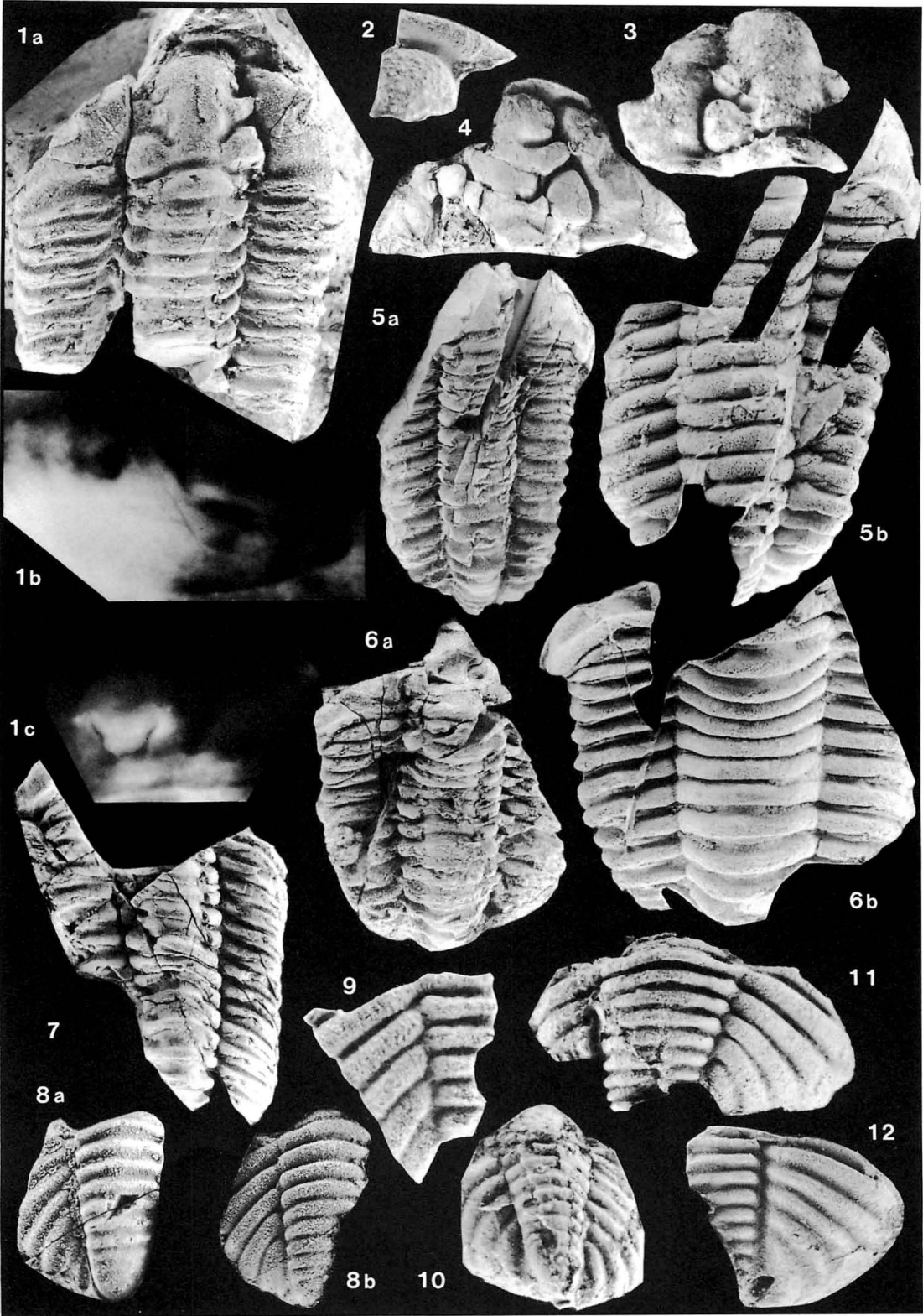
- Angelin, N. P. (1854): *Palaeontologia Scandinavica*. I: Crustacea formationis transitionis. Lund Fasc. 2, p. 21—92, pls. 25—41, Stockholm.
- Balashova, E. A. (1960): *Trilobites of the Middle and Upper Ordovician and Lower Silurian of Eastern Taimyr*. Leningrad National Univ. p. 1—111, pls. 1—6, Leningrad (in Russian).
- Barrande, J. (1846): *Notice préliminaire sur le Système Silurien et les trilobites de Bohême*. Leipzig, i—vi, 97 p.
- (1852): *Système Silurien du centre de la Bohême*. 1^{ère} partie: *Recherches paléontologiques, vol. 1, Crustacés: Trilobites*. i—xxx, 935 p., 51 pls., Prague and Paris.
- Brongniart, A. (1822): in Brongniart, A. and Desmarest, A. G., *Histoire naturelle des crustacés fossiles; les trilobites*. 154 p., pls. F, G, Levrault, Paris.
- Brünnich, M. T. (1781): *Beskrivelse over Trilobiten*. Nye Samling. Danske Vidensk. Selsk. Skrift. (not seen).
- Burmeister, H. (1843): *Die Organisation der Trilobiten*. 147 p., 6 pls., Berlin.
- Campbell, K. S. W. (1967): Trilobites of the Henryhouse Formation (Silurian) in Oklahoma. *Bull. Oklahoma Geol. Surv.* 115, p. 1—68, pls. 1—19.
- Chatterton, B. D. W. (1971): Taxonomy and ontogeny of Siluro-Devonian trilobites from near Yass, New South Wales. *Palaeontographica* Abt. A, Bd. 137, p. 1—108, pls. 1—24.
- and Campbell, K. S. W. (1980): Silurian trilobites from near Canberra and some related forms from the Yass Basin. *Ibid.*, Bd. 167, p. 77—119, pls. 9—24.
- Copper, P., Tazawa, J., Mori, K. and Kato, M. (1982): *Atrypa* (Devonian Brachiopoda) from Japan. *Trans. Proc. Palaeont. Soc. Japan, N.S.*, no. 127 (749), p. 368—374, pl. 59.
- Gill, E. D. (1945): Trilobites of the Family Calymenidae from the Palaeozoic Rocks of Victoria. *Proc. Roy. Soc. Victoria*, vol. 56 (N.S.), pt II, p. 171—185, pl. 7.
- Green, J. (1832): *A monograph of the Trilobites of North America; with colored models of the species*. 94 p. (Philadelphia).
- Hall, J. and Clarke, J. M. (1888): Descriptions of the trilobites and other Crustacea of the Oriskany, Upper Helderberg, Hamilton, Portage, Chemung and Catskill Groups. *New York Geological Survey, Palaeontology of New York*, vol. 7, p. 1—236.
- Hass, W. (1968): Trilobiten aus dem Silur und Devon von Bithynien (NW-Türkei). *Palaeontographica* Abt. A, Bd. 130, p. 60—207, pls. 1—12.
- Holloway, D. J. (1980): Middle Silurian trilobites from Arkansas and Oklahoma, U.S.A. *Palaeontographica* Abt. A, Bd. 170, p. 1—85, pls. 1—20.
- Ingham, J. K. (1977): A monograph of the upper Ordovician trilobites from the Cautley and Dent districts of Westmorland and Yorkshire. *Palaeontogr. Soc. (Monogr.)*, vol. 130 (for 1976) (546), part 3, p. 89—121, pls. 19—27.
- King, W. B. R. (1923): The Upper Ordovician rocks of the south-western Berwyn Hills. *Quart. Jour. Geol. Soc. London*, vol. 79, p. 487—507, pl. 26.
- Kobayashi, T. and Hamada, T. (1977): Devonian trilobites of Japan in comparison with Asian, Pacific and other faunas. *Palaeont. Soc. Japan, Spec. Pap.*, no. 20, 202 p., 13 pls.
- Kummerow, E. (1928): Beiträge zur Kenntnis der Fauna und der Herkunft der Diluvialgeschiebe. *Jahrb. Preuß. geol. Landesanst.*, Bd. 48, p. 1—59, pls. 1—2.
- Lindström, G. (1901): Researches on the visual organs of the trilobites. *Vetensk. Acad. Handl.*, 34 (8), p. 1—86, pls. 1—6.

- Maximova, Z. A. (1960): Palaeontological basis of the Palaeozoic stratigraphy of the Rudny Altai 7: Devonian and Carboniferous trilobites of the Rudny Altai. *Trudy VSEGEI*, vol. 7, p. 1—123, pls. 1—9 (in Russian).
- (1962): Trilobites from the Ordovician and Silurian of the Siberian platform. *Trudy VSEGEI, N.S.*, vol. 76, p. 1—176, pls. 1—13 (in Russian).
- (1967): Late Silurian and early Devonian trilobites of Central Kazakhstan. *International Symposium on the Devonian System, Calgary*, vol. 2, p. 777—787, pls. 1—4.
- (1968): Middle Palaeozoic trilobites of Central Kazakhstan. *Trudy VSEGEI, N.S.*, vol. 165, p. 1—208, pls. 1—35 (in Russian).
- (1978): Some new Devonian trilobites. *Annals of the All-Union Palaeont. Soc.*, vol. 21, p. 94—107, pl. 3 (in Russian).
- and Organova, N. M. (1959): The first discovery of remains of a Devonian fauna in West Primorie. *Doklady Acad. Nauk SSR*, vol. 128, no. 3, p. 594—595 (in Russian).
- McCoy, F. (1851): in, Sedgwick, A. and McCoy, F. A., *A synopsis of the classification of the British Palaeozoic rocks, with a detailed systematic description of the British Palaeozoic fossils in the Geological Museum of the University of Cambridge*. Fasc. 1, iii—iv, p. 1—184, pls. 1A—L, London and

Explanation of Plate 16

Figs. 1a—12. *Nipponocalymene hamadai* Kaneko, gen. et sp. nov.

- Figs. 1a—c. Paratype B, KAC-DT-0111 [PA 17150]. Incomplete individual preserved as internal mould except hypostome, of which rubber casts from external moulds are shown in Figures 3a—d of Plate 14. a, dorsal view, $\times 1$. b, right lateral, X-ray view showing hypostome approximately in position, about $\times 1.55$. c, posterior, X-ray view showing bifurcated raised area of hypostome in matrix, about $\times 1.4$.
- Fig. 2. Rubber cast from external mould of fragment of large cranium, KAC-DT-0115 [PA 17151], showing relatively long (exsag.) preglabellar furrow, dorsal view, $\times 1$.
- Fig. 3. Rubber cast from external mould of incomplete cranium, KAC-DT-0116 [PA 17152], dorsal view, $\times 1$.
- Fig. 4. Internal mould of incomplete deformed cranium, KAC-DT-0123 [PA 17153], collected by T. Ono, dorsal view, $\times 1$.
- Figs. 5a—b. Paratype C, Sasaki-Koizumi coll. [PA 17154]. Incomplete individual with hypostome shown in Figures 2a—b of Plate 14. a, dorsal view of internal mould, $\times 0.7$. b, dorsal view of rubber cast from external mould to show pitting.
- Figs. 6a—b. Paratype D, Sasaki-Koizumi coll. [PA 17670]. Incomplete individual. a, dorsal view of internal mould with displaced hypostome of external mould, from which rubber cast shown in Figures 4a—b of Plate 14 is taken, $\times 0.7$. b, dorsal view of cast from external mould, $\times 1$.
- Fig. 7. Incomplete individual, KAC-DT-0117 [PA 17671], dorsal view of internal mould, $\times 0.7$.
- Figs. 8a—b. Paratype, KAC-DT-0118 [PA 17672]. Incomplete pygidium. a, dorso-posterior view of internal mould, $\times 1$. b, dorso-posterior view of rubber cast from external mould, $\times 1$.
- Fig. 9. Rubber cast from external mould of fragment of largest pygidium, KAC-DT-0119 [PA 17673], dorso-posterior view, $\times 1$.
- Fig. 10. Rubber cast from external mould of incomplete pygidium, KAC-DT-0120 [PA 17674], dorso-posterior view, $\times 1$.
- Fig. 11. Paratype, KAC-DT-0121 [PA 17675]. Rubber cast from external mould of incomplete, somewhat depressed pygidium, dorso-posterior view, $\times 1$.
- Fig. 12. Internal mould of incomplete pygidium, KAC-DT-0122 [PA 17676], dorso-posterior view, $\times 1$.



- Cambridge.
- McLearn, F. H. (1924): Palaeontology of the Silurian Rocks of Arisaig, Nova Scotia. *Canada Dept. Mines, Geol. Surv., Mem.* 137, no. 118, geol. ser., p. 1—180, pls. 1—30.
- McNamara, K. J. (1979): Trilobites from the Coniston Limestone Group (Ashgill Series) of the Lake District, England. *Palaeontology*, vol. 22, pt. 1, p. 53—91, pls. 7—12.
- Modzalevskaya, E. A. (1967): Biostratigraphic subdivision of the Devonian in the Far East and Transbaikal region, USSR. *International Symposium on the Devonian System, Calgary*, vol. 2, p. 543—549.
- Pillet, J. (1968): Les *Calymene* dévoniens d'Europe et d'Afrique du Nord. *Ann. de Paléont. Invert.*, vol. 54, p. 67—89, pls. A—H.
- Price, D. (1982): *Calymene quadrata* King, 1923 and allied species of trilobites from the Ashgill of North Wales. *Geol. Mag.*, vol. 119, no. 1, p. 57—66, pls. 1—3.
- Prouty, W. F. (1923): in, Swartz, C. K. and Prouty, W. F., Trilobita, in Systematic palaeontology of Silurian deposits. *Maryland Geol. Surv., Silurian*, p. 1—794, pls. 1—67.
- Richter, R. and Richter, E. (1954): Die Trilobiten des Ebbe-Sattels und zu vergleichende Arten (Ordovizium, Gotlandium/Devon). *Abh. Senckenb. Naturf. Ges.*, 488, p. 1—76, pls. 1—6.
- Salter, J. W. (1865): The Trilobites of the Silurian, Devonian &c., Formations. *Palaeontogr. Soc. (Monogr.)*, vol. 17 (for 1863) (72), part 2, p. 81—128, pls. 7—14.
- Schmidt, Fr. (1894): Revision der ostbaltischen silurischen Trilobiten, Abt. 4. *Mém. Acad. imp. Sci.*, Ser. 7, 42, p. 1—93, pls. 1—6 (not seen).
- (1907): Revision der ostbaltischen silurischen Trilobiten, Abt. 6. *Ibid.*, Ser. 8, 20, p. 1—104, pls. 1—3.
- Schrank, E. (1970): Calymeniden (Trilobita) aus silurischen Geschieben. *Ber. deutsch. Ges. geol. Wiss. A, Geol-Paläont.* Bd. 15 (1), p. 109—146, pls. 1—12.
- Shirley, J. (1933): A redescription of the known British Silurian species of *Calymene* (s.l.). *Mem. Proc. Manchester lit. phil. Soc.*, vol. 77, p. 51—67, pl. 1.
- (1936): Some British trilobites of the Family Calymenidae. *Quart. Jour. Geol. Soc. London*, vol. 92, p. 384—422, pls. 29—31.
- Siveter, D. J. (1977): The Middle Ordovician of the Oslo region, Norway, 27. Trilobites of the family Calymenidae. *Norsk. geol. tidsskr.*, vol. 56 (for 1976), p. 335—396, pls. 1—13.
- (1979): *Metacalymene* Kegel, 1927, a calymenid trilobite from the Kopanina Formation (Silurian) of Bohemia. *Jour. Paleont.*, vol. 53, no. 2, p. 367—379, pls. 1—3.
- (1980): Evolution of the Silurian trilobite *Tapinocalymene* from the Wenlock of the Welsh Borderlands. *Palaeontology*, vol. 23, pt. 4, p. 783—802, pls. 97—101.
- (1983): *Calymene lawsoni* and allied species from the Silurian of Britain and their stratigraphic significance. In, Briggs, D. E. G. and Lane, P. D., Trilobites and other early arthropods: papers in honour of Professor H. B. Whittington, F. R. S. *Spec. Pap. in Palaeontology*, no. 30, p. 69—88, pls. 7—10.
- Temple, J. T. (1975): Early Llandovery trilobites from Wales with notes on British Llandovery calymenids. *Palaeontology*, vol. 18, pt. 1, p. 137—159, pls. 25—27.
- Tillman, C. G. (1960): *Spathacalymene*, an unusual new Silurian trilobite genus. *Jour. Paleont.*, vol. 34, no. 5, p. 891—895, pl. 116.
- Weber, V. N. (1932): Trilobites of the Turkestan. *Trudy VGRO, NKTP, SSR*, p. 1—157, pls. 1—4 (in Russian with English summary).
- Whittington, H. B. (1941): Silicified Trenton trilobites. *Jour. Paleont.*, vol. 15, no. 5, p. 492—522, pls. 72—75.
- (1956): Silicified Middle Ordovician trilobites: the Odontopleuridae. *Bull. Mus. Comp. Zool. Harv.*, vol. 114, no. 5, p. 155—288, pls. 1—24.
- (1959): Family Calymenidae Burmeister, 1843. in, Moore, R. C. (ed.): *Treatise on invertebrate palaeontology*, Pt. O, Arthropoda 1, Geol. Soc. Amer. and Univ. Kansas press, 560 p., 415 figs.
- (1971a): A new calymenid trilobite from the Maquoketa Shale, Iowa. In, Dutro, J. T. Jr. (ed.), *Paleozoic Perspectives: A*

- paleontological tribute to G. Arthur Copper. —(1971b): Silurian calymenid trilobites from
Smithsonian Contrib. Paleobiol., no. 3, p. the United States, Norway and Sweden.
 129—136, pls. 1—2. *Palaeontology*, vol. 14, pt. 3, p. 455—477,
 pls. 83—89.

Kitakami Mountains 北上山地, Nakazato 中里

北上山地中部デボン系中里層産の三葉虫動物群について—その2, Calymenidae 科: 本篇に於ては中部デボン系中里層 N₃ 部層産の Calymenidae 科に属する1新種を記載し, これに対し新属を提唱し *Nipponocalymene* と命名した。新属の背甲は一応 *Calymene* 属の構成概念をも充足するが, 腹板である下唇に於て本科としては極めて特異な形質を示す。即ち, 本科に於て下唇中央部前葉に突起を生じる場合には, 通常正中線上に唯1つ現われるだけであるが, 新属に於ては正中線を対称軸に1対を成して現われる。頭部前縁及び頭鞍の形態から, 新属は *Calymene* 属の内, Schrank (1970) の分類による *tentaculata* グループに, とりわけこのグループのカザクスタン産の種に最も良く対比され得る。恐らくこれ等に由来するものと考えられる。

金子 篤

797. INTRASPECIFIC VARIATION IN THREE SPECIES OF *GLOSSAULAX*
(GASTROPODA: NATICIDAE) FROM THE LATE CENOZOIC STRATA IN
CENTRAL AND SOUTHWEST JAPAN*

RYUICHI MAJIMA

Institute of Geoscience, University of Tsukuba, Ibaraki 305, Japan

Abstract. The intraspecific variation within three *Glossaulax* species, *G. hyugensis* (Shuto), *G. nodai*, n. sp. and *G. hagenoshitensis* (Shuto), which had flourished in the late Cenozoic waters of Japan, was studied on the basis of more than 600 individuals collected from 24 localities. The three species overlap stratigraphically and geographically, and are distinguished from other *Glossaulax* species by having a nearly flat umbilical wall and a spiral angulation dividing the base and the umbilical wall.

“Dimorphic” variation is recognized in the callus morphology of the adults of *G. hyugensis* and *G. hagenoshitensis*. One adult variant of *G. hyugensis* is similar to that of *G. hagenoshitensis*, and the other adult variant of the former species is similar to that of the latter, whereas the frequency of the similar adult variants of the two species is extremely different. *G. nodai*, however, is uniform in callus morphology throughout growth. In the callus morphology, the juvenile of *G. hyugensis* and that of *G. hagenoshitensis* are similar to *G. nodai*, and to one form of the adult “dimorphic” variation of *G. hyugensis*, respectively. Furthermore, *G. hagenoshitensis* is divisible into two allopatric forms in the sculpture of sub-sutural area and of umbilical wall margin. The mode of the ontogenetic variations of the three species is explained by a heterochronic model in which an imaginary ancestral species is presumed. *G. hagenoshitensis* has been taxonomically confused with *Polinices sagamiensis* Pilsbry and *Glossaulax reiniana* (Dunker), but is clearly distinguished from these two species on the basis of umbilical morphology.

Introduction

Late Cenozoic strata distributed along the Pacific coast of southwest Japan yield abundant warm-water molluscan species, collectively called the Kakegawa Fauna (Otuka, 1939; Chinzei, 1978). Japanese paleontologists have provided taxonomical and evolutionary studies for many taxa from these strata: for example, *Umboonium* by Makiyama (1925), Suzuki (1934) and Sugi-

yama (1935); *Siphonalia* by Makiyama (1941); *Paphia* by Shuto (1957); *Anadara* by Noda (1965); and *Cryptopecten* by Hayami (1973).

Despite the large numbers of naticid gastropods from these strata, they have been little studied except for Shuto's (1964) description of species from the late Miocene to early Pleistocene Miyazaki Group of southeast Kyushu. Shuto (1964) proposed the new species *Polinices (Glossaulax) hyugensis* and *P. (G.) hagenoshitensis*, both of which have been generally considered to be endemic and rare in the

*Received April 26, 1984; Read January 22, 1984, Annual Meeting at Kyoto University.

Miyazaki Group. However, the two species, especially in *G. hagenoshitensis*, occur abundantly in the Kakegawa Fauna. The apparent rarity of *G. hagenoshitensis* is partly because it has been confused with *Polinices sagamiensis* Pilsbry and *Glossaulax reiniana* (Dunker). *Glossaulax hyugensis*, *G. hagenoshitensis* and their closely related species *G. nodai*, n. sp. are characterized by a nearly flat umbilical wall and a spiral angulation dividing the base and the umbilical wall, by which they are easily distinguished from *P. sagamiensis* and other *Glossaulax* species.

G. hyugensis and *G. hagenoshitensis* show "dimorphic" variations at the adult stages and their juveniles differ, to varying degrees, from the adults. *G. nodai*, n. sp., however, has a uniform shell morphology throughout growth. Furthermore, *G. hagenoshitensis* is divisible into two allopatric forms. The three species can therefore be divided into ten phenotypes: *G. hyugensis* has one juvenile and two adult phenotypes; *G. hagenoshitensis* two juvenile and four adult phenotypes; and *G. nodai* one phenotype. The aim of this study is to describe the ten phenotypes of the three *Glossaulax* species; to evaluate the intraspecific variations of the three species as species characters; to propose a heterochronic model to explain how the differences of the ontogenetic variation among the three species occur phylogenetically; to provide revised diagnoses for *G. hyugensis* and *G. hagenoshitensis*; and to propose the new species *G. nodai*.

The term "phenotype" used in this study is somewhat of a misnomer because the juvenile forms of *G. hyugensis* and *G. hagenoshitensis* are also designated as "phenotype." In the model of heterochrony proposed herein, this term will be used in the same sense as growth stage.

Morphological terminology in the present paper conforms to that adopted by Marinovich (1977, text-fig. 10) except for "umbilical wall" which shows the umbilical side of body whorl excluding funicle and above it. In the three *Glossaulax* species, umbilical wall is sharply separated from the base by a spiral angulation.

The specimens studied here are preserved in

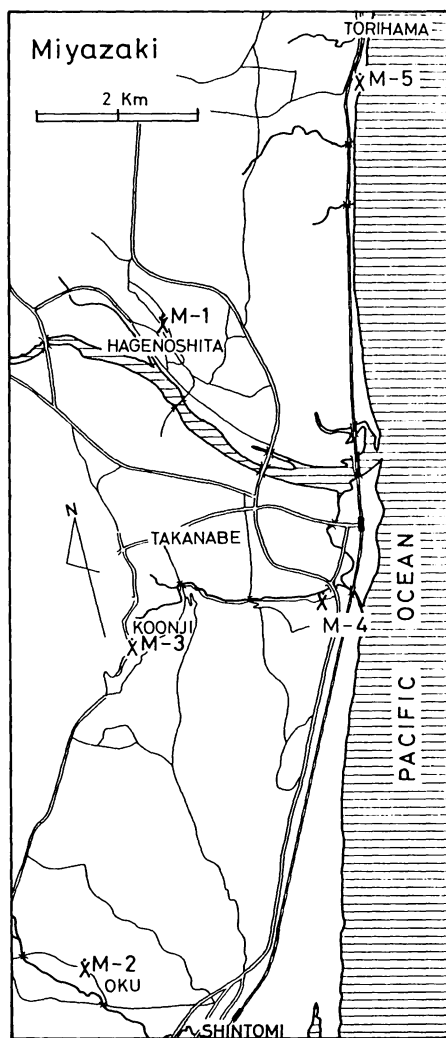
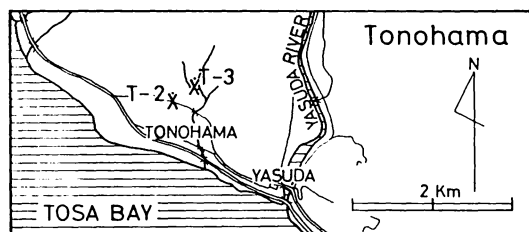
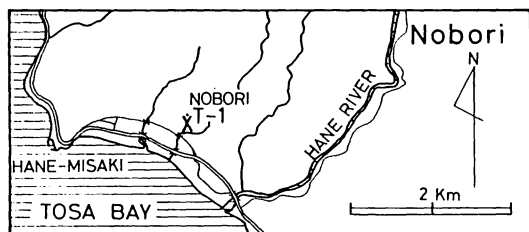
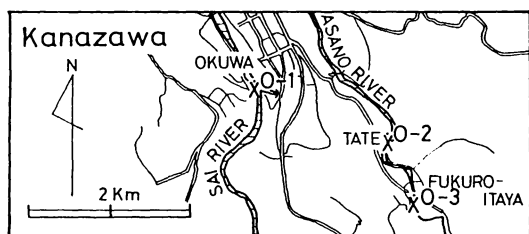
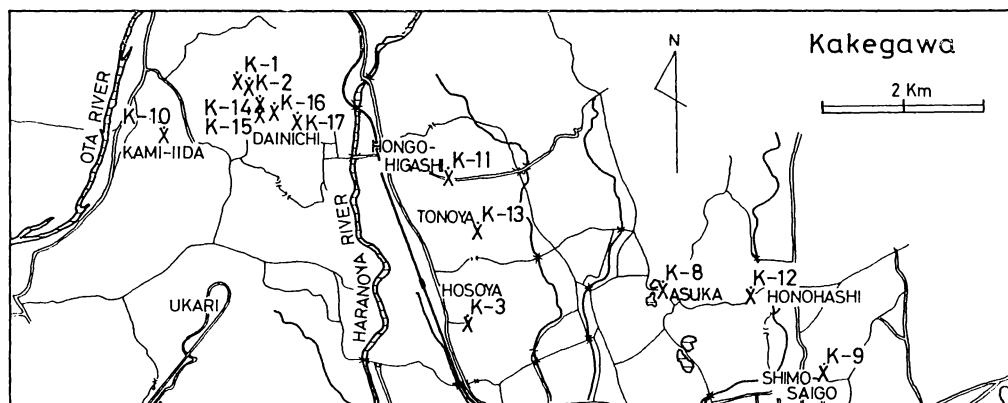
Institute of Geoscience, University of Tsukuba (IGUT), Geological Institute of Yokohama National University (GIYU), and Department of Geology, Faculty of Science, Kyushu University (GK).

Localities

All specimens studied here were obtained from late Cenozoic strata in central and southwest Japan (Text-fig. 1). The chronology of these strata is mainly based upon planktonic foraminiferal biostratigraphy, and radiometric and magnetostratigraphic datings (Tsuchi *ed.*, 1979; 1981). These strata range in age from late Pliocene to early Pleistocene. The stratigraphic positions of fossil localities and numbers of specimens examined from each locality are summarized in Table 1. The formations and localities treated in this study are in the following geographic areas (Text-fig. 1):

Miyazaki area.—This area is situated in the eastern part of Miyazaki Prefecture. The five localities (Locs. M-1–5) in this area are assigned to the late Pliocene to early Pleistocene Takanabe Member of the Koyu Formation of the Miyazaki Group (Shuto, 1961). The Takanabe Member is composed mainly of well bedded siltstone, within which intercalated, thin (less than 1 m) sandstone beds have yielded the specimens studied herein. Shuto (1961) recognized six fossil horizons in the Miyazaki Group: from the first to the sixth fossil horizons in ascending order. Among them, the fourth to sixth fossil horizons occur in the Takanabe Member; that is, the fourth fossil horizon at Locs. M-1, M-2 and M-3, the fifth at Loc. M-4 and the sixth at Loc. M-5 (Table 1). The Pliocene-Pleistocene boundary is drawn between the fifth and sixth fossil horizons (Shuto, 1983).

M-1: Road cut at Hagenoshita, Takanabemachi, Koyu County (lat. 32°08.8'N.; long. 131°31.1'E.); fine-grained sandstone. M-2: Road cut at Oku, Shintomi-machi, Koyu County (lat. 32°47.7'N.; long. 132°29.2'E.); fine-grained sandstone. M-3: Road cut at Koonji, Takanabemachi, Koyu County (lat. 32°06.7'N.; long.



Text-fig. 1. Maps showing fossil localities. See Shikama and Masujima (1969) for the Loc. N-1 in the Kamakura area.

Table 1. Stratigraphic and geographic distributions of the specimens of *Glossaulax hyugensis* (Shuto), *G. nodai*, n. sp. and *G. hagenoshitensis* (Shuto) examined in this study. The numbers in parentheses show number of specimens. The specimens are repositied in Institute of Geoscience, University of Tsukuba (IGUT), Geological Institute of Yokohama National University (GIYU), and Department of Geology, Faculty of Science, Kyushu University (GK).

Formation	Species		<i>Glossaulax</i>	<i>Glossaulax</i>
	<i>hyugensis</i> (Shuto)	<i>nodai</i> n. sp.	<i>hagenoshitensis</i> (Shuto) (Phenotypes 3Ja, 3Ia and 3Ua)	<i>hagenoshitensis</i> (Shuto) (Phenotypes 3Jb, 3Ib, and 3Ub)
Miyazaki Area Miyazaki Group Sixth fossil horizon Early Pleistocene		M-5: IGUT no. 15698(1)		
Fifth fossil horizon Late Pliocene				M-4: GK. L7987(1)
Fourth fossil horizon Late Pliocene	M-1: IGUT no. 15699(50) GIYU no. 570(1) GK. L8009(1) M-2: IGUT no. 15701(30) M-3: GIYU no. 571(2)		M-1: IGUT no. 15700(46) GIYU no. 568(8) GK. L8003(1) M-2: IGUT no. 15702(16) M-3: GIYU no. 571(7)	
Nobori and Ionohama Areas Ionohama Group Ananai Formation Late Pliocene	T-2: IGUT no. 15694(25) IGUT no. 15693(28)		T-3: IGUT no. 15692(1)	
Nobori Formation Late Pliocene	T-1: IGUT no. 15691(9)		T-1: IGUT no. 15690(2)	
Kakegawa Area Kakegawa Group Upper Kakegawa Formation Hosoya Member Early Pleistocene				K-3: IGUT no. 15717(18)
Lower Kakegawa Formation Tenno Member Late Pliocene	K-9: IGUT no. 15716(3)		K-8: IGUT no. 15714(15) K-9: IGUT no. 15715(2)	
Dainichi Member Late Pliocene		K-13: IGUT no. 15695(1) IGUT no. 15696(2) K-17: IGUT no. 15697(6)	K-12: IGUT no. 15712(11)	K-1: IGUT no. 15703(152) K-2: IGUT no. 15704(47) K-10: IGUT no. 15705(121) K-11: IGUT no. 15707(21) K-13: IGUT no. 15713(3) K-14: IGUT no. 15709(11) K-15: IGUT no. 15710(6) K-16: IGUT no. 15711(17) K-17: IGUT no. 15706(48)
Kamakura Area Nojima Formation Early Pleistocene		N-1: GIYU no. 562(1) GIYU no. 563(1) GIYU no. 564(1)		N-1: GIYU no. 567(8)
Kanazawa Area Omna Formation Early Pleistocene				O-1: IGUT no. 15688(10) O-2: IGUT no. 15718(2) O-3: IGUT no. 15689(1)

131°30.2'E.); sandstone. M-4: Road cut at Nihonmatsu, Takanabe-machi, Koyu County (loc. MI-5551 of Shuto, 1961, lat. 32°06.7'N.; long. 131°31.7'E.); fine-grained sandstone. M-5: Construction excavation at Torihama fishing port, Kawaminami-machi, Koyu County (lat. 32°10.1'N.; long. 131°33.1'E.); fine-grained sandstone.

Nobori and Tonohama areas.—The two areas are located in the southeastern part of Kochi Prefecture. The late Pliocene Tonohama Group, which is divided into the Nobori, Nahari and Ananai Formations in ascending order (Katto *et al.*, 1953), is exposed in these areas. The Nobori Formation (Loc. T-1) consists mainly of massive siltstone, and the Ananai Formation (Locs. T-2 and T-3) is mainly massive sandstone with sporadic pebbles.

T-1: Large quarry at Nobori, Hane-machi, Muroto County (lat. 33°22.2'N.; long. 134°03.5'E.); siltstone. T-2: Road cut, about 450 m north from Tonohama Village, Yasuda-machi, Aki County (lat. 33°26.6'N.; long. 133°58.2'E.); fine-grained sandstone. T-3: Stream-side cliff in small valley, about 350 m northwest from Higashidani Village, Yasuda-machi, Aki County (lat. 33°26.7'N.; long. 133°58.4'E.); fine- to medium-grained sandstone.

Kakegawa area.—This area is situated in the southwestern part of Shizuoka Prefecture. The Kakegawa Group yields the fossils studied at thirteen localities (Locs. K-1–3, 8–17). The Kakegawa Group is divided into the Lower Kakegawa, Upper Kakegawa and Soga Formations in ascending order (Makiyama and Sakamoto, 1957). The Lower Kakegawa Formation is divided into two members: the Dainichi Sand (Locs. K-1, 2, 10–17) below and the Tenno Sand (Locs. K-8, 9) above. The basal part of the Upper Kakegawa Formation is designated the Hosoya Tuffaceous Silt Member (Loc. K-3). The Pliocene-Pleistocene boundary coincides with a tuff bed (Hosoya Tuff) in the lowermost part of the Hosoya Tuffaceous Silt Member (Tsuchi and Ibaraki *in* Tsuchi *ed.*, 1979).

K-1: Stream-side cliff in small valley, about 700 m northwest from Dainichi Village, Fukuroi

City (lat. 34°48.7'N.; long. 137°56.4'E.); fine- to medium-grained sandstone with pebbles. K-2: Stream-side cliff in small valley, about 120 m southeast from Loc. K-1 (lat. 34°48.7'N.; long. 137°56.4'E.); fine- to medium-grained sandstone with pebbles. K-3: Road cut near Kakegawa Baseball Field, about 650 m southeast from Hosoya National Railway Station, Kakegawa City (lat. 34°47.1'N.; long. 137°58.2'E.); silt-pebble bearing medium-grained sandstone intercalated in tuffaceous siltstone. K-8: Road cut at Asuka, Kakegawa City (lat. 34°47.3'N.; long. 137°59.9'E.); fine- to medium-grained sandstone. K-9: Road cut at Shimo-Saigo, Kakegawa City (lat. 34°46.7'N.; long. 138°01.2'E.); silty sandstone. K-10: Road-side cliff, about 500 m east from Kami-Iida Village, Mori-machi, Suchi County (lat. 34°48.4'N.; long. 137°55.7'E.); fine- to medium-grained sandstone with pebbles. K-11: Road cut, about 500 m southeast from Hongo-Higashi Village, Kakegawa City (lat. 34°48.1'N.; long. 137°58.0'E.); fine- to medium-grained sandstone. K-12: Road cut at the east entrance of small tunnel, about 250 m southwest from Honohashi Village, Kakegawa City (lat. 34°47.3'N.; long. 138°00.6'E.); conglomerate with medium-grained sandstone matrix. K-13: Small tunnel cut, about 300 m east from Tonoya Village, Kakegawa City (lat. 34°47.7'N.; long. 137°58.3'E.); fine-grained sandstone. K-14: Small river-side cliff, about 500 m north from Dainichi Village, Fukuroi City (lat. 34°48.6'N.; long. 137°56.5'E.); fine- to medium-grained sandstone. K-15: Small river-side cliff, about 200 m south from Loc. K-14 (lat. 34°48.4'N.; long. 137°56.5'E.); fine- to medium-grained sandstone. K-16: Road cut, about 250 m east from Loc. K-14 (lat. 34°48.5'N.; long. 137°56.6'E.); fine- to medium-grained sandstone. K-17: Road cut, about 1000 m west from Haranoya National Railway Station, boundary between Fukuroi and Kakegawa Cities (lat. 34°48.4'N.; long. 137°56.8'E.); fine- to medium-grained sandstone.

Kamakura area.—This area is located in the base of Miura Peninsula, Kanagawa Prefecture. At only one locality (Loc. N-1) of this area, fossils studied herein have been collected from the early Pleistocene Nojima Formation of the Kazusa Group. The Nojima Formation is composed mainly of tuffaceous fine-grained sand-

stone or siltstone with many scoriaceous or pumiceous patches (Shikama and Masujima, 1969).

N-1: Large sand quarry, about 900 m north-east from Kitakamakura National Railway Station, Kamakura City (loc. 318-II of Shikama and Masujima, 1969): tuffaceous fine- to medium-grained sandstone with pebbles.

Kanazawa area.—This area is situated in the central part of Ishikawa Prefecture. The three localities (Locs. O-1–3) in this area belong to the early Pleistocene Omma Formation which is composed mainly of medium-grained sandstone.

O-1: River bed of the Sai River, about 1000 m southeast from the Okuwa bridge, Okuwamachi, Kanazawa City (lat. $36^{\circ}31.6'N$.; long. $136^{\circ}41.2'E$.); fine- to medium-grained sandstone. O-2: River-side cliff of the Asano River, Tate-machi, Kanazawa City (lat. $36^{\circ}31.3'N$.; long. $136^{\circ}42.4'E$.); fine- to medium-grained sandstone. O-3: Transported subangular boulder, on the river floor of the Asano River, about 150 m west from the streets of Fukuroitaya-machi, Kanazawa City (lat. $36^{\circ}30.8'N$.; long. $136^{\circ}42.5'E$.); fine-grained sandstone.

Associated faunas

The Kakegawa, Omma-Manganji (=Omma-Manganzi) and Kuroshio Faunas (Chinzei, 1978) contain the three *Glossaulax* species.

The Kakegawa Fauna, warm-water molluscs of late Miocene to early Pleistocene age, occurs in strata along the Pacific coast of southwest Japan, including the Miyazaki Group (Locs. M-1–5), the Tonohama Group (Locs. T-1–3) and the Kakegawa Group (Locs. K-1–3, 8–17). The fauna is characterized by extinct, shallow, warm-water species, such as *Anadara castellata* (Yokoyama), *Glycymeris nakamurai* Makiyama, *Amusiopecten praesignis* (Yokoyama), *Venericardia panda* (Yokoyama), *Suchium mysticum* (Yokoyama), *S. obsoletum* (Makiyama), *S. suchiense* (Yokoyama), *Turritella perterebra* Yokoyama, *Babylonia elata* Yokoyama, *Baryspira okawai* (Yokoyama) and others. The three

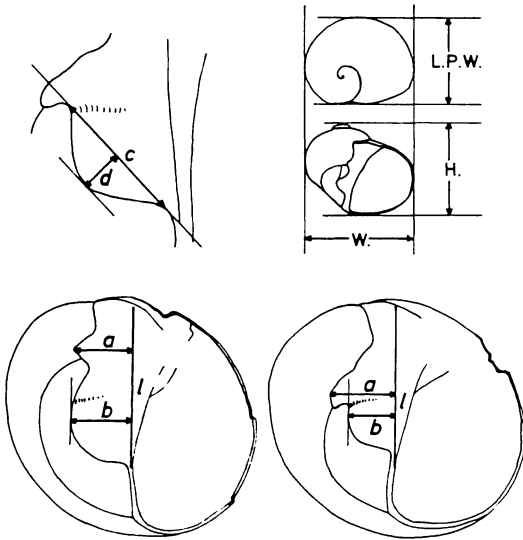
Glossaulax species are most frequently found in the Kakegawa Fauna (Table 1).

The Omma-Manganzi Fauna, cold-water molluscs of Pliocene to early Pleistocene age, occurs in strata along the Japan Sea coast of Japan that include the Omma Formation (Locs. O-1–3). This fauna is characterized by extinct, shallow, cold-water species, such as *Anadara amacula elongata* Noda, *Mizuhopecten tokyoensis hokurikuensis* (Akiyama), *Pseudamiantis tauensis* (Yokoyama), *Suchium akitanum* (Suzuki), *Turritella saishuensis* Yokoyama and others. Among the three *Glossaulax* species, only *G. hagenoshitensis* is found in the Omma-Manganzi Fauna (Table 1). Several warm-water species are rarely associated with the Omma-Manganzi Fauna (Ogasawara, 1981). This is considered to be caused by the Paleo-Tsushima current, a branch of the warm-water Paleo-Kuroshio current, which flowed into the Japan Sea through Tsushima Strait at that time. The rare occurrence of *G. hagenoshitensis* in the Omma Formation is interpreted as having been influenced by this current.

The Kuroshio Fauna which flourishes in the modern warm waters under the influence of Kuroshio current first appeared in the early to middle Pleistocene. *G. hagenoshitensis* and *G. nodai* are found in the Kuroshio Fauna at the Loc. N-1 of the early Pleistocene Nojima Formation. Although the molluscan fauna of the Loc. N-1 indicates shallow warm waters, it lacks any characteristic species of the Kakegawa Fauna (Shikama and Masujima, 1969).

Descriptions of intraspecific variations of the three *Glossaulax* species

Measurements.—Intraspecific variation within each of the three *Glossaulax* species is best shown by the differences in the shape of callosity. To illustrate their variations, four values of the callus were measured (Text-fig. 2): *a* is the maximum width of the parietal callus, and *b* is the maximum width of the umbilical callus; both are measured normal to line *l* (Text-fig. 2) which coincides with the angulation developed along



Text-fig. 2. Measurements of the three *Glossaulax* species. *a*: Maximum width of parietal callus. *b*: Maximum width of umbilical callus. *l*: A line coinciding with angulation developed along inner apertural margin. *c*: Length from the anterior end of umbilical callus to the apex of depression between parietal and umbilical calluses. *d*: Maximum width of adaxial half of umbilical callus. *W.*: Width of shell. *H.*: Height of shell. *L.P.W.*: Shell length perpendicular to *W.* and *H.*

the inner apertural margin. However, some specimens, especially *G. nodai* and juvenile form of *G. hyugensis*, have not the distinctly developed angulation. In such cases, the position of line *l* is approximated. The value *c* is the length from the anterior end of umbilical callus to the apex of depression between the parietal callus and umbilical callus (sulcus) (Text-fig. 2). The value *d* is the maximum width of the adaxial half of the umbilical callus, and is measured normal to line *c* (Text-fig. 2).

The values *a*, *b*, *c* and *d* are measured by the following photographic method. (1) The parietal and umbilical calluses are set almost parallel to the film surface. (2) The specimen is photographed, and the photographic print is enlarged ($\times 2$ – $\times 5$). (3) The lines, *a*, *b*, *c*, *d* and *l* are drawn on the print, and the lengths on the print, *a'*,

b', *c'* and *d'*, are measured. (4) The true values *a*, *b*, *c* and *d* are calculated from the enlarged print.

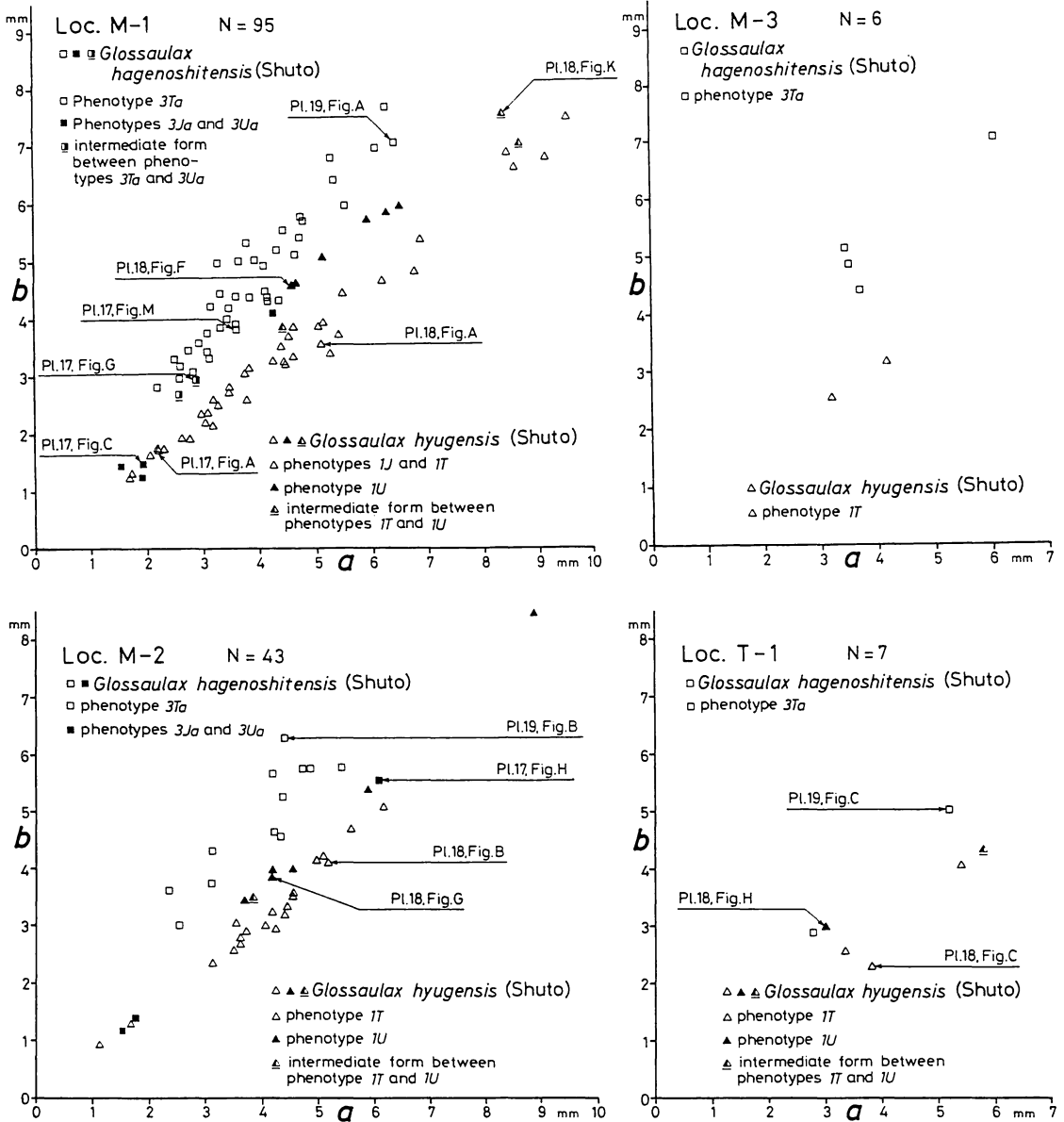
The intraspecific variations of the parietal and umbilical calluses are well illustrated by the scatter diagrams of *a* and *b* (Text-figs. 3, 4, 5 and 6), and that of *c* and *d/c* (Text-fig. 7). The intraspecific variations of the three *Glossaulax* species are described below.

The variation of Glossaulax hyugensis (Shuto).—The specimens of *G. hyugensis* collected from Locs. M-1, M-2, M-3, T-1, T-2 and K-9 (Table 1) can be divided into three morphologically different groups (phenotypes *1J*, *1T* and *1U*) which occur together at Locs. M-1 and M-2 (Text-fig. 3), and T-2 (Text-fig. 4), where they occur abundantly.

Phenotype *1J* is a juvenile form (Pl. 17, Figs. Aa–Bb), with value *a* less than about 3 mm and *b* less than about 2 mm. Phenotype *1J* is characterized by a wedge-shaped anterior lobe of parietal callus which is developed along the posterior margin of umbilicus, and by a subtrigonal umbilical callus. The anterior lobe of parietal callus always protrudes more than the umbilical callus ($a > b$) and the former callus is attached to the latter by a shallow groove.

Phenotype *1T* is a typical adult form (Pl. 18, Figs. Aa–Eb) and differs from phenotype *1J* by the shape of its umbilical callus. Phenotype *1T* possesses a subquadrate umbilical callus. Phenotype *1J* gradually changes to phenotype *1T* with growth (Text-fig. 7).

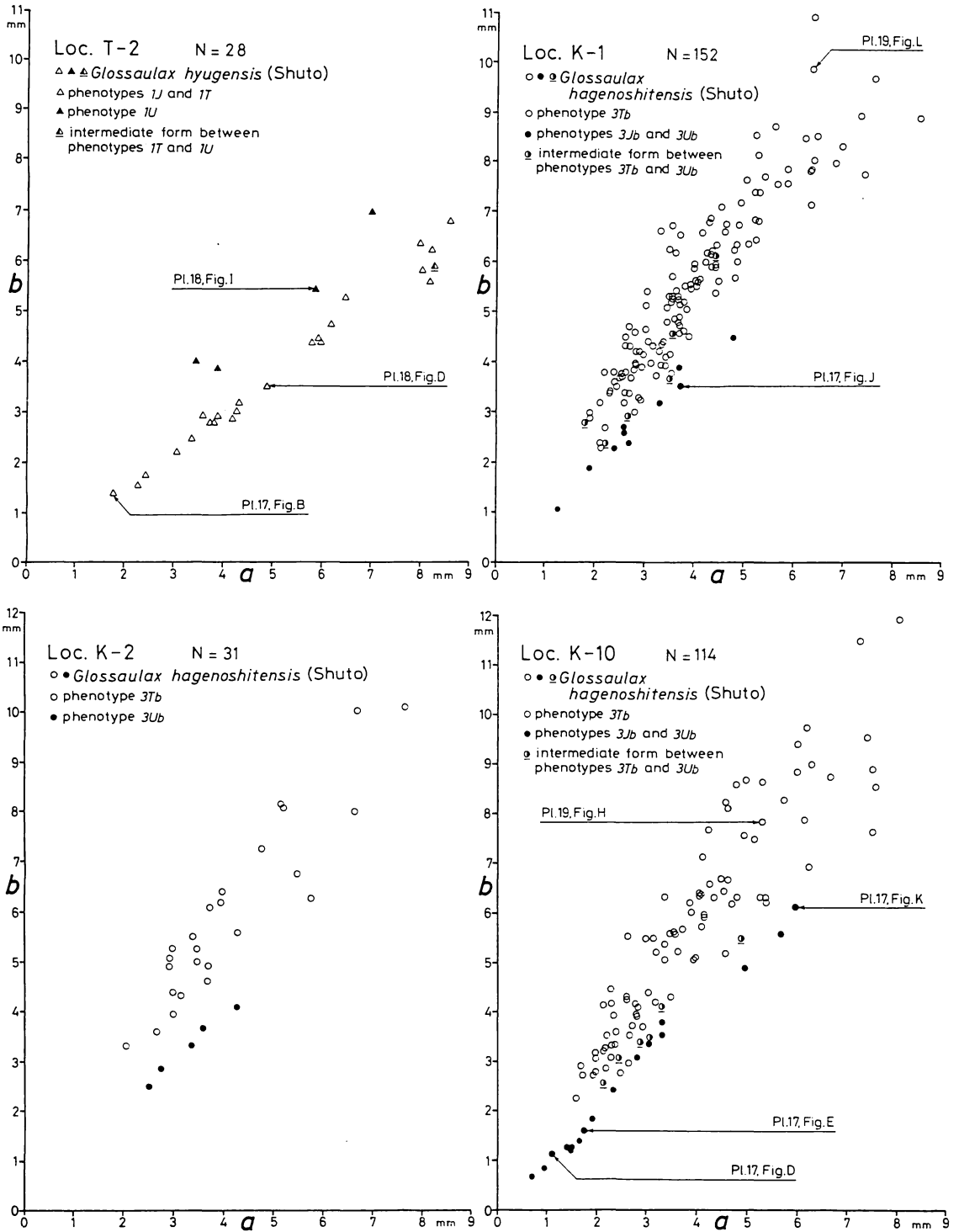
Phenotype *1U* is an unusual adult form (Pl. 18, Figs. Fa–Jb) characterized by having a very weakly developed anterior lobe of parietal callus and a subquadrate to semicircular umbilical callus. The umbilical callus has a shallow transverse groove at the center to posterior portion but it may be indistinct. In phenotype *1U*, the degree of protrusion of the parietal and umbilical calluses is almost equal ($a = b$). There are a few intermediate forms between phenotypes *1T* and *1U* (Pl. 18, Figs. Ka–b). In the scatter diagrams of *a* and *b*, the intermediate forms do not always occupy their intermediate place (Loc. T-2 in Text-fig. 4).



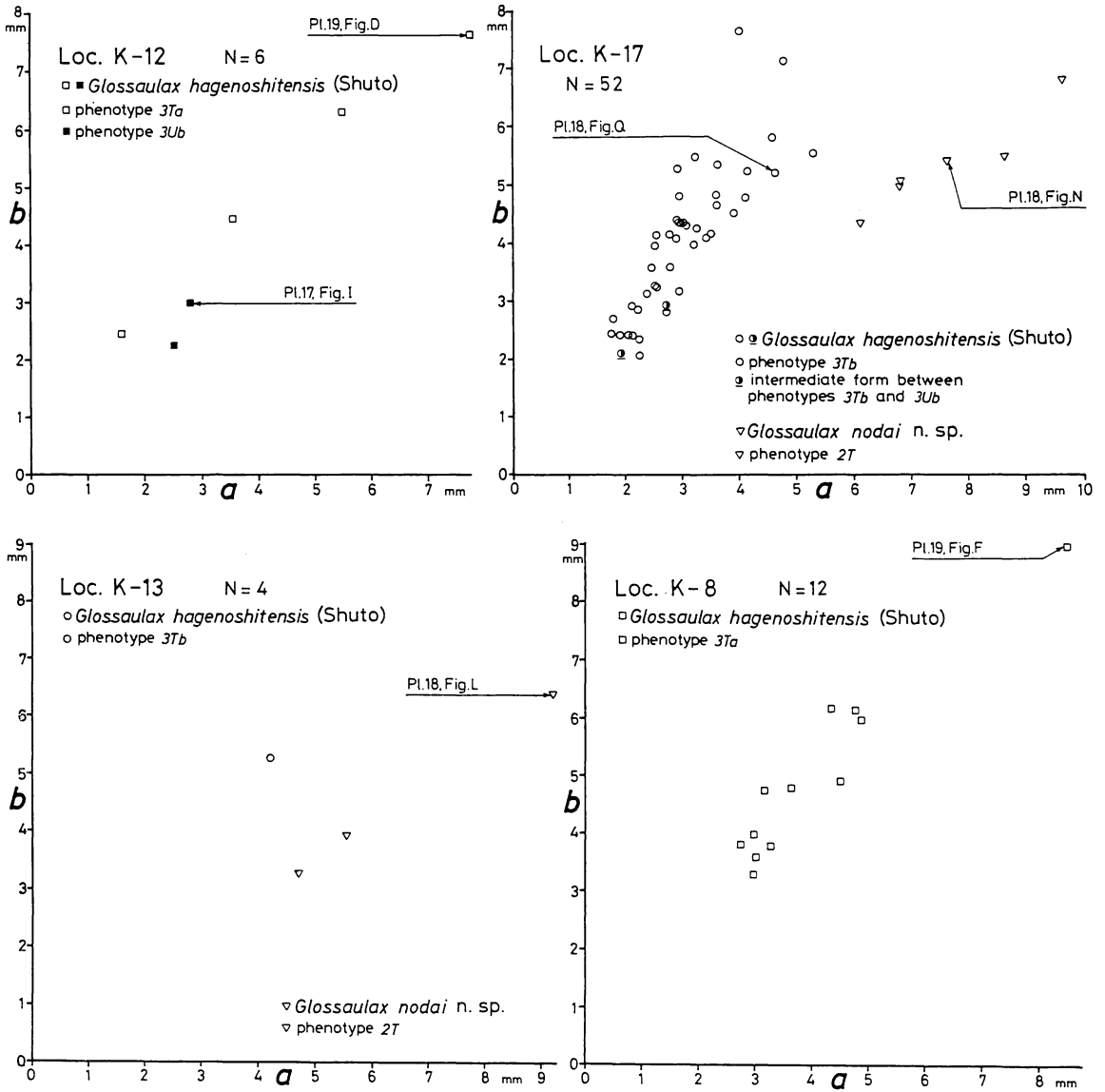
Text-fig. 3. Scatter diagrams of *a* and *b* (Text-fig. 2) for *Glossaulax hyugensis* (Shuto) and *G. hagenoshitensis* (Shuto) at Locs. M-1, M-2, M-3 and T-1.

The variation of Glossaulax nodai, n. sp.—The specimens of *G. nodai* collected from Locs. M-5, K-13, K-17 and N-1 (Table 1) are morphologically uniform (phenotype 2T: Pl. 18, Figs. La–Ob). They are characterized by having a wedge-shaped anterior lobe of parietal callus and a subtrigonal umbilical callus. Pheno-

type 2T is morphologically similar to the phenotype 1J of *G. hyugensis* (Pl. 17, Figs. Aa–Bb); the former differs from the latter only in its greater size (Text-fig. 7). The juvenile form of *G. nodai* is unknown but it is likely to be morphologically almost identical with the adult form (phenotype 2T) judging from the callus form of the smallest



Text-fig. 4. Scatter diagrams of *a* and *b* (Text-fig. 2) for *Glossaulax hyugensis* (Shuto) at Loc. T-2 and *G. hagenoshitensis* (Shuto) at Locs. K-1, K-2 and K-10.

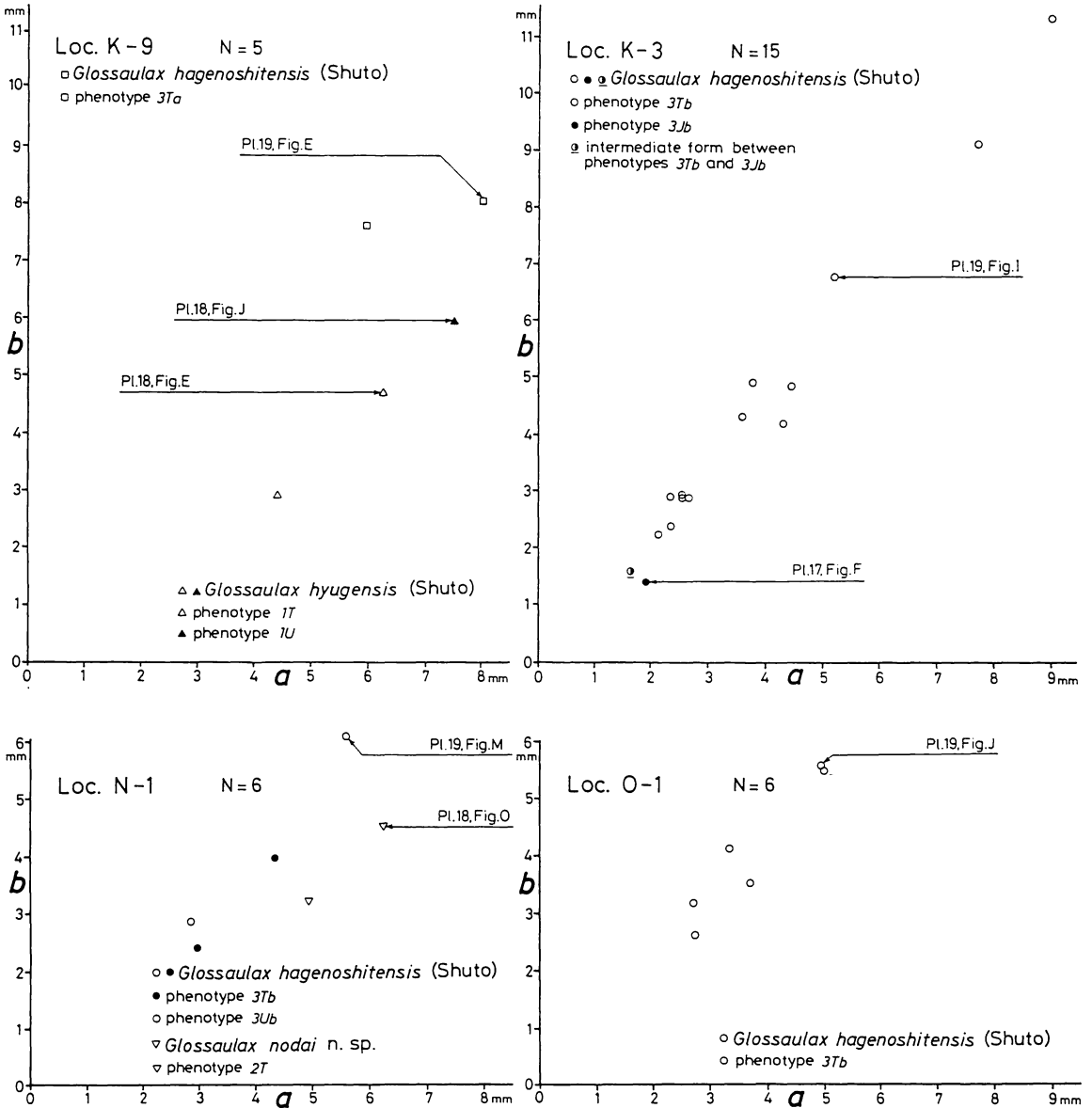


Text-fig. 5. Scatter diagrams of *a* and *b* (Text-figs. 2) for *Glossaulax hagenoshitensis* (Shuto) at Locs. K-12 and K-8, and *G. hagenoshitensis* (Shuto) and *G. nodai*, n. sp. at Locs. K-17 and K-13.

specimen of phenotype 2T (Text-fig. 7).

The variation of Glossaulax hagenoshitensis (Shuto).—The specimens of *G. hagenoshitensis* collected from 23 localities (Table 1) can be divided into six morphologically different groups (phenotypes 3Ja, 3Ta, 3Ua, 3Jb, 3Tb and 3Ub). They can be also divided into two allopatric groups, one group comprising phenotypes 3Ja,

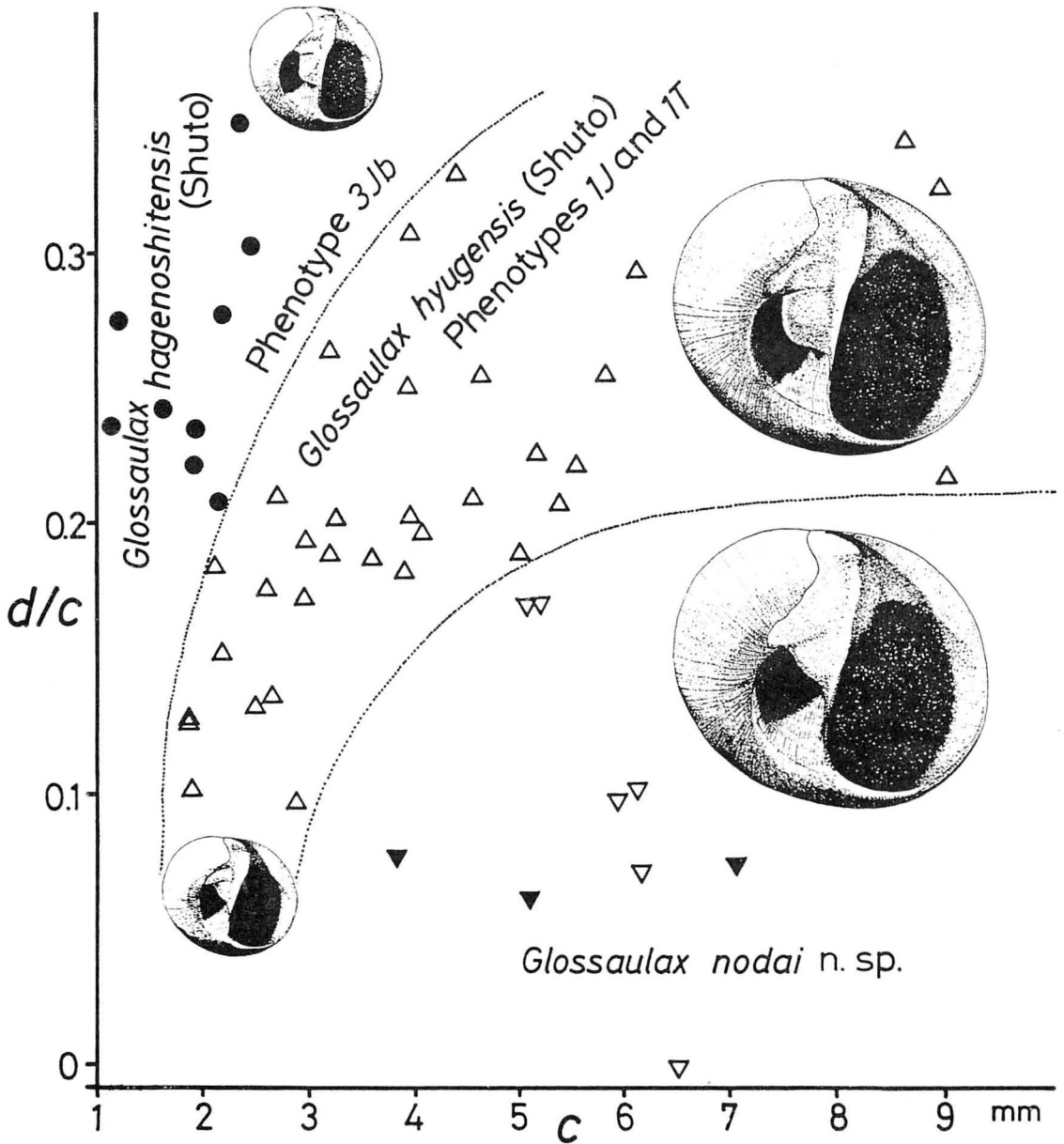
3Ta and 3Ua, and the other is phenotypes 3Jb, 3Tb and 3Ub. Phenotypes 3Jb, 3Tb and 3Ub are characterized by a subsutural, minutely incised band and a spiral ridge along the outer margin of the umbilical wall, while phenotypes 3Ja, 3Ta and 3Ua lack these characters (Text-fig. 8). The latter phenotypes, however, rarely possess a very weakly developed subsutural band



Text-fig. 6. Scatter diagrams of *a* and *b* (Text-fig. 2) for *Glossaulax hyugensis* (Shuto) and *G. hagenoshitensis* (Shuto) at Loc. K-9, *G. hagenoshitensis* (Shuto) at Locs. K-3 and O-1, and *G. hagenoshitensis* and *G. nodai*, n. sp. at Loc. N-1.

(Pl. 17, Fig. Ha) and a spiral ridge of the umbilical wall. In the localities where specimens occur abundantly, all the phenotypes 3Ja, 3Ta and 3Ua occur together at Locs. M-1 and M-2 (Text-fig. 3) and all the phenotypes 3Jb, 3Tb and 3Ub at Locs. K-1 and K-10 (Text-fig. 4).

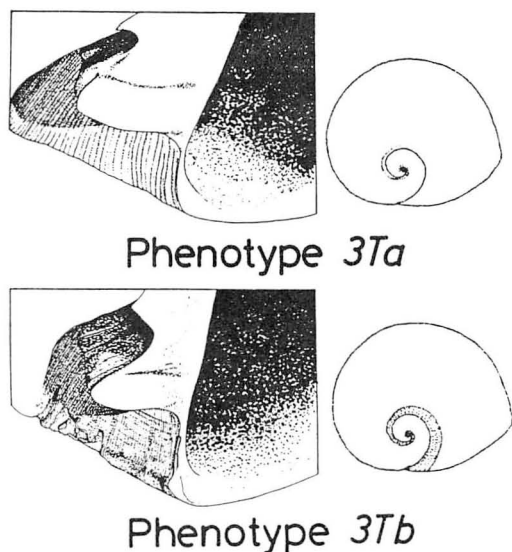
Phenotypes 3Ja (Pl. 17, Figs. Ca–b) and 3Jb (Pl. 17, Figs. Da–Fb) are juvenile forms smaller than about 2 mm for values *a* and *b*. They are characterized by the possession of a wedge-shaped anterior lobe of parietal callus and a subquadrate umbilical callus. The parietal callus protrudes



Text-fig. 7. Scatter diagram of c and d/c (Text-fig. 2) for phenotype 3Jb of *Glossaulax hagenoshitensis* (Shuto) (black circle: Loc. K-10), phenotypes 1J and 1T of *G. hyugensis* (Shuto) (white triangular: Loc. M-1) and *G. nodai*, n. sp. (black reverse triangular: Loc. K-13; white reverse triangular: Loc. K-17).

somewhat more than the umbilical callus ($a \geq b$), and the former is attached to the latter with a shallow groove. The shape of callosity is similar to that of the phenotype 1T of *G. hyu-*

gensis, but phenotypes 3Ja–b (3Ja + 3Jb) differ from phenotype 1T in the small size (Text-fig. 7), and in the subsutural and umbilical wall sculpture of phenotype 3Jb.



Text-fig. 8. Sculpture of subsutural area and umbilical wall margin of phenotypes *3Ta* and *3Tb* of *Glossaulax hagenoshitensis* (Shuto), characterizing two allopatric forms. Populations including phenotypes *3Jb*, *3Tb* and *3Ub* are distinguished from those including phenotypes *3Ja*, *3Ta* and *3Ub* by having a subsutural, minutely incised band and a weak to strong spiral ridge along the umbilical wall margin.

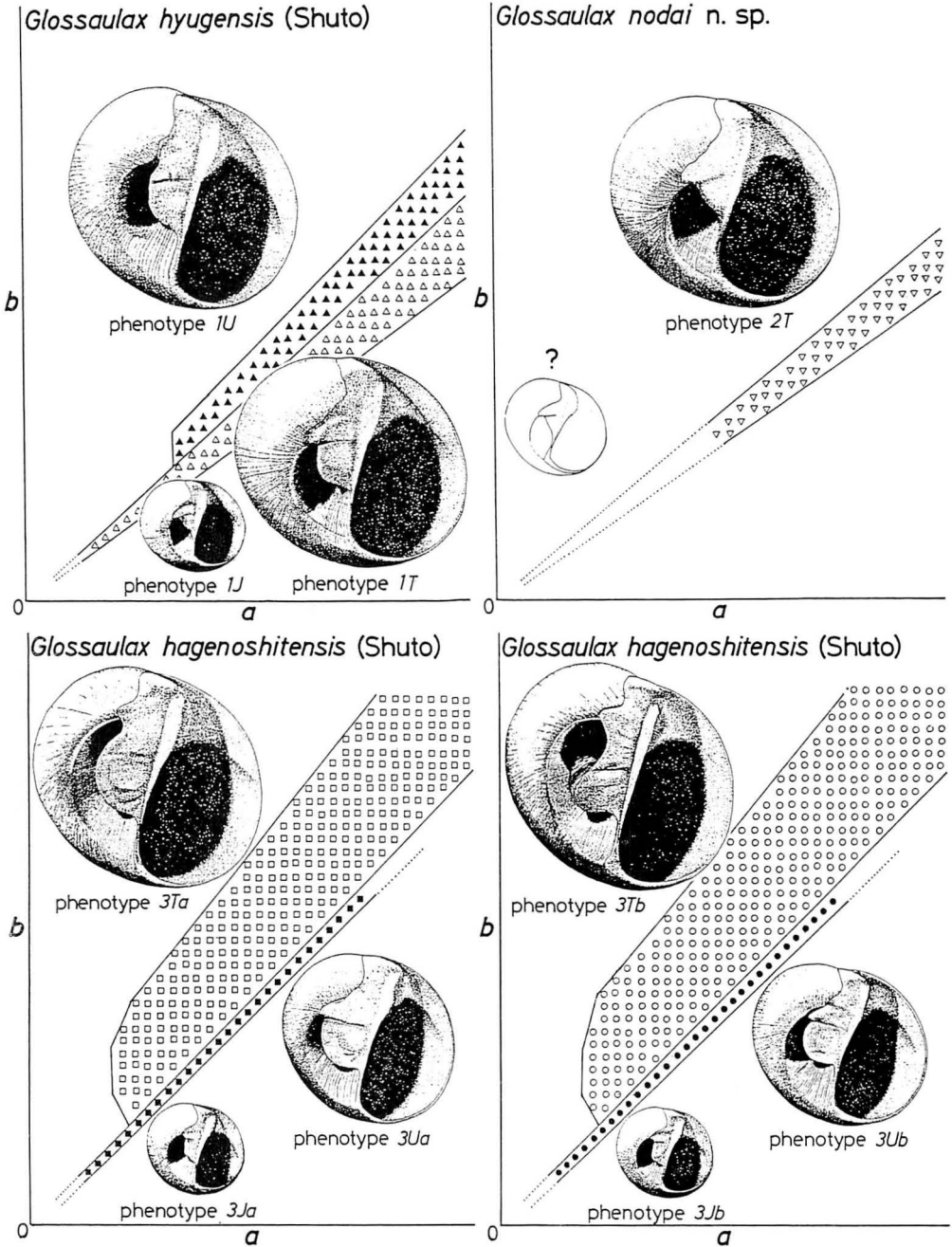
Phenotypes *3Ta* (Pl. 17, Figs. Ma–c, Pl. 18, Figs. Pa–b, Pl. 19, Figs. Aa–Fc) and *3Tb* (Pl. 18, Figs. Qa–c, Pl. 19, Figs. Ga–Mc) are typical adult forms. They are characterized by having a prominent anterior lobe of parietal callus and a semicircular to tongue-like umbilical callus. In some specimens, the anterior lobe of parietal callus is indistinct (Pl. 18, Figs. Pa–b). The umbilical callus usually protrudes more than the parietal callus ($a < b$); the former callus is separated from the latter by a narrowly to broadly rounded sulcus. There is a shallow transverse groove on the umbilical callus at its posterior portion but the groove disappears in some specimens. Phenotypes *3Ta–b* (*3Ta* + *3Tb*) are similar to the phenotype *1U* of *G. hyugensis* but differ slightly from the latter by having a stronger funicle and a rather deep sulcus.

Phenotypes *3Ua* (Pl. 17, Figs. Ha–Ic) and

3Ub (Pl. 17, Figs. Ja–Kc) are unusual adult forms. They are characterized by having a wedge-shaped anterior lobe of parietal callus and a prominently swollen subquadrate umbilical callus. The degree of protrusion of the parietal callus is almost the same as that of the umbilical callus ($a = b$). Phenotypes *3Ja* and *3Jb* gradually change with growth into phenotypes *3Ua* and *3Ub*, respectively. There are a few intermediate forms between phenotypes *3Ta* and *3Ua* (Pl. 17, Figs. Ga–c: the holotype of *G. hagenoshitensis*), and also between *3Tb* and *3Ub*. In the scatter diagrams of a and b , the intermediate forms between phenotypes *3Tb* and *3Ub* do not always occupy their intermediate place (Loc. K-1 in Text-fig. 4). The shape of the callosity of phenotypes *3Ua–b* (*3Ua* + *3Ub*) is very similar to that of phenotype *1T* of *G. hyugensis*, but the umbilical callus of the former phenotypes is relatively larger than the latter. The umbilical opening of phenotypes *3Ua–b* is, therefore, more slender than in the phenotype *1T* of *G. hyugensis*.

Discussion on intraspecific variations of the three *Glossaulax* species

From the analysis of variations of the callus morphologies of the three *Glossaulax* species, their intraspecific variations have been reconstructed and summarized (Text-fig. 9). *G. hyugensis* and *G. hagenoshitensis* show “dimorphic” variations in their adult stages, which are morphologically very similar to each other, but *G. nodai* does not show such variation. The following discussions are based upon two assumptions that (1) the mortality rates of the three species did not extremely differ among the growth stages, and that (2) the fossil population from each locality did not undergo selective post-mortem transportation. The rarity of the juvenile form observed in Loc. M-2 (Text-fig. 3), Locs. K-1 and K-2 (Text-fig. 4), and Locs. K-17 and K-8 (Text-fig. 5), is due to that some or many juvenile forms are artificially damaged during the collection at some localities where fragile specimens occur, and to that juvenile form may be overlooked at some localities



Text-fig. 9. Summary of ontogenetic variations of the umbilical parts of *Glossaulax hyugensis* (Shuto), *G. nodai*, n. sp., and two allopatric forms of *G. hagenoshitensis* (Shuto). Phenotype symbols are the same as in Text-figs. 3, 4, 5 and 6. The variation range of *a* and *b* of each phenotype is approximately illustrated, and the number of each symbol does not mean the frequency.

where the species is rare.

Intraspecific variation of the callus morphology within the three Glossaulax species also plays important roles in specific differentiation.—The phenotypes 1J, 1T and 1U of *G. hyugensis* correspond ontogenetically with the phenotypes 3Ja–b, 3Ua–b and 3Ta–b of *G. hagenoshitensis*, respectively. In the adult “dimorphic” variations of the two species, frequency of the phenotype 1T (1U) of *G. hyugensis* is much greater (smaller) than that of its corresponding phenotypes 3Ua–b (3Ta–b) of *G. hagenoshitensis* (Text-figs. 3, 4, 5 and 6). The two species are easily distinguished from each other by the difference of the frequency between ontogenetically corresponding adult phenotypes.

G. nodai resembles phenotypes 1J and 1T of *G. hyugensis*, and also phenotypes 3Ja–b and 3Ua–b of *G. hagenoshitensis*. However, intraspecific variation within *G. nodai* shows only one form throughout growth, which is quite distinct from the adult “dimorphic” variations of both *G. hyugensis* and *G. hagenoshitensis*.

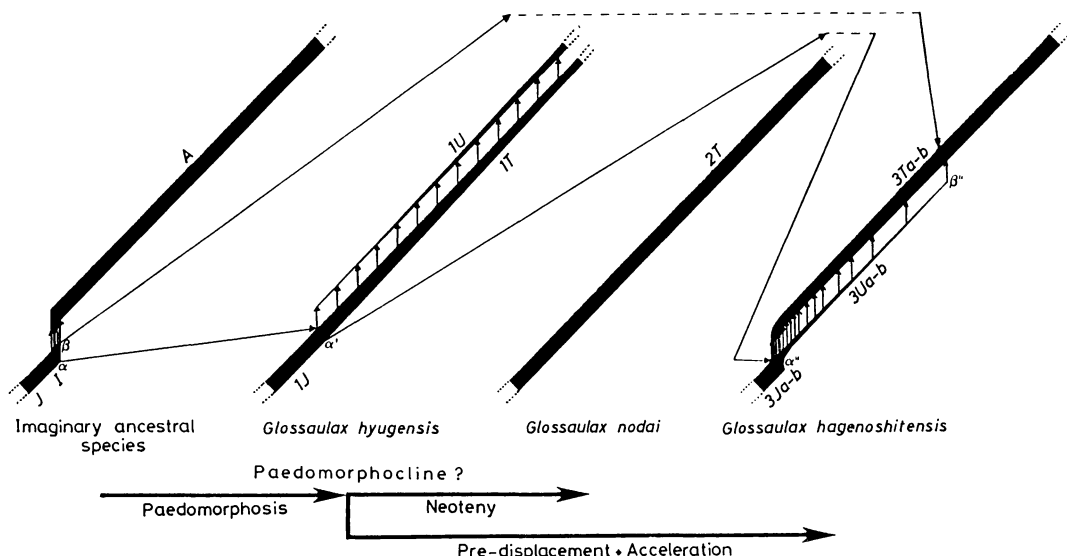
The two allopatric forms of *G. hagenoshitensis*, which are divisible by the sculpture of subsutural area and umbilical wall margin (Text-fig. 8), show analogous variations in the shapes of parietal and umbilical calluses (Text-fig. 9). I consider the two allopatric forms of *G. hagenoshitensis* to be environmentally controlled, and to be interpopulational variation within a single species, regarding their corresponding parietal and umbilical callus variations as a species character.

The “dimorphic” variations represented by the adult phenotypes 1T and 1U of G. hyugensis, and 3Ta–b and 3Ua–b of G. hagenoshitensis are not expressions of sexual dimorphism.—If the growth points, which show the first appearances of the unusual adult form (phenotype 1U) of *G. hyugensis* and the typical adult form (phenotypes 3Ta–b) of *G. hagenoshitensis* in their growth series (Text-figs. 3, 4 and 9), were interpreted as representing the stages of sexual maturity, their “dimorphic” variations might represent sexual dimorphism. However, I do not

consider the “dimorphic” variations of the two species to be sexually controlled. The frequency of the phenotype 1T (1U) to all adult shells of *G. hyugensis* is much greater (smaller) than that of its ontogenetically corresponding phenotypes 3Ua–b (3Ta–b) to all adult shells of *G. hagenoshitensis* at some localities where they occur abundantly (Text-figs. 3 and 4). If the “dimorphic” variations of the two species were regarded as sexual, ontogenetically corresponding phenotypes (1T and 3Ua–b; 1U and 3Ta–b) would represent the same sex, and one could hardly explain the fact that the frequency of the corresponding phenotypes of the two species are extremely different, and that phenotypes 3Ua–b lack the specimens comparable in size with the larger specimens of phenotype 1T (Tables 2 and 4). The different frequency is not environmentally controlled because the two species sympatrically occur at Locs. M-1, M-2, M-3, T-1 and K-9 (Text-figs. 3 and 6; Table 1).

Comparable morphologies between juvenile and adult forms among the three Glossaulax species are interpreted as heterochrony.—A heterochronic model is proposed to explain why *G. nodai* does not show such “dimorphic” variation as *G. hyugensis* and *G. hagenoshitensis* show, why ontogenetically corresponding adult phenotypes between *G. hyugensis* and *G. hagenoshitensis* possess extremely different frequency, and why the adult phenotypes 3Ua–b of *G. hagenoshitensis* lack the specimens comparable in size with the larger specimens of phenotypes 3Ta–b. The term “phenotype” in the following lines are used in the same sense as growth stage as noted in the chapter of introduction.

In this model, an imaginary ancestral species of the three *Glossaulax* species is presumed (Text-fig. 10). All individuals of this imaginary ancestral species pass through the three different growth stages represented by three phenotypes, J (juvenile), I (intermediate) and A (adult) in growth order. In the shapes of parietal and umbilical calluses, phenotypes J, I and A correspond, respectively, with phenotypes 1J (*G. hyugensis*) and 2T (*G. nodai*), phenotypes 1T (*G. hyugensis*) and 3Ja–b (*G. hagenoshitensis*),



Text-fig. 10. A model of ontogenetic development and heterochrony of *Glossaulax hyugensis* (Shuto), *G. nodai*, n. sp., and *G. hagenoshitensis* (Shuto). Mode of the ontogenetic development of each species, which is given by the black column(s), is illustrated as comparable with the individual distribution of each phenotype plotted in the scatter diagrams of *a* and *b* (Text-figs. 3, 4, 5 and 6). The width of each column illustrates the frequency of each phenotype. In this model, an imaginary ancestral species of the three *Glossaulax* species is presumed, and all its individuals pass through the three growth stages which are morphologically represented by phenotypes, *J*, *I* and *A* in growth order. Phenotypes *J*, *I* and *A* morphologically correspond, respectively, with phenotypes *1J* and *2T*, phenotypes *1T* and *3Ja-b*, and phenotypes *1U* and *3Ta-b*. The timing of the onset of the development from phenotype *I* to phenotype *A* slightly varies with the individual, in which the two critical growth stages α and β are recognized and defined, respectively, as the stages where the smallest and largest individuals of phenotype *I* begin their development toward phenotype *A*. The short vertical arrows between the two columns exhibit the development, from phenotype *I* to phenotype *A*, of the individuals. The critical growth stage α' of *G. hyugensis*, and α'' and β'' of *G. hagenoshitensis* are literally corresponding with the critical growth stages α and β of the imaginary ancestral species as given by the oblique or horizontal arrows. The mode of the ontogenetic development of *G. hyugensis*, *G. nodai* and *G. hagenoshitensis* can be explained by heterochronic evolution from this imaginary ancestral species.

and phenotypes *1U* (*G. hyugensis*) and *3Ta-b* (*G. hagenoshitensis*). Phenotype *J* gradually changes into phenotype *I* with growth but phenotype *I* relatively rapidly changes into phenotype *A*. The timing of the onset of the development from phenotype *I* to phenotype *A* slightly varies with the individual, in which two critical growth stages are recognized: one (stage α) is defined as the stage for the smallest individual to begin its development from *I* to *A*, and the other (stage β) is the stage for the

largest one.

In Text-fig. 10, the mode of the growth of the imaginary ancestral species is given by two black columns. Phenotypes *J* and *I* are represented by one short column but phenotype *A* has the other long column. Individuals of each phenotype grow from base to top of each column. Short vertical arrows between the two columns exhibit the rapid development from phenotype *I* to phenotype *A* in individuals. The width of the column illustrates the fre-

quency of each phenotype. The critical growth stages α and β therefore coincide, respectively, with the right and left corners of the top of the column of phenotypes *J* and *I*. The equivalent explanations apply to the columns of *G. hyugensis*, *G. nodai* and *G. hagenoshitensis* (Text-fig. 10). The columns in Text-fig. 10 are illustrated as comparable with the individual distribution of each phenotype plotted in the scatter diagrams of *a* and *b* (Text-figs. 3, 4, 5 and 6).

Among the three *Glossaulax* species which overlap stratigraphically and geographically, *G. hyugensis* occurs in the oldest strata. Shuto (1964) recorded *G. hyugensis* from the first fossil horizon (late Miocene) of the Miyazaki Group. *G. nodai* and *G. hagenoshitensis*, on the other hand, first appeared in late Pliocene strata (Table 1).

Glossaulax hyugensis is thought to have evolved from the imaginary ancestral species by paedomorphosis. Paedomorphosis is the morphological expression which is observed in phylogeny as the retention of ancestral juvenile characters by later ontogenetic stages of descendants (Gould, 1977). Ontogenetically corresponding critical growth stage between the imaginary ancestral species and *G. hyugensis* is given by an arrow ($\alpha \rightarrow \alpha'$) in Text-fig. 10. The adult stage of *G. hyugensis* does not largely reach the critical growth stage β of the imaginary ancestral species, and many specimens of phenotype *1T*, as the result of the paedomorphosis, remain without the onset of the development toward phenotype *1U*. This is the reason why *G. hyugensis* possesses larger numbers of phenotype *1T* than phenotype *1U*.

Glossaulax nodai is thought to have evolved from *G. hyugensis* by paedomorphosis. The adult stage of *G. nodai* never reaches the critical growth stage α' (Text-fig. 10) of *G. hyugensis*. In other words, all of phenotype *2T*, as the result of paedomorphosis, remain without the onset of the development toward the "next stage". This is the reason why *G. nodai* does not show such "dimorphic" variation as *G. hyugensis* and *G. hagenoshitensis* show.

Glossaulax hagenoshitensis is thought to have evolved from *G. hyugensis* by peramorphosis. Peramorphosis (Alberch *et al.*, 1979) is the morphological expression which is observed in phylogeny as the repetition of ancestral adult stages in embryonic or juvenile stages of descendants (Gould, 1977). The critical growth stage β'' (Text-fig. 10), which is shown by the largest individuals of phenotypes *3Ua-b* of *G. hagenoshitensis*, ontogenetically corresponds with the critical growth stage β of the imaginary ancestral species ($\beta \rightarrow \beta''$ in Text-fig. 10). In other words, all the individuals of phenotypes *3Ua-b*, as the result of peramorphosis, have already begun their development toward phenotypes *3Ta-b* until the critical growth stage β'' . This is the reason why *G. hagenoshitensis* possesses larger numbers of phenotypes *3Ta-b* than *3Ua-b*, and why phenotypes *3Ua-b* lack the specimens comparable in size with the larger specimens of phenotypes *3Ta-b*.

As McNamara (in press) has summarized, the comparison of the rates of the development of characters, and of adult sizes between heterochronic ancestor and descendant play important roles as keys to the identification of heterochronic processes in fossil material.

Glossaulax nodai is considered to have evolved from *G. hyugensis* by neotenic process. Neoteny is a reduced rate of morphological development during the juvenile phase, which results in a morphologically retarded adult (McNamara in press). The adult of paedomorph *G. nodai* (attaining 50.0 mm in height, Table 3) is larger in size than that of apaedomorph *G. hyugensis* (attaining 36.3 mm in height, Table 2). In neotenic process, the descendant adult is often larger in size than the ancestral adult due to delayed onset of sexual maturity.

Glossaulax hagenoshitensis is considered to have evolved from *G. hyugensis* by the combination of pre-displacement and acceleration. The peramorph *G. hagenoshitensis* begins its "post-larval" ontogeny with subquadrate umbilical callus (phenotypes *3Ja-b*) which morphologically corresponds with that of the adult phenotype *1T* of aparamorph *G. hyugensis*. This process

is interpreted to be pre-displacement (Alberch *et al.*, 1979), which is the initiation of development of one or a number of organs or structures of the descendants at a relatively earlier stage of development of the whole organism, with respect to the ancestor (McNamara in press). Relatively larger umbilical callus of phenotypes *3Ua-b* of peramorph *G. hagenoshitensis* reasonably supports this interpretation. On the other hand, the majority of individuals of phenotypes *3Ja-b* and *3Ua-b* of *G. hagenoshitensis* begin their morphological development toward phenotypes *3Ta-b* at a smaller size. This is inferred from the individual distribution of *G. hagenoshitensis* plotted in the scatter diagrams of *a* and *b* (Text-figs. 3 and 4): that is, the population of *G. hagenoshitensis* already possessed relatively larger numbers of phenotypes *3Ta-b* than *3Ua-b* at the stage where phenotypes *3Ta-b* first appeared in the growth series. This fact may be explained by the acceleration of the rate of development in the early ontogenetic stage of *G. hagenoshitensis*. Acceleration is an increase in the rate of morphological development during ontogeny (McNamara in press). Alberch *et al.* (1979) believed that it is possible for the combination of peramorphic processes to be operating concurrently in a single species.

In the acceleration process, the descendant adult is often smaller in size than the ancestral adult due to acceleration in the onset of sexual maturity. However, it is difficult to compare absolutely the size of *G. hyugensis* with that of *G. hagenoshitensis*. The largest individual of phenotype *3Ta* (attaining 34.5 mm in height, Table 4) is smaller than that of phenotype *1U* (36.3 mm) of *G. hyugensis*, but phenotype *3Tb* (attaining 46.6 mm in height, Table 4) is larger than the latter species. Odhner (1913) and Marincovich (1977) reported the shell size of *Cryptonatica clausa* (Broderip and Sowerby), a common boreal naticid, varies in accordance with different environments. In the acceleration process of the evolution from *G. hyugensis* to *G. hagenoshitensis*, therefore, it is not known whether the onset of sexual maturity is also

accelerated.

If *G. hyugensis* evolved from the imaginary ancestral species by neoteny, the paedomorphic lineage: the imaginary ancestral species → *G. hyugensis* → *G. nodai* (Text-fig. 10) may be interpreted as a paedomorphocline (McNamara, 1982). The evolution of *G. hagenoshitensis*, which is considered to have evolved from *G. hyugensis* by peramorphosis, seems to be inconsistent with the heterochronic clinal model of McNamara (1982), who discussed the difficulty of reverse speciation along a heterochronic cline. However, if the imaginary ancestral species was extinct, there is the possibility that the peramorph *G. hagenoshitensis* did evolve from the paedomorphocline. This is able to have occurred if the niche, which previously had been occupied by the imaginary ancestral species, became empty. There was thus no effective block (competitive exclusion) to reverse speciation.

As is well known, naticids prey on the infaunal mollusks, especially bivalves. If the three *Glossaulax* species prey on different mollusks inhabiting different substratum depth, the environmental gradient along which the paedomorphocline and one peramorphosis (Text-fig. 10) have developed, may be considered to be difference in depth of their preys. This interpretation may allow the apparently sympatric occurrences in the heterochrony among the three *Glossaulax* species: that is, paedomorph *G. nodai* and peramorph *G. hagenoshitensis* occur together at Locs. K-13, K-17 and N-1, and aperamorph *G. hyugensis* and peramorph *G. hagenoshitensis* occur together at Locs. M-1, M-2, M-3, T-1 and K-9 (Table 1).

Systematic paleontology

Family NATICIDAE Forbes, 1838

Subfamily POLINICINAE Finlay and Marwick, 1937

Genus *Glossaulax* Pilsbry, 1929

Type species.—*Natica reclusiana* Deshayes, 1839, by original designation.

Glossaulax hyugensis (Shuto, 1964)

Pl. 17, Figs. Aa—Bb, Pl. 18, Figs. Aa—Kb.

Polinices (*Glossaulax*) *hyugensis* Shuto, 1964, p. 282—284, pl. 42, figs. 3, 5, 13, 15, pl. 43, figs. 9, 10, 12, text-figs. 1, 2.

Not *Polinices* cfr. *hyugensis* Shuto: Suehiro, 1979, p. 89, pl. 16, figs. 2a—b [= *Glossaulax didyma coticazae* (Makiyama, 1926)].

Polinices (*Glossaulax*) aff. *reiniana* (Dunker): Shuto, 1964, p. 285—286, pl. 42, fig. 1, text-fig. 3 [not *P. (G.) reiniana* (Dunker, 1877)].

Holotype.—GK. L8009 (Pl. 18, Figs. Aa—b), from the fourth fossil horizon of Shuto (1961), the late Pliocene to early Pleistocene Takanabe Member of the Koyu Formation (Loc. M-1).

Revised diagnosis.—Medium-sized and globose to weakly elongate shell characterized by a spiral angulation dividing the base and the umbilical wall, almost flat umbilical wall, weak funicle, and by showing three forms of callosity (Text-fig. 9).

Juvenile form (phenotype *1J*: Pl. 17, Figs. Aa—Bb): Anterior lobe of parietal callus wedge-shaped and covering posterior margin of umbilicus; umbilical callus subtrigonal and attached to parietal callus with a shallow groove.

Typical adult form (phenotype *1T*: Pl. 18, Figs. Aa—Eb): Shape of anterior lobe of parietal callus almost identical with juvenile form but umbilical callus subquadrate.

Unusual adult form (phenotype *1U*: Pl. 18, Figs. Fa—Jb): Anterior lobe of parietal callus very weak to nearly lacking; umbilical callus subquadrate to semicircular with a weak to indistinct transverse groove at its central to posterior portion.

Description.—Shell moderate in size and in thickness, globose to weakly elongate in form; body whorl greatly inflated; shoulder slightly concave; nuclear whorls 1-1/2, smooth, separated from the first conch whorl by a weak groove; postnuclear whorls 2-1/2 in holotype, almost occupied by body whorl. Spiral sculpture of microscopic, closely spaced, minutely wavy costellae, and of very weak subsutural ridge

which is most distinct in early conch whorls and starts from the second one; axial sculpture of incremental growth lines that are most distinct at base. Parietal callus moderately thick, moderately filling posterior apertural angle; anterior lobe very strong, wedge-shaped (phenotypes *1J* and *1T*), or weak to nearly lacking (phenotype *1U*). Umbilicus broadly and deeply open, horn-like form, deeply excavating anterior inner lip of aperture; umbilical callus subtrigonal (phenotype *1J*) to subquadrate (phenotype *1T*), or subquadrate to semicircular (phenotype *1U*); funicle weak. Umbilical wall almost smooth except for incremental growth lines and reliable number of spiral striae, separated from the base by an acute (phenotype *1J*) to subacute (phenotypes *1T* and *1U*) angulation. Posterior inner margin of aperture distinctly angulate but weakly rounded in juvenile specimens (phenotype *1J*); anterior inner lip and outer lip thin except for gradually thickening anteriorly; basal lip weakly thickened.

Remarks.—The measurements of the largest specimen of *G. hyugensis* from each locality are given in Table 2.

Glossaulax didyma didyma (Röding), common in Japanese Pliocene to Recent warm to cold waters, is similar to the unusual adult form (phenotype *1U*) of *G. hyugensis*, but the former species differs from the latter in having a rounded base and an umbilical wall sculptured with a very shallow but wide spiral depression around the funicle. Additionally, *G. didyma didyma* has a variant which has been called *G. hosoyai* (Kira) by Japanese malacologists. The “*G. hosoyai*”-type individual of *G. didyma didyma* is characterized by having a very stout shell and an umbilicus almost closed by a heavy and large umbilical callus, similar to what some previous workers have recognized as a form of *G. reclusiana* (Deshayes) (*G. reclusiana imperforata* (Dall): see pl. 29, fig. 7 of Marinovich, 1977). Therefore, the two species are also distinguished from each other by their ranges of variations.

Glossaulax reiniana (Dunker) (Pl. 17, Figs. Oa—b), common in the Japanese late Pliocene to

Table 2. Measurements (in mm) of the largest specimens of phenotypes 1T and 1U of *Glossaulax hyugensis* (Shuto) at each locality. Abbreviations are shown in Text-fig. 2 except for N. W. (Number of whorls).

Phenotype 1T					
Loc.	W.	L.P.W.	H.	N.W.	Specimen
M-1	39.8	30.3	32.6+	5+	IGUT no. 15699-40
M-2	23.3+	18.4	20.7	4.5+	IGUT no. 15701-20
M-3	15.6+	14.4	ca.15.5	4.5	GIYU no. 571-1
T-1	25.6	20.8	20.7+	4.5+	IGUT no. 15691-2
T-2	33.5+	29.1	32.2+	5+	IGUT no. 15693-1
K-9	24.5+	22.0	20.5	4.5+	IGUT no. 15716-2

Phenotype 1U					
Loc.	W.	L.P.W.	H.	N.W.	Specimen
M-1	30.5+	25.8	30.1	3.5+	IGUT no. 15699-48
M-2	ca.38.7	32.2	36.3	4.5+	IGUT no. 15701-28
T-1	17.0+	15.2	16.1	2.5+	IGUT no. 15691-6
T-2	33.9+	30.4	33.0	5.5	IGUT no. 15694-26
K-9	ca.33.8	26.8	22.6+	2.5+	IGUT no. 15716-3*

*Slightly deformed

Table 3. Measurements (in mm) of the largest specimen of phenotype 2T of *Glossaulax nodai*, n. sp. at each locality. Abbreviations are shown in Text-fig. 2 except for N. W. (Number of whorls).

Phenotype 2T					
Loc.	W.	L.P.W.	H.	N.W.	Specimen
M-5	49.9	41.4	50.0	4.5+	IGUT no. 15698**
K-13	40.9	32.3	36.4	6	IGUT no. 15695*
K-17	28.2+	27.3	27.3+	5.5	IGUT no. 15697-5**
N-1	20.5+	22.4	23.6+	4+	GIYU no. 563**

*Holotype **Paratype

Table 4. Measurements (in mm) of the largest specimens of phenotypes 3Ta, 3Ua, 3Tb and 3Ub of *Glossaulax hagenoshitensis* (Shuto) at each locality. Abbreviations are shown in Text-fig. 2 except for N. W. (Number of whorls).

Phenotype 3Ta					
Loc.	W.	L.P.W.	H.	N.W.	Specimen
M-1	29.8	24.8	29.0	4.5+	IGUT no. 15700-43
M-2	17.4+	17.3	18.3	4.5	IGUT no. 15702-13
M-3	29.6	23.3	24.5	4.5+	GIYU no. 571-7
T-1	25.5	20.0	22.8+	5+	IGUT no. 15690-1
T-3	17.9	13.9	15.1	5	IGUT no. 15692
K-8	37.4	33.0	34.5	5+	IGUT no. 15714-14
K-9	28.3+	26.2	ca.28.6	4.5+	IGUT no. 15715-2
K-12	ca.31.5	27.2	ca.29.7	4.5+	IGUT no. 15712-8

Phenotype 3Ua					
Loc.	W.	L.P.W.	H.	N.W.	Specimen
M-1	17.3+	12.9	15.5	4.5+	IGUT no. 15700-21
M-2	19.8	15.0	16.2	3.5+	IGUT no. 15702-10
K-12	12.8	10.3	11.2	4+	IGUT no. 15712-3

Phenotype 3Tb					
Loc.	W.	L.P.W.	H.	N.W.	Specimen
M-4	28.0	23.6	19.6+	4+	GK. L7987
K-3	29.6+	27.0	27.3+	5+	IGUT no. 15717-17
K-1	40.1	31.1	35.2	5+	IGUT no. 15703-122
K-2	45.5	38.3	46.6	4+	IGUT no. 15704-47
K-10	44.0	37.8	42.7	4.5+	IGUT no. 15705-116
K-11	38.1+	33.3	32.0	4.5+	IGUT no. 15707-1
K-13	36.9	32.3	34.5	5+	IGUT no. 15713-3
K-14	32.3+	28.8	22.8+	4.5+	IGUT no. 15709-5
K-15	24.2+	24.9	22.2	4.5+	IGUT no. 15710-5
K-16	30.2+	25.3	25.2+	4.5+	IGUT no. 15711-14
K-17	35.8+	31.7	36.1	4+	IGUT no. 15706-48
N-1	30.3+	24.5	ca.27.0	3.5+	GIYU no. 567-3
O-1	28.7	23.5	28.5	3.5+	IGUT no. 15688-1
O-2	15.6+	13.4	11.7+	5	IGUT no. 15718-2
O-3	16.7	13.3	14.1	5	IGUT no. 15689

Phenotype 3Ub					
Loc.	W.	L.P.W.	H.	N.W.	Specimen
K-1	22.0	16.0	16.3	4+	IGUT no. 15703-59
K-2	18.0	13.5	13.5	4.5+	IGUT no. 15704-13
K-10	23.1	18.4	18.1	4.5+	IGUT no. 15705-56
K-11	14.7+	12.9	11.9	4+	IGUT no. 15707-5
N-1	17.6+	15.3	17.0	4.5	GIYU no. 567-2

Recent warm waters, is similar to the juvenile (phenotype *IJ*) and typical adult (phenotype *IT*) forms of *G. hyugensis*, but the former species is distinguished from the latter in having an umbilical wall sculptured with a deep spiral groove around the funicle.

Glossaulax nodai, n. sp.

Pl. 18, Figs. La—Ob.

Holotype.—IGUT no. 15695 (Pl. 18, Figs. La—b), from the late Pliocene Dainichi Member of the Lower Kakegawa Formation (Loc. K-13).

Paratypes.—IGUT no. 15698 (Pl. 18, Figs. Ma—b), from the sixth fossil horizon of Shuto (1961), the late Pliocene to early Pleistocene Takanabe Member of the Koyu Formation (Loc. M-5); IGUT nos. 15696-1—2, from the same locality as the holotype (Loc. K-13); IGUT nos. 15697-1—6 (Pl. 18, Figs. Na—b), from the same member as the holotype (Loc. K-17); GIYU nos. 562, 563 (Pl. 18, Figs. Oa—b) and 564, from the early Pleistocene Nojima Formation (Loc. N-1).

Etymology.—This species is named for Professor Hiroshi Noda of Institute of Geoscience, University of Tsukuba, who introduced the present writer to the paleontology of the Naticidae.

Diagnosis.—Medium-sized and globose shell characterized by a spiral angulation dividing the base and the umbilical wall, almost flat umbilical wall, weak funicle and by one form of callosity (Text-fig. 9). Anterior lobe of parietal callus wedge-shaped, developing along posterior margin of umbilicus; umbilical callus subtriangular and attached to parietal one with a weak to indistinct groove.

Description.—Shell moderate in size and in thickness, globose in form; body whorl greatly inflated; shoulder slightly concave; nuclear whorls 2-1/2, smooth, separated from the first conch whorl by a weak groove; postnuclear whorls 3 in holotype, almost occupied by body whorl; suture moderately impressed. Spiral sculpture of microscopic, closely spaced, minutely wavy costellae, and of very weak ridge at subsutural part which starts from the second

conch whorl and changes into two or three weak costellae in later whorls of larger specimens; axial sculpture of incremental, prosoclinal growth lines that are most distinct at base. Parietal callus moderately thick, moderately filling posterior apertural angle; anterior lobe very strong, wedge-shaped. Umbilicus broadly and deeply open, horn-like form, and deeply excavates anterior inner lip of aperture; umbilical callus weakly developed, subtrigonal in form; funicle weak to indistinct; umbilical wall almost smooth except for incremental growth lines and many spiral striae, separated from the base by a subacute angulation. Posterior inner margin of aperture weakly rounded; anterior inner lip and outer lip thin except for gradually thickening anteriorly; basal lip weakly thickened.

Remarks.—The measurements of the largest specimen of *G. nodai* from each locality are given in Table 3. There are no species comparable with *G. nodai* except for *G. hyugensis* and *G. hagenoshitensis*. *G. nodai* is easily distinguished from *G. hyugensis* and *G. hagenoshitensis* by the range of morphological variation (Text-fig. 9).

Glossaulax hagenoshitensis (Shuto, 1964)

Pl. 17, Figs. Ca—Kc, Ma—c,

Pl. 18, Figs. Pa—Qc, Pl. 19, Figs. Aa—Mc.

Polinices (*Neverita*) *sagamiensis* Pilsbry: Shuto, 1964, p. 281—282 [in part], pl. 42, fig. 2 [not *P. (N.) sagamiensis* Pilsbry, 1904; not pl. 42, figs. 8 and 14, showing imperfect specimens].

Polinices sagamiensis Pilsbry: Itoigawa and Shibata in Morishita, 1977, pl. 30, fig. 18 [not *P. sagamiensis* Pilsbry, 1904].

Polinices (*Glossaulax*) *hagenoshitensis* Shuto, 1964, p. 284—285, pl. 42, fig. 10, text-fig. 1.

Neverita (*Glossaulax*) *reiniana* (Dunker): Kaseno and Matsuura, 1965, pl. 2, figs. 32, 33 [not *N. (G.) reiniana* (Dunker, 1877)].

Holotype.—GK. L8003 (Pl. 17, Figs. Ga—c), from the fourth fossil horizon of Shuto (1961), the late Pliocene to early Pleistocene Takanabe Member of the Koyu Formation (Loc. M-1).

Revised diagnosis.—Medium-sized and globose to globose elongate shell characterized by a spiral angulation dividing the base and the umbilical wall, strong funicle, and by showing two allopatric (Text-fig. 8) and three sympatric (Text-fig. 9) forms. Two allopatric forms: One form possesses a very weakly developed subsutural spiral ridge which is most distinct in early conch whorls, and a flat umbilical wall (phenotypes 3Ja, 3Ta and 3Ua); the other form has a subsutural, minutely incised band and a strong to weak spiral ridge along the outer margin of the umbilical wall (phenotypes 3Jb, 3Tb and 3Ub) (Text-fig. 8). Three sympatric forms, characterized by shapes of parietal and umbilical calluses, are as follows:

Juvenile form (phenotypes 3Ja–b: Pl. 17, Figs. Ca–Fb): Anterior lobe of parietal callus wedge-shaped and covering posterior margin of umbilicus; umbilical callus subquadrate and attached to parietal callus with a shallow groove.

Typical adult form (phenotypes 3Ta–b: Pl. 17, Figs. Ma–c, Pl. 18, Figs. Pa–Qc, Pl. 19,

Figs. Aa–Mc): Anterior lobe of parietal callus prominent but rarely indistinct; umbilical callus semicircular to tongue-like, separated from parietal callus by a narrowly to broadly rounded sulcus; transverse groove on umbilical callus weak to indistinct, situated posteriorly.

Unusual adult form (phenotypes 3Ua–b: Pl. 17, Figs. Ha–Kc): Shape of callosity is nearly identical with that of juvenile form but umbilical callus relatively larger and more swollen.

Description.—Shell relatively large (phenotype 3Tb) or relatively small (phenotype 3Ta) in size, moderate in thickness, globose to globose elongate in form; body whorl greatly inflated with slightly concave to flattened shoulder; nuclear whorls 2-1/2, smooth, separated from the first conch whorl with a weak groove; postnuclear whorls 2-1/2 in holotype; suture moderately impressed. Spiral sculpture of microscopic, closely spaced, minutely wavy costellae, and of subsutural, very weakly developed ridge in early conch whorls (phenotypes 3Ja, 3Ta and 3Ua) or subsutural, minutely incised band

Explanation of Plate 17

Figs. Aa–Bb. Phenotype 1J of *Glossaulax hyugensis* (Shuto): Aa–b, IGUT no. 15699-2, Loc. M-1, $\times 2.2$; Ba–b, IGUT no. 15694-1, Loc. T-2, $\times 2.2$.

Figs. Ca–b. Phenotype 3Ja of *Glossaulax hagenoshitensis* (Shuto): IGUT no. 15700-1, Loc. M-1, $\times 2.1$.

Figs. Da–Fb. Phenotype 3Jb of *Glossaulax hagenoshitensis* (Shuto): Da–b, IGUT no. 15705-1, Loc. K-10, $\times 2.8$; Ea–b, IGUT no. 15705-4, Loc. K-10, $\times 2.5$; Fa–b, IGUT no. 15717-1, Loc. K-3, $\times 2.3$.

The small letters of a and b of A–F indicate, respectively, front and basal views of specimen.

Figs. Ga–c. Intermediate form between phenotypes 3Ta and 3Ua of *Glossaulax hagenoshitensis* (Shuto): holotype, GK. L8003, Loc. M-1, $\times 2.0$.

Figs. Ha–Ic. Phenotype 3Ua of *Glossaulax hagenoshitensis* (Shuto): Ha–c, IGUT no. 15702-10, Loc. M-2, $\times 1.3$; Ia–c, IGUT no. 15712-3, Loc. K-12, $\times 1.9$.

Figs. Ja–Kc. Phenotype 3Ub of *Glossaulax hagenoshitensis* (Shuto): Ja–c, IGUT no. 15703-26, Loc. K-1, $\times 1.6$; Ka–c, IGUT no. 15705-48, Loc. K-10, $\times 1.4$.

The small letters a, b and c of G–K indicate, respectively, apical, front and basal views of specimen.

Figs. La–c. *Neverita incei* (Philippi): IGUT no. 15719-5, Stradbroke Island, Queensland, Australia (Recent), $\times 1.2$.

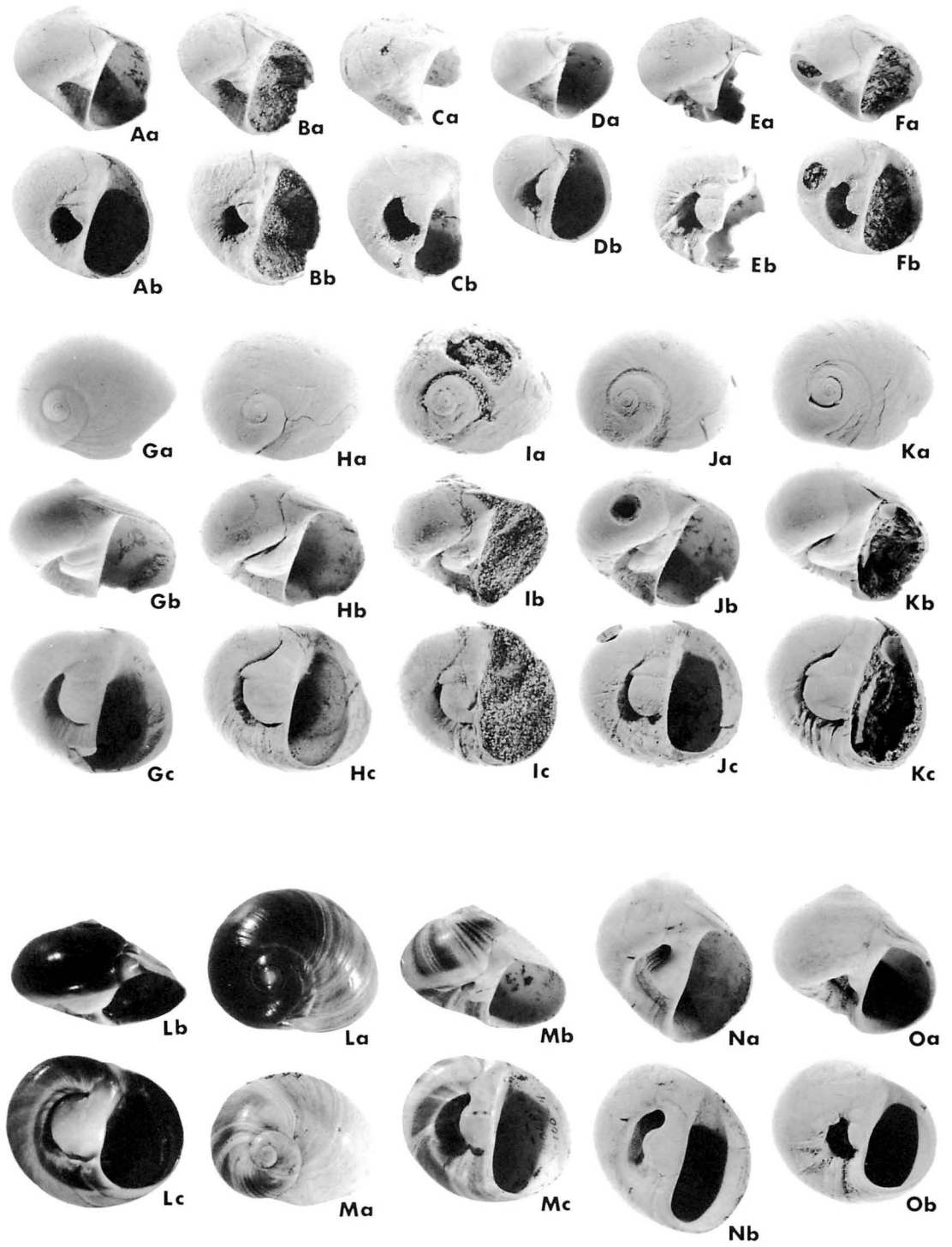
Figs. Ma–c. Phenotype 3Ta of *Glossaulax hagenoshitensis* (Shuto): GIYU no. 568-3, Loc. M-1, $\times 1.1$.

The small letters a, b and c of L–M indicate, respectively, apical, front and basal views of specimen.

Figs. Na–b. *Polinices sagamiensis* Pilsbry: IGUT no. 15721-4, Loc. K-1, $\times 0.6$.

Figs. Oa–b. *Glossaulax reiniana* (Dunker): IGUT no. 15722-13, Loc. O-1, $\times 1.1$.

The small letters a and b of N–O indicate, respectively, front and basal views of specimen.



(phenotypes *3Jb*, *3Tb* and *3Ub*), both of which start from the second conch whorl; axial sculpture of incremental, prosoclinal growth lines that are most distinct at base and below suture. Parietal callus moderately to strongly developed, moderately filling posterior apertural angle; anterior lobe strong but rarely indistinct. Umbilicus broadly (phenotypes *3Ja-b* and *3Ta-b*) to narrowly (phenotypes *3Ua-b*) open, horn-like to U-shaped in form, deeply excavating anterior inner lip of aperture; sulcus indistinct (phenotypes *3Ja-b* and *3Ua-b*) or distinct (phenotypes *3Ta-b*); umbilical callus moderate (phenotypes *3Ja-b* and *3Ta-b*) to large (phenotypes *3Ua-b*) in size, subquadrate (phenotypes *3Ja-b* and *3Ua-b*) or semicircular to tongue-like (phenotypes *3Ta-b*) in form, all forms with strong funicle. Umbilical wall weakly sculptured with incremental growth lines and reliable number of spiral striae, may be with a weak to distinct ridge at its outer margin (phenotypes *3Jb*, *3Tb* and *3Ub*), and sharply separated from the base by an acute angulation. Posterior inner margin of aperture distinctly to moderately angulate; anterior inner lip and outer lip thin except for gradually thickening anteriorly; basal lip weakly (phenotypes *3Ja*, *3Ta* and *3Ua*) or strongly (phenotypes *3Jb*, *3Tb* and *3Ub*) thickened.

Remarks.—The measurements of the largest specimen of *G. hagenoshitensis* from each locality are given in Table 4. A specimen illustrated by Martin (1905) as *Natica ampla* Philippi from the middle Pliocene Sonde bed of Java, Indonesia (pl. 39, fig. 628 in Martin, 1905) seems to be identical to the phenotype *3Ta* or *3Tb* of *G. hagenoshitensis*. Unfortunately it is difficult to be certain of this, based on Martin's single illustration.

Neverita incei (Philippi), a common Australian shallow water species (Cernohorsky, 1972, p. 100, pl. 26, fig. 6; Wilson and Gillett, 1980, p. 38, pl. 18, figs. 4–4b) illustrated in Pl. 17, Figs. La–c, very closely resembles the phenotype *3Tb* of *G. hagenoshitensis* in having a subsutural, weakly incised band, spiral angulation dividing the base and the umbilical wall, and a distinct ridge along the outer margin of an almost flat

umbilical wall, but it differs slightly from the phenotype *3Tb* by being small in size (up to 30 mm in length (Cernohorsky, 1972)), and by having a relatively large umbilical callus sculptured with many weak wrinkles. *N. incei* shows dimorphic variation in its coloration. One colored form is represented by flesh-tone whorls, with white base and white umbilical callus. The other colored form has dark purple whorls, brown base and brown umbilical wall; brown base is separated from purple whorls by a narrow white spiral band; umbilical callus is white with light brown margin (Pl. 17, Figs. La–c). Though the coloration of many specimens of *G. hagenoshitensis* has been lost, a few specimens from the Takanabe Member of the Koyu Formation at Loc. M-1 preserve color (Pl. 17, Figs. Ma–c): namely, the whorls are dark gray but become gradually paler toward the aperture and suture; base and umbilical wall are dark brown, and separated from the dark gray whorls by a light yellowish spiral band; callus is white. The color pattern of the second colored form of *N. incei* (Pl. 17, Figs. La–c) and that of the specimen of *G. hagenoshitensis* from the Takanabe Member (Pl. 17, Figs. Ma–c), therefore, closely resemble each other. *N. incei* seems to be a descendant of *G. hagenoshitensis* but the former species is also similar to *Neverita josephina* (Risso), the type species of *Neverita*, which ranges in age from Oligocene to Recent in Europe (Švagrovský, 1982). To confirm the phylogenetic relation between *G. hagenoshitensis* and *N. incei*, further investigation is necessary.

Glossaulax hagenoshitensis has been taxonomically confused with *Polinices sagamiensis* Pilsbry in the Kakegawa Fauna and with *Glossaulax reiniana* (Dunker) in the Omma-Manganzi Fauna. A specimen illustrated by Shuto (1964) as *Polinices (Neverita) sagamiensis* from the Koyu Formation (pl. 42, fig. 2 in Shuto, 1964: Pl. 19, Figs. Ga–c) is identified with the phenotype *3Tb* of *G. hagenoshitensis*. Phenotype *3Tb* has been also confused with *P. sagamiensis* by Itoigawa and Shibata in Morishita (1977) in the Dainichi Member of the Lower Kakegawa Formation (pl. 30, fig. 18 in Itoigawa and

Shibata in Morishita, 1977). *P. sagamiensis* occurs from the Dainichi Member of the Lower Kakegawa Formation (Pl. 17, Figs. Na–b) and the Ananai Formation, but only in small numbers. *P. sagamiensis* is distinguished from *G. hagenoshitensis* by having a rounded base, smooth umbilical callus and a shallow groove around the funicle (Pl. 17, Figs. Na–b). A specimen illustrated by Kaseno and Matsuura (1965) as *Neverita (Glossaulax) reiniana* from the Omma Formation (pl. 2, figs. 32, 33) is identified with phenotype 3Tb of *G. hagenoshitensis*. Though *G. reiniana* occurs in the Omma Formation (Pl. 17, Figs. Oa–b) in association with *G. hagenoshitensis* at Loc. O-1, it is distinguished from the latter species by having a small umbilical callus and a strong groove around the funicle.

Among the specimens of *G. hagenoshitensis*, a few specimens (Pl. 19, Figs. Ba–c, Ia–c) have been shallowly (Pl. 19, Figs. Ba–c) or deeply (Pl. 19, Figs. Ia–c) bored in the anterior end of umbilical callus. When Wrigley (1949) described the English Eocene and Oligocene Naticidae, he mentioned:

“In several of the species described in this paper a few specimens have been bored by a parasite or commensal. The boring is always in the same place, . . . , at the rear of the

middle plug. This parasite, or whatever it was, knew exactly where to find the thickest part of the shell, and in a place which was conveniently adjacent to excreta. These borings are never bevelled like the usual perforations in molluscan shells Until their true nature is noticed they falsify the appearance of the plug and columellar border.”

The borings of the specimens (Pl. 19, Figs. Ba–c, Ia–c) are considered to be due to a parasite or commensal.

Concluding remarks

The intraspecific variation in the three *Glossaulax* species, *G. hyugensis* (Shuto), *G. nodai*, n. sp., and *G. hagenoshitensis* (Shuto) was studied on the basis of more than 600 individuals collected from 24 localities. *G. hyugensis* and *G. hagenoshitensis* show “dimorphic” variations at the adult stages and their juveniles differ, to varying degrees, from the adults. *G. nodai*, however, has an uniform shell morphologies throughout growth. The mode of the ontogenetic variations of the three species is explained by a model of heterochronic evolution in which an imaginary ancestral species is presumed.

The three important results of the present

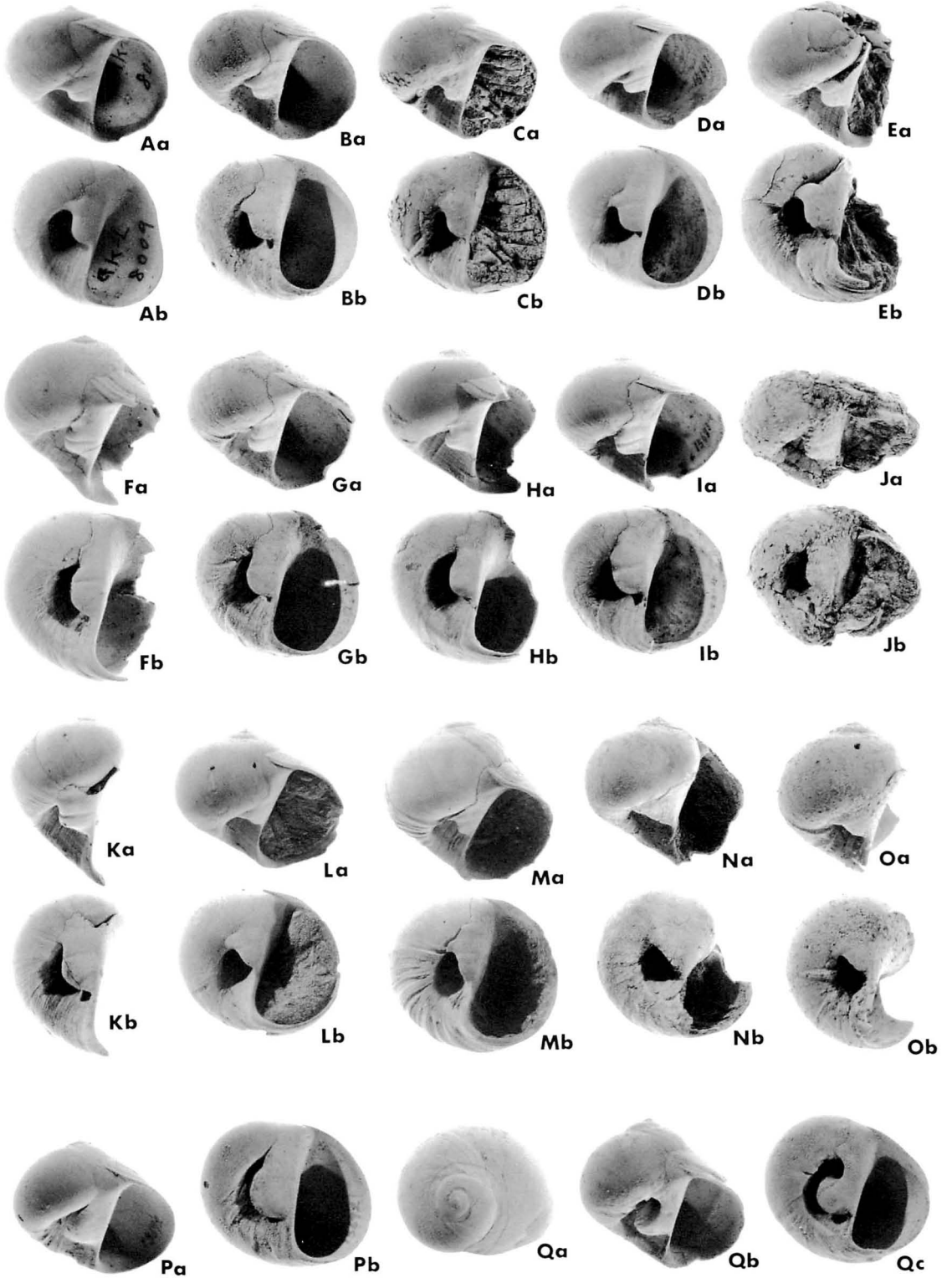
Explanation of Plate 18

- Figs. Aa–Eb. Phenotype 1T of *Glossaulax hyugensis* (Shuto): Aa–b, holotype, GK. L8009, Loc. M-1, $\times 1.3$; Ba–b, IGUT no. 15701-23, Loc. M-2, $\times 1.2$; Ca–b, IGUT no. 15691-7, Loc. T-1, $\times 1.4$; Da–b, IGUT no. 15693-7, Loc. T-2, $\times 1.2$; Ea–b, IGUT no. 15716-1, Loc. K-9, $\times 1.1$.
- Figs. Fa–Jb. Phenotype 1U of *Glossaulax hyugensis* (Shuto): Fa–b, IGUT no. 15699-44, Loc. M-1, $\times 1.1$; Ga–b, IGUT no. 15701-19, Loc. M-2, $\times 1.2$; Ha–b, IGUT no. 15691-6, Loc. T-1, $\times 1.5$; Ia–b, IGUT no. 15693-4, Loc. T-2, $\times 0.9$; Ja–b, IGUT no. 15716-3, Loc. K-9, $\times 0.8$.
- Figs. Ka–b. Intermediate form between phenotypes 1T and 1U of *Glossaulax hyugensis* (Shuto): IGUT no. 15699-40, Loc. M-1, $\times 0.8$.
- Figs. La–Ob. Phenotype 2T of *Glossaulax nodai*, n. sp.: La–b, holotype, IGUT no. 15695, Loc. K-13, $\times 0.6$; Ma–b, paratype, IGUT no. 15698, Loc. M-5, $\times 0.9$; Na–b, paratype, IGUT no. 15697-6, Loc. K-17, $\times 0.9$; Oa–b, paratype, GIYU no. 563, Loc. N-1, $\times 1.0$.
- Figs. Pa–b. Phenotype 3Ta of *Glossaulax hagenoshitensis* (Shuto): IGUT no. 15692, Loc. T-3, $\times 1.4$.

The small letters a and b of A–P indicate, respectively, front and basal views of specimen.

- Figs. Qa–c. Phenotype 3Tb of *Glossaulax hagenoshitensis* (Shuto): IGUT no. 15706-39, Loc. K-17, $\times 1.1$.

The small letters a, b and c of Q indicate, respectively, apical, front and basal views of specimen.



study are briefly summarized as follows:

1. The apparent dimorphic variations of both *G. hyugensis* and *G. hagenoshitensis* are interpreted as different growth stages on the basis of the model of heterochronic evolution (Text-fig. 10). The two adult forms of both species indicate continuous variation but not discontinuous one. There is no essential difference among the individuals of each species except for the continuously different timing of the onset of development toward the next growth stage (phenotypes *1U* and *3Ta-b*).

2. The three species are best characterized by the range of morphological variation including the difference of the frequency of the adult phenotypes of each species. In the morphological variation of the three species (Text-fig. 9), the typologically similar forms are classified into different species (phenotypes *1J* and *2T*; *1T* and *3Ja-b*; *1T* and *3Ua-b*; *1U* and *3Ta-b*) and the typologically different forms into the same species (phenotypes *1T* and *1U*; *1J* and *1U*; *3Ta-b* and *3Ua-b*; *3Ja-b* and *3Ta-b*). The ranges of the morphological variations of the three *Glossaulax* species are confronted with the typological methodology.

3. The three species are one of the most dominant and characteristic molluscan species of the Kakegawa Fauna and some of them have been misidentified with other naticid species.

Acknowledgments

The author wishes to thank Professor Hiroshi Noda (University of Tsukuba), Dr. Louie Marinovich, Jr. (U.S. Geological Survey, Menlo Park, California), Dr. Kenneth J. McNamara (Western Australian Museum), and Dr. Norman F. Sohl (U.S. Geological Survey, Washington, D.C.), who kindly read the manuscript and provided invaluable comments. Thanks are due to Professors Hisayoshi Igo, Naoaki Aoki, and Dr. Fujio Masuda (all of University of Tsukuba) for reading the manuscript and giving valuable advice. This paper has greatly benefited from the criticisms by the scientists mentioned above. Remnant errors of logic and expression are

entirely mine.

I am indebted to Dr. Nelly Hooper Ludbrook (Australia) for giving valuable information of *Neverita incei*, and to Professor Tsugio Shuto (Kyushu University), and Professor Yoshikazu Hasegawa and Mr. Kimihiko Ozaki (both of Yokohama National University) for their permission to observe the specimens preserved in their universities. I am also grateful to Dr. Kazutaka Amano (Joetsu University of Education), Dr. Makoto Ito (University of Tsukuba), Mr. Hirokazu Takahashi (University of Tsukuba Senior High School at Komaba) and Mr. Tomonori Shibata (Arabian Oil Company) for their different kinds of help and suggestion giving during the course of this study.

Finally I wish to thank an anonymous referee for reading the manuscript and offering suggestions for its improvement.

References

- Alberch, P., Gould, S. J., Oster, G. F. and Wake, D. B. (1979): Size and shape in ontogeny and phylogeny. *Paleobiology*, vol. 5, no. 3, p. 296-317.
- Cernohorsky, W. O. (1972): *Marine shells of the Pacific, Volume II*. Pacific Publication, Sydney, 411 p.
- Chinzei, K. (1978): Neogene molluscan faunas in the Japanese Islands: An ecological and zoogeographical synthesis. *Veliger*, vol. 21, no. 2, p. 155-170.
- Gould, S. J. (1977): *Ontogeny and phylogeny*. Harvard University Press, Cambridge, Massachusetts, 501 p.
- Hayami, I. (1973): Discontinuous variation in an evolutionary species, *Cryptopecten vesiculosus*, from Japan. *Jour. Paleont.*, vol. 47, no. 3, p. 401-420.
- Itoigawa, J. and Shibata, H. in Morishita, A. ed. (1977): *Illustrations of the standard fossils of Japan*. Asakura Shoten, Tokyo, 242 p. (in Japanese).
- Kaseno, Y. and Matsuura, N. (1965): Pliocene shells from the Omma Formation around Kanazawa City, Japan. *Sci. Rep., Kanazawa Univ.*, vol. 10, no. 1, p. 27-62, pls. 1-20.
- Katto, J., Nakamura, J. and Takayanagi, Y. (1953): Stratigraphical and paleontological

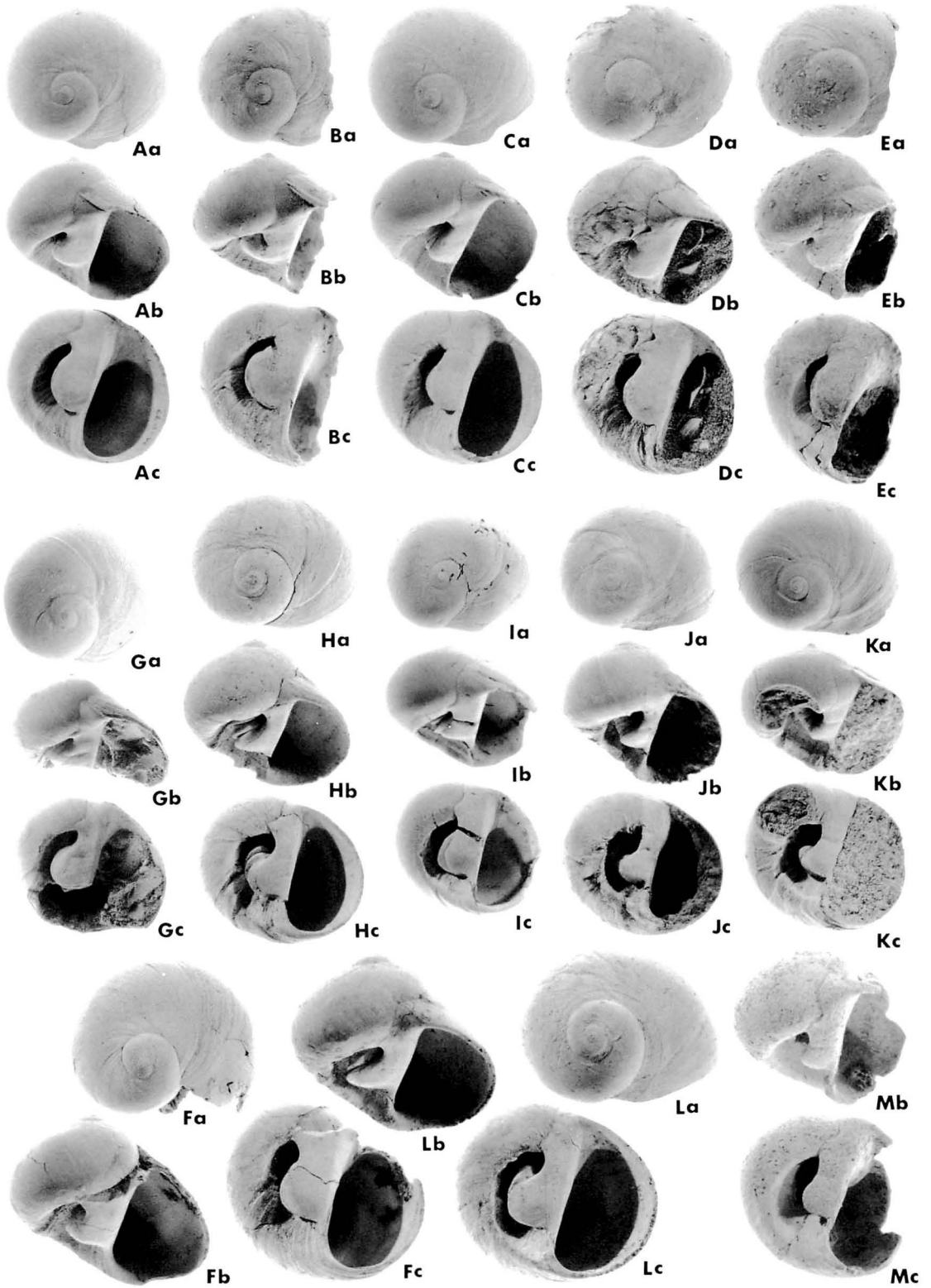
- studies of the Tonohama Group, Kochi Prefecture, Japan. *Res. Rep., Kochi Univ.*, vol. 2, no. 32, p. 1–15 (in Japanese).
- Makiyama, J. (1925): The evolution of *Umboonium*. *Japan. Jour. Geol. Geogr.*, vol. 3, nos. 3–4, p. 118–130, pl. 3.
- (1941): Evolution of the gastropod genus *Siphonalia* with accounts on the Pliocene species of Totomi and other examples. *Mem. Coll. Sci., Kyoto Imp. Univ.*, [B], vol. 16, no. 2, p. 75–93, pls. 1–4.
- and Sakamoto, T. (1957): Explanatory text of the geological map of Japan, 1:50,000, "Mitsuke and Kaketsuka" Sheets. *Geol. Surv. Japan*, 43 p. (in Japanese with English abstract).
- Marincovich, L., Jr. (1977): Cenozoic Naticidae (Mollusca: Gastropoda) of the Northeastern Pacific. *Bull. Am. Paleont.*, vol. 70, no. 294, p. 169–494, pls. 17–42.
- Martin, K. (1905): Die Fossilien von Java. *Samml. Geol. Reichsmus. Leiden*, Mollusken, Heft 8, p. 221–281, pls. 34–41.
- McNamara, K. J. (1982): Heterochrony and phylogenetic trends. *Paleobiology*, vol. 8, no. 2, p. 130–142.
- (in press): A guide to the nomenclature of heterochrony. *Jour. Paleont.*
- Noda, H. (1965): Some fossil *Anadara* from southwest Japan. *Trans. Proc. Palaeont. Soc. Japan, N.S.*, no. 59, p. 92–109, pls. 10–11.
- Odhner, N. H. (1913): Northern and Arctic invertebrates in the collection of the Swedish State Museum. VI. Prosobranchia. 2. *K. Svenska Vetenskapsakad., Handl.*, vol. 50, no. 5, p. 1–89, pls. 1–5.
- Ogasawara, K. (1981): Paleogeographic significance of the Omma-Manganzian fauna of the Japan Sea Borderland. *Saito Ho-on Kai Mus., Res. Bull.*, no. 49, p. 1–17, pls. 1–2.
- Otuka, Y. (1939): Tertiary crustal deformation in Japan (with short remarks on Tertiary palaeontology). *Jubilee Pub. Commen. Prof. H. Yabe's 60th Birthday*, p. 481–519.
- Shikama, T. and Masujima, A. (1969): Quantitative studies of the molluscan assemblages in the Ikego-Nojima Formation. *Sci. Rep., Yokohama National Univ.*, [2], no. 15, p. 61–94, pls. 5–7.
- Shuto, T. (1957): Fossil *Paphia* from the Miyazaki Group (Palaeontological study of the Miyazaki Group-III). *Japan. Jour. Geol. Geogr.*, vol. 29, nos. 1–3, p. 139–160, pl. 12.
- (1961): Palaeontological study of the Miyazaki Group — a general account of the fauna. *Mem. Fac. Sci., Kyushu Univ.*, [D], vol. 10, no. 2, p. 73–206.
- (1964): Naticid Gastropoda from the Miyazaki Group (Palaeontological study of the Miyazaki Group-X). *Trans. Proc. Palaeont. Soc. Japan, N.S.*, no. 55, p. 281–293, pls. 42–43.
- (1983): Geologic history and faunal similarity of the Pliocene-Pleistocene molluscs in Southwest Japan. In Kotaka, T. and Ogasawara, K. eds.: *Origin and migration of Japanese Cenozoic Molluscs*. Tohoku University, Sendai, p. 77–79 (in Japanese).
- Suehiro, M. (1979): Upper Miocene molluscan fauna of the Fujina Formation, Shimane Prefecture, West Japan. *Bull. Mizunami Fossil Mus.*, no. 6, p. 65–100, pls. 10–16 (in Japanese with English abstract).
- Sugiyama, T. (1935): On the variation of the shells of living and fossil *Umboonium* from

Explanation of Plate 19

Figs. Aa–Fc. Phenotype 3Ta of *Glossaulax hagenoshitensis* (Shuto): Aa–c, IGUT no. 15700-45, Loc. M-1, ×0.9; Ba–c, IGUT no. 15702-13, Loc. M-2, ×1.2; Ca–c, IGUT no. 15690-1, Loc. T-1, ×1.0; Da–c, IGUT no. 15712-8, Loc. K-12, ×0.8; Ea–c, IGUT no. 15715-2, Loc. K-9, ×0.8; Fa–c, IGUT no. 15714-14, Loc. K-8, ×0.8.

Figs. Ga–Mc. Phenotype 3Tb of *Glossaulax hagenoshitensis* (Shuto): Ga–c, GK. L7987, Loc. M-4, ×0.9; Ha–c, IGUT no. 15705-108, Loc. K-10, ×0.8; Ia–c, IGUT no. 15717-15, Loc. K-3, ×0.9; Ja–c, IGUT no. 15688-1, Loc. O-1, ×0.8; Ka–c, IGUT no. 15689, Loc. O-3, ×1.5; La–c, IGUT no. 15703-109, K-1, ×0.8; Mb–c, GIYU no. 567-3, Loc. N-1, ×0.9.

The small letters a, b and c of A–M indicate, respectively, apical, front and basal views of specimen.



- Japan, and its evolution (Part 2). *Jour. Geol. Soc. Japan*, vol. 42, no. 503, p. 449—482 (in Japanese).
- Suzuki, K. (1934): A few evidence on the evolution of *Umbonium*. *Jour. Geol. Soc. Japan*, vol. 41, no. 485, p. 67—81 (in Japanese).
- Švagrovský, J. (1982): Archaeogastropoda und Mesogastropoda des oberen Badenien von Borský Mikuláš (No-Teil des Wiener Beckens) und ihre stratigraphische Bedeutung. *Geol. Carpath.*, vol. 33, no. 1, p. 3—50, pls. 1—10.
- Tsuchi, R. ed. (1979): *Fundamental data on Japanese Neogene bio- and chronostratigraphy*. Shizuoka University, Shizuoka, 156 p.
- ed. (1981): *Fundamental data on Japanese Neogene bio- and chronostratigraphy. —Supplement—* Shizuoka University, Shizuoka, 126 p.
- Wilson, B. R. and Gillett, K. (1980): *Australian shells*. A. H. & W. Reed PTY Ltd., Sydney, 153 p., 58 pls.
- Wrigley, A. (1949): English Eocene and Oligocene Naticidae. *Proc. Malac. Soc. London*, vol. 28, no. 1, p. 10—30.

Aki 安芸, Ananai 穴内, Asuka 飛鳥, Dainichi 大日, Hagenoshita 禿の下, Hane-machi 羽根町, Haranoya 原谷, Higashidani 東谷, Hongo-Higashi 本郷東, Honohashi 方の橋, Kami-lida 上飯田, Koonji 光音寺, Koyu 児湯, Nahari 奈半利, Nihonmatsu 二本松, Oku 奥, Okuwa (Omma) 大桑, Sai 犀, Shimo-Saigo 下西郷, Shintomi-machi 新富町, Suchi 周智, Takanabe-machi 高鍋町, Tate-machi 館町, Tonohama 唐ノ浜, Tonoya 殿谷, Torihama 通浜, Yasuda-machi 安田町

西南日本後期新生代層産の *Glossaulax* (ツメタガイ属) (腹足綱: タマガイ科) の3種の種内変異: 日本の後期新生代の海に栄えた *Glossaulax* の3種, *Glossaulax hyugensis* (Shuto), *G. nodai*, n. sp. および *G. hagenoshitensis* (Shuto) の種内変異を24産地から採集した約600個体の標本を使って研究した。この3種は、層序的に、また地理的に分布が重なり、そして他の *Glossaulax* の種と平滑な臍孔壁および殻底と臍孔壁を分ける蝶状な角によって区別される。

“二型的”な変異が、*G. hyugensis* と *G. hagenoshitensis* の成員の滑層の形態に認められる。*G. hyugensis* の成員の一方の変異型は *G. hagenoshitensis* の成員の一方の変異型に似ており、また *G. hyugensis* の成員のもう一方の変異型は *G. hagenoshitensis* の成員のもう一方の変異型に似る。それにもかかわらず、この2種の類似した変異型の傾度は、極端に異なっている。*G. nodai* は、しかし、成長を通じて一定の滑層の形態を示す。滑層の形態に関して、*G. hyugensis* の幼貝は *G. nodai* に似ており、また *G. hagenoshitensis* の幼貝は、*G. hyugensis* の成員の“二型的”な変異の一方の変異型に似る。さらに、*G. hagenoshitensis* は、縫合下と臍孔壁の周辺の彫刻で、2つの異所的な変異型に分けることができる。この3種の発生上の変異の様式は、想像上の祖先種を仮定した heterochrony のモデルによって説明される。

G. hagenoshitensis は、*Polinices sagamiensis* Pilsbry と *Glossaulax reiniana* (Dunker) に分類学上混同されていたが、臍孔部の形態に基づいて、これら2種から明確に区別される。

間島隆一

798. ONTOGENIES OF TWO MIDDLE CAMBRIAN CORYNEXOCHID
TRILOBITES FROM THE CANADIAN ROCKY MOUNTAINS*

CHUNG-HUNG HU

Department of Earth Science, Taiwan Normal University, Taipei

Abstract. The present report describes the ontogenetic developments of *Fieldaspis quadriangularis*, n. sp. and *Albertella limbata* Rasetti from the Middle Cambrian, Alberta, Canada. The morphogenic characteristics of these two species during their different ontogenetic stages are similar to those of *Bathyriscus fimbriatus* Robison and *Ptarmigania aurita* Resser from the North American continent. The similar ontogenetic characteristics make them a natural taxonomic group and possibly descendants from a common ancestor.

Introduction

The purpose of the present report is to illustrate the ontogenetic developments of *Fieldaspis quadriangularis*, n. sp. and *Albertella limbata* Rasetti. The studied materials were collected from the Mount Weed section, Banff National Park, Alberta, Canada. They come from the Mount Whyte and Cathedral formations (the *Plagiura-Poliella* and *Albertella* zones) of the Middle Cambrian. The collections were made during the Second International Symposium on the Cambrian System, Field-trip 2 to Canadian Rocky Mountains, Alberta and British Columbia in 1981. The morphogenic characteristics of these two trilobites are similar and can be subdivided into five metamorphic stages, i.e., anaprotaspid, metaprotaspid, paraprotaspid, early meraspid, and late meraspid. These are briefly defined as follows.

In the anaprotaspid stage, the shield is with or without an axial lobe but with a longitudinal median furrow, a large frontal lobe, and a small terminal portion; the metaprotaspid has a cylindrical axis, with or without axial segments; the

paraprotaspid shield shows the presence of a protopygidium and a well-segmented axial lobe; the early meraspid cranidium has a broad cylindrical glabella expanded both anteriorly and posteriorly, and the presence of a narrow anterior border; the late meraspid cranidium has an expanded anterior glabella, broad anterior border, and broad anterior fixigenal area.

The ontogenetic characteristics of *Fieldaspis quadriangularis* and *Albertella limbata* are closely similar to those of *Bathyriscus fimbriatus* Robison (1967) and *Ptarmigania aurita* Resser (Hu, 1971) as reported from the Middle Cambrian of North America. The protaspis of all these species possesses rather narrow anterior second and third axial segments, a forwardly expanded frontal lobe, a large palpebral lobe; the meraspid cranidia are trapezoidal in outline; the cylindrical glabella is expanded both anteriorly and posteriorly, and protrudes anteriorly; the palpebral lobe is rather large. Evidently that these four species of trilobites are a natural taxonomic group and with a close phylogenetic relationship.

The ontogenetic developments of the present trilobites are differentiated from that of the

*Received June 10, 1984.

ptychoparioids: *Crassifimbria walcotti* (Resser) (Palmer, 1958), *Glyphaspis* cf. *parkensis* Rasetti (Hu, 1971), *Ehmaniella burgessensis* Rasetti (Hu, 1984), *Sao hirsuta* Barrande (Whittington, 1959), *Trymatospis convexus* Hu and *Yuknessaspis santaquinensis* Hu (Hu, 1972) from the Middle Cambrian in having protaspis with a rather weakly developed axis and the absence of the second to third axial segments; the meraspid cranium has a large palpebral lobe and a somewhat forwardly expanded glabella. These different morphologic features of the two groups of trilobites clearly show that they are phylogenetically unrelated and had independent ancestral stocks.

The author wishes to express his thanks to Dr. J. D. Aitken, Geological Survey of Canada, Calgary, Alberta for guidance of the field trip and personal help. Thanks go to Dr. K. E. Caster, University of Cincinnati, Ohio for reading over the present manuscript and corrected with the English text. The figured specimens are all stored in the Geology Museum, University of Cincinnati, Ohio (UCGM).

Systematic paleontology

Genus *Fieldaspis* Rasetti, 1951

Fieldaspis quadriangularis, n. sp.

Pl. 20, Figs. 1–29, Text-figs. 1 A–N.

Diagnosis.—Cranidium quadrate in outline, convex, with cylindrical glabella slightly expanded forwardly; four pairs of glabellar furrows are seen; no preglabellar field is present, but there is a narrow anterior border; fixigenae narrow, flat, and occupied by a pair of large palpebral rings; posterior fixigenae narrow and of about the same width as the occipital ring; librogenae sickle-shape and elongate; hypostoma acute, triangular and ankylosed with the rostrum; pygidium semicircular and with a pair of long caudal spines.

Description.—The quadrate cranium has a rather large cylindrical glabella which is moderately convex, and has no preglabellar field, but there is a narrow anterior border elevated

along the anterior glabellar margin; the glabella is convex above the flattened fixigenae, it is demarked by a dorsal furrow and has four pairs of glabellar furrows; the anterior first pair of furrows are faint and protrude forwardly; the second pair are deeper than the first pair and extend horizontally; the third and fourth pairs are deeper and more distinct than the anterior two pairs; they are directed posterolaterally; the anterior facial sutures are slightly divergent and convex; the posterior facial suture runs almost parallel to the narrow posterior fixigenal border; the long palpebral ring is convex and well delimited by a palpebral furrow; no occipital spine or tubercle is known, but faint wrinkles are present along the posterior margin.

The librogena is narrowly elongate and has a medium-sized genal spine; the narrow ocular platform is convex, elevated from the lateral marginal furrow to the large ocular ring; both of the lateral and posterior marginal furrows are well defined and connected at the genal angle roundly.

The hypostoma is triangular in outline and ankylosed to a narrow rostrum; the median body is oval-elongate and convex, and has a U-shape posterior inner marginal border; the sides of the median body are distinctly impressed by a pair of elongate pits, and flattened antero-lateral wings are present.

The pygidium is transverse and nearly sub-quadrate with posteriorly arched marginal border; the convex axis is divided into two distinct axial rings and a large terminal portion which is possibly made up of two or three rudimentary axial rings; the pleural lobe is gently convex, well demarked by a pair of intropleural furrows, and two to four pairs of faint grooves; a pair of long slender caudal spines extend posterolaterally from the first to second pygidial segments; the axial rings are each marked with a median tubercle.

The skeletal surface is covered by faint to medium coarse granules; both anterior glabella and anterior median hypostomal margin are impressed by a rounded pit; a few coarse granules occur along the anterior cranial border, and faint ridges are parallel to the lateral border

of the rostrum.

Remarks.—The studied materials were collected from the base of the Mount Weed Section far below the *Albertella limbata* Rasetti and *Plagiura cerops* (Walcott) zones, and above the *Olenellus* Zone. The trilobite fragments are embedded in a dark grey, faintly crystalline limestone. The present species is represented by abundant adult and immature skeletons, which show the very well preserved ontogenetic sequence. This species is differentiated from *F. furcata* Rasetti, *F. bilobata* Rasetti, and *F. superba* Rasetti (Rasetti, 1951) by its quadrate cranium, broader anterior fixigenae, and less divergent anterior facial suture; the pygidium possesses a pair of large caudal spines, and the pygidial axis bears median tubercles; the posterior marginal border is well defined.

Locality and horizon.—Mount Weed Section, near Bow Lake, Banff National Park, Alberta; Mount Whyte Formation, *Plagiura*-“*Poliella*” Zone, Middle Cambrian.

Fieldaspis quadriangularis, n. sp., ontogeny

Anaprotaspid stage (Pl. 20, Figs. 1–6 & Text-figs. 1A, B). The shield is round with both anterior and posterior margins curving inwardly, and moderately convex; the measurement of the shield is 0.26 to 0.38 mm in length (sag.); the axial lobe is a longitudinal furrow, which suggests the gut position; no axial ring is observed but two to three pairs of pits are present besides of the median furrow; the triangular frontal lobe expands forwardly from the median furrow and with a pair of lateral eyebrow ridges extending laterally; the fixigenal area is broad and moderately convex; the shield is possibly surrounded by a narrow flat marginal border.

The morphogenesis of the instars during present stage indicates that the earliest skeleton has a longitudinal furrow along the axial region but in the later anaprotaspid the shield axis possesses a large frontal lobe, two to three pairs of axial knobs, and a small terminal portion.

Metaprotaspid stage (Pl. 20, Figs. 7, 8 & Text-

fig. 1C). The shield is round, moderately convex, with the anterior margin straight, and the posterior margin curving inwardly; the measurement of the shield is 0.42 to 0.40 mm in sagittal length; the axial lobe is possibly faintly defined by three central rings, a small terminal portion, and a large frontal lobe; these central rings are made from three pairs of central knobs from the previous stage; the convex rounded frontal lobe is extended with a pair of eyebrow ridges extending from the anterolateral sides and running a short distance to connect with the palpebral ridge; a pair of distinct frontal pits is marked at the sides of the frontal lobe where the palpebral lobes are initiated; the narrow well-defined palpebral lobe runs posterolaterally from the frontal pits for a short distance and ends before reaching the transverse mid-line of the shield; the terminal portion is a small semi-circular node that is elevated at the posterior median margin; the surface of the shield is covered by faint granules; the narrow flat marginal border surrounds the posterior half of the shield, and forms a pair of short spines at the posterolateral margin.

Paraprotaspid stage (Pl. 20, Figs. 9, 10, 12, 13 & Text-figs. 1D, E). The shield is convex and round to trapezoidal in outline; the sagittal length of the shield varies from 0.50–0.66 mm; the axial lobe contains a large rounded frontal lobe three transverse rings, and a small terminal portion; these are all well-defined by dorsal and ring furrows; the frontal lobe has a similar structure to that of previous stage with a pair of eyebrow ridges and distinct pits; the posterior shield margin is equal to or broader than the occipital ring and bears a pair of saw-teeth located at the lateral ends; the surface of the skeleton is covered by faint granules, and there is a narrow flat margin along the posterior and lateral margins.

The distinct morphologic characteristics of the present stage are: the axial nodes are complete and the median furrow is absent; the posterior fixigenal border increases in width from narrow to broad, which suggests the presence of the protopygidium or the thoracic

segments.

Early meraspid stage (Pl. 20, Figs. 14–16 & Text-fig. 1F). The cranidium is trapezoidal in outline, moderately convex, and the sagittal length is 0.75 to 1.25 mm; the glabella is oblong, gently expanded anteriorly from the second glabellar furrow; the first glabellar segment or the frontal lobe is a larger segment than the following and protrudes into the frontal furrow; the second to fourth glabellar segments are faintly dissected ring furrows, and the convex subtriangular occipital ring bears a small median tubercle; a narrow anterior border appears in front of the glabella and arches forwardly; the frontal pits which were well marked in the previous stage now becomes shallower; the paired palpebral ring is parenthetic and extends from the sides of the first glabellar segment to end before reaching the posterior fixigenal furrow; the posterior fixigenal border is about as wide as the occipital ring; the surface is granulate and a median impression is marked in front of the anterior glabellar margin.

The morphogenesis of the present stage is: the anterior border appears; the glabellar furrows are complete; both anterior and posterior facial sutures increase in length.

Late meraspid stage (Pl. 20, Figs. 17, 18 & Text-figs. 1 I, H). The cranidium is moderately convex and measurement is about 1.50 to 2.50 mm in sagittal length; the glabella expands forwardly from the posterior second glabellar furrow with a rounded anterior margin; the four pairs of glabellar furrows are complete and the posterior parts of the first glabella are deeply impressed and the following are shallow; the occipital ring is subtriangular, convex, and bearing a minute median tubercle; the elevated anterior border arches forwardly and is well delimited by an anterior furrow; the narrow palpebral lobe is well defined by the palpebral furrow; it is elevated and situated posteriorly to the transverse midline of the glabella; the anterior facial suture is short, slightly divergent, and convex; the posterior fixigenal area is triangular and the post-fixigenal border is about the same width as that of the occipital ring;

the fixigenal area is broad and flat between the dorsal furrow and the palpebral lobe. The cranial surface is covered by faint granules and a median impression is situated in front of the anterior glabellar margin.

The present stage is differentiated from previous stage in having a broader anterior border, broader anterior fixigenal area, and posteriorly located palpebral lobe. A pair of additional glabellar furrows appears at the sides of the anterior first glabellar segment.

The growth of the pygidium (Pl. 20, Figs. 23, 24, 26, 28 & Text-figs. 1L, N). A small pygidium measured about 0.3 mm in sagittal length is made of three freely articulated segments and a small terminal plate; the axial lobe is convex above the pleuron; the axial ring is well separated by a ring furrow and bears a dorsal spine on each axial ring. The pleural bands each project into a pair of posteriorly directed spines. Judging from the pygidial structures this pygidium to the protaspid stage. The next pygidium (Pl. 20, Figs. 26, 28) in size measured from 1.2 to 0.75 mm in sagittal length. It is composed of three segments and a terminal portion. If this pygidium is compared to the earlier stage, it is clear that the pygidial segments are all ankylosed as a plate and show the adult structure; however, their posterior marginal border still remains incomplete, *i.e.*, the marginal saw-teeth are absent. Therefore, these specimens are judged as representing meraspid pygidia.

Growth of the librevena (Pl. 20, Figs. 11, 12). The morphogenic characteristics of the librevena during its different growth stage shows progressive reduction of the length of the genal spine and an increase in the width of the ocular platform.

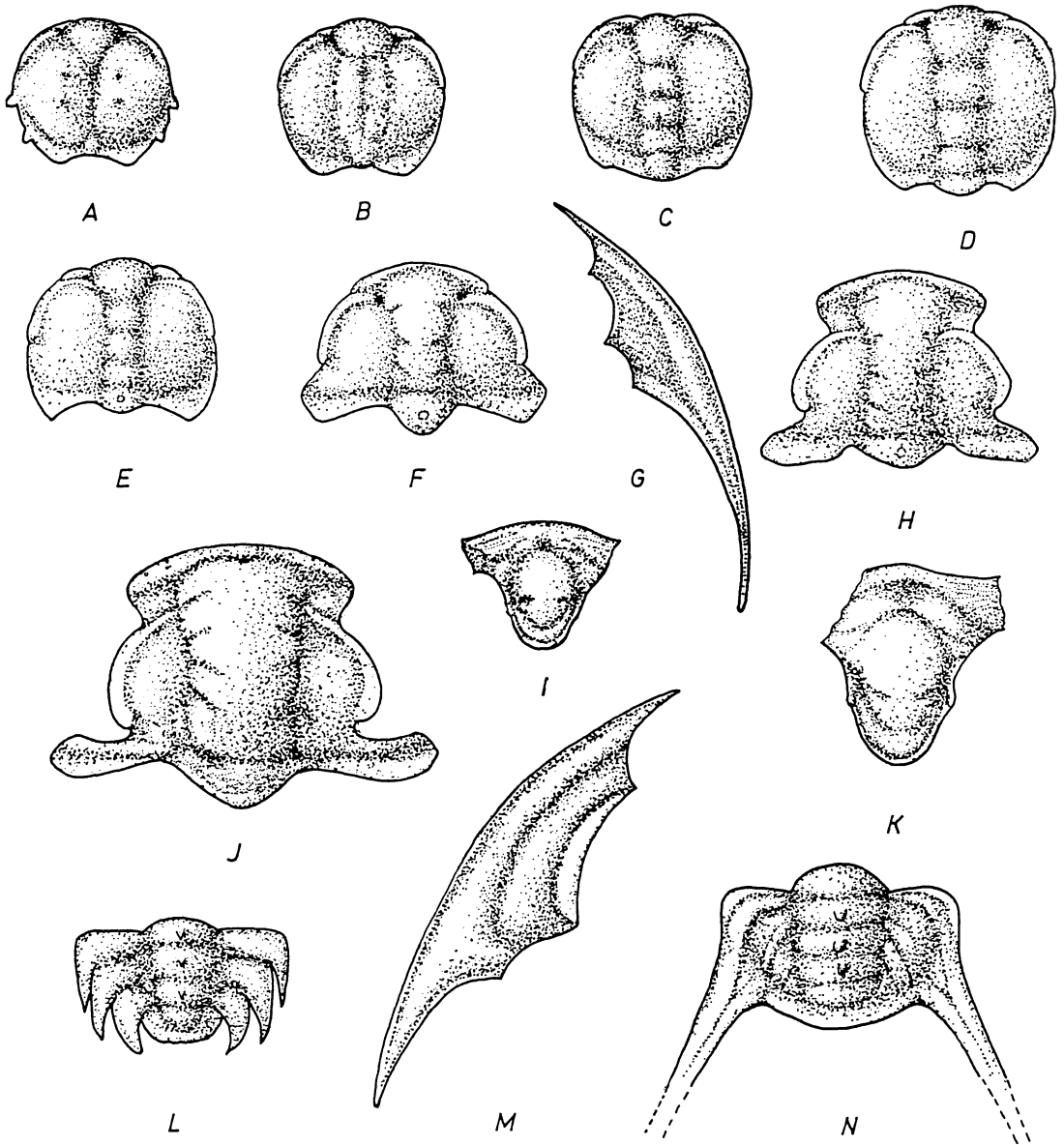
Genus *Albertella* Walcott, 1908

Albertella limbata Rasetti, 1951

Pl. 21, Figs. 1–32, Text-figs. 2 A–N.

Albertella limbata Rasetti, 1951, p. 154, pl. 18, figs. 8–17.

Remarks.—A small piece of dark grey, finely



Text-fig. 1. *Fieldaspis quadriangularis*, n. sp.

A, B, two anaprotaspis shields, showing the median axial furrow and possibly coelomic nodes. $\times 50$; C, a metaprotaspis, showing the completion of the axial lobes and the axial segments. $\times 42$; D, E, two paraprotaspis shields, showing the broadening of the posterior fixigenal border. $\times 23$, $\times 20$; F, an early meraspis cranium; notice the presence of the anterior border. $\times 18$; G, a meraspis libregena, showing the long slender genal spine and the lateral furrow extending into the genal spine. $\times 3.5$; H, a late meraspis cranium, showing the protruded anterior glabella and the broadening of the anterior fixigenal area. $\times 8$; J, a holaspis cranium. $\times 3.7$; I, K, immature and holaspis hypostomata, showing the association of the rostrum. $\times 9$, $\times 3$; L, an early meraspis pygidium. $\times 31$; M, an adult libregena. $\times 3$; N, an adult pygidium, showing the caudal spines and the axial tubercles. $\times 4.5$.

crystalline fossiliferous limestone was collected from the same locality as *Fieldaspis quadrangularis* but stratigraphically slightly higher in the *Albertella* Zone. The studied material contains rather abundant mature and immature skeletons. They show ontogenetic preservation very well. This trilobite is comparable to some occurrences those reported by Rasetti (1951) from the same general area.

Additional description.—The libregena is crescentic in outline, moderately convex, and has a rather large ocular ring; both the anterior facial suture and the posterior facial suture lines are short; the ocular platform is narrow anteriorly and broadens posteriorly; it is faintly marked by radial ridges; the lateral and the posterior marginal furrows meet at the genal angle, and run for a short distance into the genal spine. The hypostoma is acutely triangular in outline, convex, and surrounded by a narrow marginal border along the posterior and lateral margins; the convex median body is nearly triangular and surrounded by a U-shape posterior furrow and a pair of lateral elongate pits. The thoracic segment is well impressed by a broad ring and intrapleural furrows; the axial ring and the pleural lobe are of the same width; the pleural lobe terminates in a slender posterolaterally directed spine.

Locality and horizon.—Mount Weed Section, near Bow Lake, Banff National Park, Alberta; Cathedral Formation, *Albertella* Zone, Middle Cambrian.

Albertella limbata Rasetti, ontogeny

Anaprotaspis stage (Pl. 21, Figs. 1, 2 & Text-figs. 2A, B). The shield is round, moderately convex, and measures 0.26 mm in sagittal length; the axial lobe is narrow and depressed as a longitudinal median furrow; the rounded frontal lobe is convex with a pair of deeply demarked pits situated anterolaterally; the paired eyebrow shape ridges extend in front of the pits — the sides of the frontal lobe, and run posterolaterally for a short distance; the posterior half of the axial lobe is slenderly elevated into a small terminal node at the shield margin. This suggests the initial portion of the occipital ring. The

lateral lobe is rather broader than the axis, convex, and surrounded by a narrow deflated marginal border; the surface of the shield is smooth to faintly granulate; there are possibly two pairs of short marginal spines at the lateral and posterolateral shield margins.

Metaprotaspis stage (Pl. 21, Figs. 3–6 & Text-fig. 2C). The shield is round to quadrate in outline, convex; it measures about 0.25 to 0.35 mm in length (sag.); the axial lobe is well developed but axial rings are indistinguishable; the frontal lobe is broad, larger than the following axia, convex, and well marked by a pair of lateral pits; the paired eyebrow ridges extend from the anterolateral frontal lobe for a short distance; a pair of palpebral lobes is developed behind the frontal pits and extend anterolaterally to the transverse mid-line of the shield; the narrow axial lobe is well-defined by furrows and the axial ring is poorly developed; but a few pairs of pits are faintly marked along the axial furrow, which suggests the presence of the axial segments; the terminal node is small, convex, and situated at the posterior shield margin; the pleural lobe is twice as wide as the axis, convex, and no marginal border is visible. The surface of the shield is rough or faintly granulate; certain specimen shows faint cephalic segmental furrows on the pleural region.

The ontogenetic characteristics of this stage are: the axial lobe increases in broadness; unsegmented or segmented axial lobe tapering posteriorly or expanded at both anterior and posterior ends from the anterior second axial ring; the axial furrows increase in depth from shallow to well recognizable.

Paraprotaspis stage (Pl. 21, Figs. 7–11 & Text-figs. 2D, E). The cranium is quadrate to trapezoidal in outline, moderately convex; the sagittal length varies 0.50 to 0.65 mm; the axial lobe is deeply demarked anteriorly and expands forwardly and posteriorly from the second axial ring; the first axial ring or the frontal lobe is the largest, convex, with a pair of lateral pits lying behind the eyebrow ridges; the narrow palpebral lobe is well defined by a furrow, and is elevated along the anterolateral margin of the shield; the following axial rings

increase the size from the anterior second to fourth, and there is a small terminal node representing the occipital ring; all of the axial rings are well separated by transverse ring-furrows; the pleural lobe is about twice as wide as the axis, convex, and has a very well developed post-fixigenal border; the fixigenal margin is surrounded by a narrow flat border; the surface of the shield is covered by faint granules; a pair of large tubercle is marked at the sides of the posterior fourth axial ring-furrow.

The morphogenesis of the instars during the present stage is: the cranium changes from quadrate to trapezoidal in outline and the glabellar ring is well defined; the posterior fixigenal border increases in width and the protopygidium appears.

Early meraspid stage (Pl. 20, Figs. 12–14, 16 & Text-fig. 2F). The cranium is trapezoidal in outline, moderately convex, and is about 0.85 to 1.7 mm in length (sag.); the axial lobe is deeply demarcated by dorsal furrows and expands forwardly from the occipital ring furrow with a large-sized frontal lobe; the axial rings are well delimited by transverse ring furrows which are shallow across the central line and deeply incised to the dorsal furrows; the subtriangular occipital

ring is convex and bears a minute median tubercle; a narrow anterior border appears in front of the glabella; the large narrow palpebral ring is parenthetical and extends from the sides of the frontal lobe posteriorly to the narrow post-fixigenal area; the post-fixigenal border is deeply defined by a border furrow and is less broad than the occipital ring; the surface of the shield is faintly granulate and a few coarse granules are present; the anterior margin of the frontal lobe is marked with a distinct median pit.

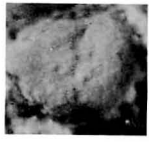
A nearly triangular pygidium composed of 5 to 6 freely articulated segments is assigned to the present stage. The first segment is the largest and with the pleural bands protruding posterolaterally; the following segments are small and have their pleural ends projected posteriorly; the axis is about the same width as the pleural lobe and well demarcated by axial ring furrows; the intrapleural furrow of each segment is deep and broad, and is subparallel to the pleural bands; the axial rings all possess a single but slender median spine.

During the present stage the cranium appears as a narrow anterior border; the glabella changes from tapering forward to expanded forward; the posterior fixigena decrease in

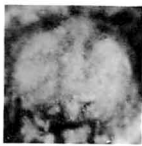
Explanation of Plate 20

Figs. 1–29. *Fieldaspis quadriangularis*, n. sp.

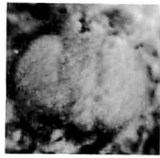
- 1–6, a growth series of anaprotaspid shields; notice the incomplete axial lobe. 1–4, $\times 50$; 5, $\times 45$, 6, $\times 43$.
- 7, 8, two metaprotaspid shields, showing the genesis of the axial lobe. $\times 38$, $\times 42$.
- 9, 10, 12, 13, several paraprotaspid shields, showing the lateral expansion of the posterior fixigenal border and the possible presence of the protopygidium. $\times 32$, $\times 23$, $\times 20$, $\times 22$.
- 11, a broken libregena. $\times 3$. (paratype).
- 14–16, three early meraspid crania; note the presence of the anterior border and the completion of the glabellar furrows. 14, 15, $\times 18$; 16, $\times 13$.
- 17, 18, two late meraspid crania, showing the forwardly protruded glabella, broad anterior fixigenal area, and the posteriorly located palpebral lobe. $\times 8$, $\times 7$.
- 19, 25, a meraspid hypostoma and an holaspid hypostoma. $\times 9$, $\times 3$. (paratypes).
- 20, 21, 27, lateral and dorsal views of two broken crania. 20, 21, $\times 3.7$; 27, $\times 4$. (21, 22, holotype; 27, paratype).
- 22, a complete libregena beside a partly broken thoracic segment. $\times 3.5$.
- 23, 24, 26, three mature and immature pygidia. $\times 4.5$; $\times 31$; $\times 10$, (paratypes).
- 28, a paraprotaspid cranium and a meraspid pygidium. $\times 14$. (paratype).
- 29, a small piece of limestone, showing the abundance of the immature skeletons. $\times 13$.



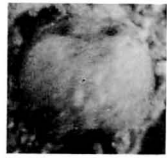
1



2



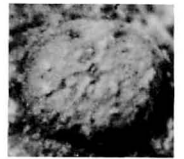
3



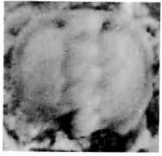
4



5



6



7



8



9



10



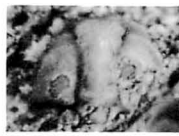
11



12



13



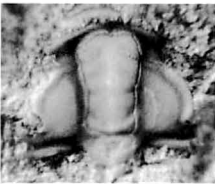
14



15



16



17



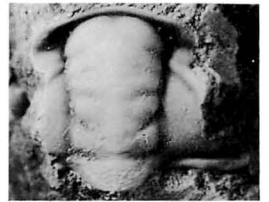
18



19



20



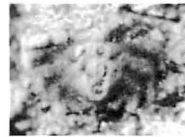
21



22



23



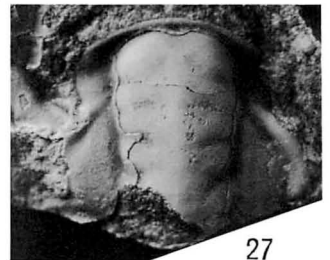
24



25



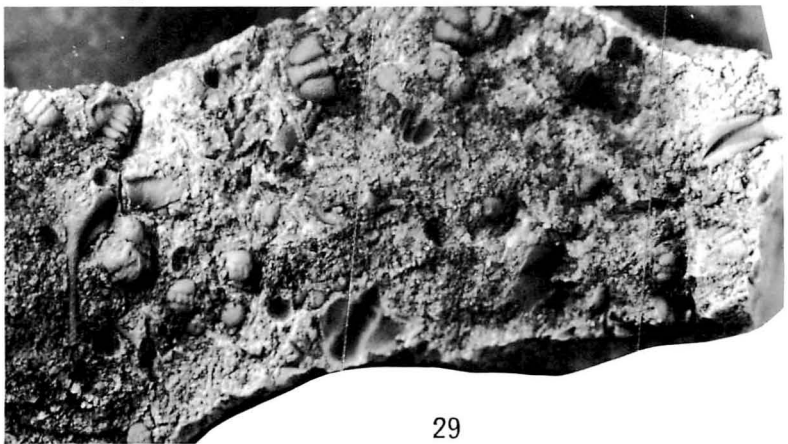
26



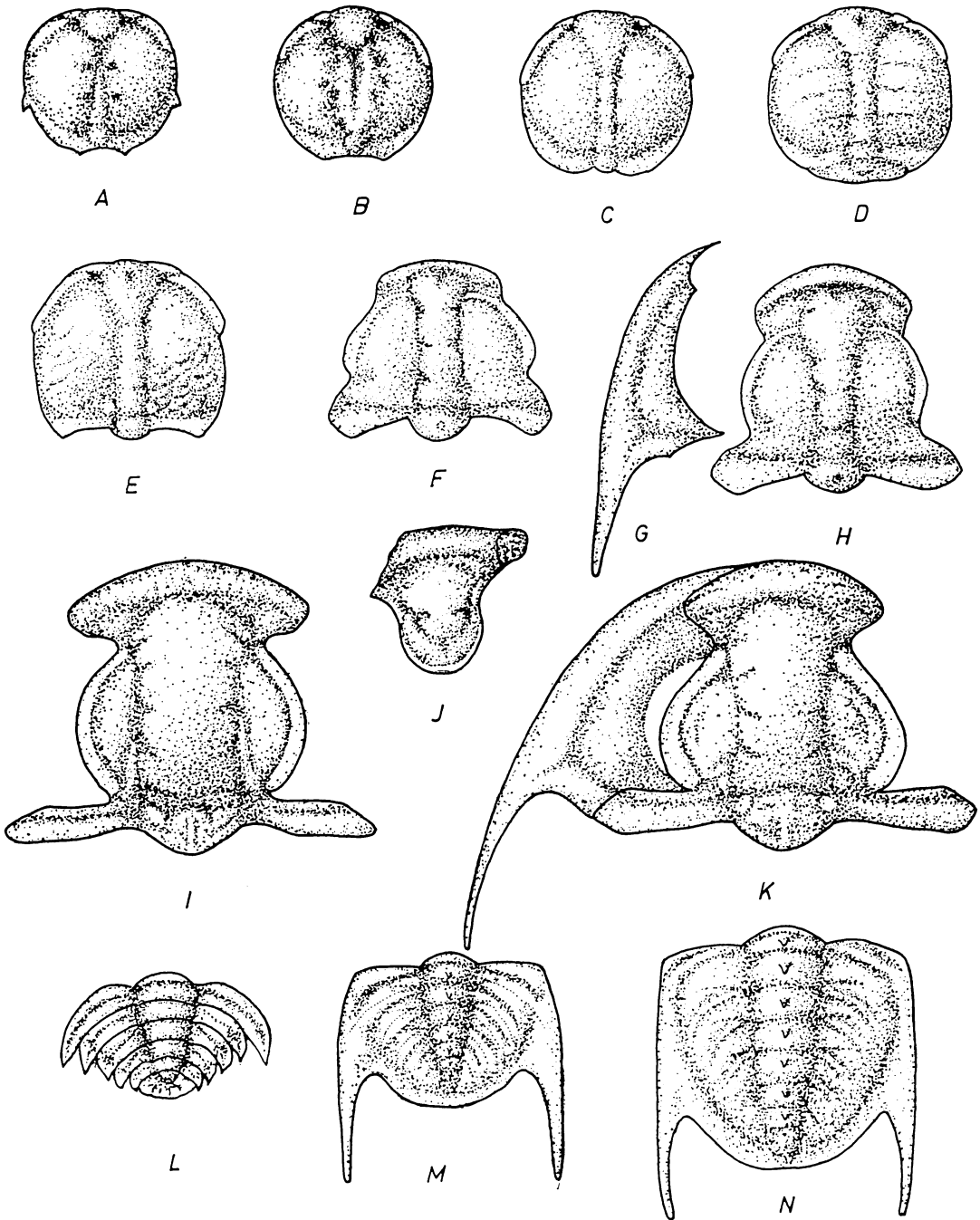
27



28



29

Text-fig. 2. *Albertella limbata* Rasetti

A, B, anaprotaspides, $\times 57$; C, metaprotaspis, $\times 50$; D, E, two paraprotaspides, $\times 38$, $\times 29$; F, early meraspis cranidium, $\times 20$; H, late meraspis cranidium, $\times 15$; G, a meraspis libregena, $\times 16$; I, K, two holaspis cranidia, $\times 9$, $\times 4$; J, a late meraspis hypostoma associated with a part of rostrum, $\times 15$; L, early meraspis pygidium, $\times 20$; M, late meraspis pygidium, $\times 15$.

broadness; the palpebral lobe increases in size and the posterior facial suture-line is divergent-posterolaterally to laterally straight.

Late meraspid stage (Pl. 21, Figs. 17, 18, 21 & Text-fig. 2H). The cranidium is elongate subquadrate in outline, convex, and is about 1.80 to 2.80 mm in length (sag.); the glabella is deeply impressed by dorsal furrrows, which expand forwardly with a rounded anterior margin; the glabellar furrows are complete, except that the posterior is incomplete; the occipital ring is large, subtriangular, convex, and bearing a median tubercle; the anterior brim is narrow, concave, and with the marginal border turned upward; the parenthetical palpebral lobe is deeply demarcated by a palpebral furrow; it runs posterolaterally from the anterior first glabellar furrow to the base of the occipital furrow; the anterior facial suture is divergent-anterolaterally and the posterior one, while divergent, is straight and almost to the posterior fixigenal border. The surface is covered by faint granules and an impression is present in front of the glabella.

A small triangular hypostoma (Pl. 21, Fig. 15 & Text-fig. 2J) is arbitrarily assigned to the present stage; it is ankylosed with an arched

rostrum anteriorly; the oval median body is convex and elevated from the marginal border by a distinct furrow; the posterior median body is occupied by a pair of transverse knobs laterally; the U-shaped inner marginal border is broad and convex, and demarcated by a broad border furrow; the outer marginal border is rather narrow and elevated from the border furrow; the anterior hypostoma is impressed by a median depression.

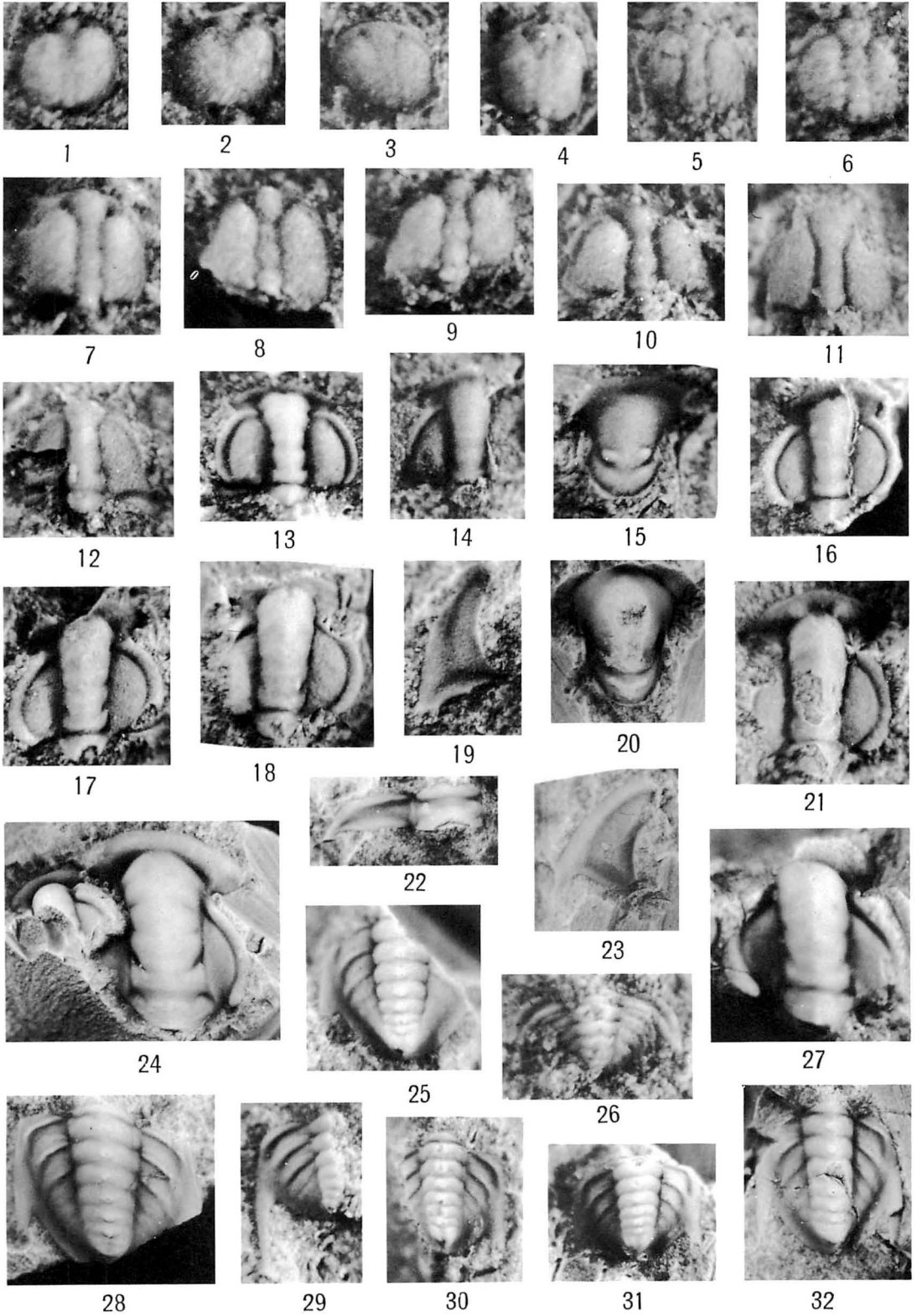
The rostrum is arched anteriorly with its lateral end broader than the central portion, convex, and chevron-shape; the surface is possibly marked by parallel ridges at its lateral ends.

The supposedly late meraspid pygidium (Pl. 21, Figs. 29–31 & Text-fig. 2M) has a quadrate outline, convex, with the axial lobe tapering slightly posteriorly; the axial lobe is made of 6–7 convex axial rings and a terminal portion; these are well separated by ring-furrows; each of the axial rings is occupied by a slender median tubercle or a short spine directed vertically; the well-segmented pleural lobe is equal to or slightly broader than the axis and has a pair of large caudal spines directed posteriorly; the surface is covered by faint granules.

Explanation of Plate 21

Figs. 1–32. *Albertella limbata* Rasetti

- 1, 2, two anaprotaspides, showing the narrow poorly developed axial lobe. $\times 57$.
- 3–6, a few metaprotaspides, showing the presence of the axis. 3–5, $\times 50$; 6, $\times 45$.
- 7–11, several paraprotaspid cranidia, showing the well developed fixigenal border and the suggestion of the presence of the protopygidium. 7, $\times 38$; 8, $\times 34$; 9, $\times 37$; 10, $\times 36$; 11, $\times 29$.
- 12–14, 16, four early meraspid cranidia, showing the presence of the anterior border and the parenthetic palpebral lobes. 12, $\times 21$; 13, $\times 20$; 14, $\times 16$; 16, $\times 12$.
- 17, 18, 21, three late meraspid cranidia, showing the completion of the glabellar furrows and the lengthening of the glabella. 17, $\times 13$; 18, $\times 15$; 21, $\times 10$.
- 15, an immature hypostoma ankylosed with the rostrum. $\times 15$.
- 20, an adult hypostoma, showing the elongation of the median body. $\times 4.5$.
- 19, 23, two incomplete libregenae. $\times 15$; $\times 5$.
- 22, part of a thoracic segment. $\times 6$.
- 24, 27, two adult cranidia, showing the morphologic varieties of the fixigenal lobe and the glabella. $\times 3.8$; $\times 9.3$.
- 26, an early meraspid pygidium. $\times 20$.
- 29–31, three late meraspid pygidia. 29, $\times 15$; 30, $\times 8.6$; 31, $\times 7.7$.
- 25, 28, 32, three holaspid pygidia. $\times 9.5$; $\times 5$; $\times 5$.



The morphogenesis of the present stage is: the glabellar furrows are nearly complete; the palpebral ring increases in size; the post-fixigenal area becomes narrower; the anterior facial suture is divergently convex, and the posterior one is divergently parallel to the fixigenal border. The pleural lobe of the pygidium decreases in width and becomes equal in width to that of the axis.

References

- Aitken, J. D. (1981): The Cambrian System in the southern Canadian Rocky Mountains, Alberta and British Columbia (Second International Symposium on the Cambrian System). *Guide book for field trip 2*. 61 p. (USGS, Colorado).
- Hu, C-H. (1971): Ontogeny and sexual dimorphism of lower Paleozoic Trilobita. *Palaeontographica Americana*, vol. 7, no. 44, p. 31—155.
- (1972): Ontogenies of two Middle Cambrian trilobites from Wasatch Mountains, Utah. *Acta Geol. Taiwanica*, no. 15, p. 41—50 (Taiwan).
- (1984): Ontogenesis of *Ehmaniella burgensensis* Rasetti (Trilobita) from the Burgess Shale, Middle Cambrian, Yoho Park, British Columbia. *Palaeont. Soc. Japan, Proc. Trans., N.S.*, 135, p. 395—400, pl. 76.
- Palmer, A. R. (1958): Morphology and ontogeny of a lower Cambrian ptychoparioid trilobite from Nevada. *Jour. Paleont.*, vol. 32, p. 154—170, pls. 25, 26.
- Rasetti, F. (1951): Middle Cambrian stratigraphy and faunas of the Canadian Rocky Mountains. *Smith. Mis. Coll.*, vol. 116, no. 5, 277 p.
- Robison, R. A. (1967): Ontogeny of *Bathyriscus fimbriatus* and its bearing on affinities of corynexochid trilobites. *Jour. Paleont.*, vol. 41, no. 1, p. 213—221, pl. 24, text-figs. 1—5.
- Whittington, H. B. (1959): Ontogeny of Trilobita: Treatise on invertebrate paleontology, Arthropoda 1, Pt. O, *Geol. Soc. America & Univ. Kansas Press*, p. 127—145 (Lawrence).

カナダのロッキー山地産の中期カンブリア紀 Corynexochid 三葉虫 2 種の個体発生: カナダ・アルバータ産の中期カンブリア紀の *Fieldaspis quadriangularis*, n. sp. と *Albertella limbata* Rasetti の個体発生を記述した。この 2 種は、個体発生の種々の段階での形態形成の特徴が北米大陸の *Bathyriscus fimbriatus* Robison と *Ptarmigania aurita* Resser のそれに類似する。類似した個体発生の特徴はそれらが自然分類上同一グループに属すると共に、恐らく共通の祖先に由来することを示している。 胡忠恒

行 事 予 定

	開 催 地	開 催 日	講演申込締切
1986年 年会・総会	東北大学・他	1986年1月31日～2月2日	1985年11月30日

講演申込先：113 東京都文京区弥生 2-4-16 日本学会事務センター 日本古生物学会 行事係

お 知 ら せ

○1986年度年会・総会は昭和61年1月31日～2月2日に東北大学および戦災復興記念館で行なわれますが、今回から年会・総会にかぎり、プレプリント（講演予稿集）を次の要領で作成することになりました。講演をされる予定の方は御面倒ですが、あらかじめ御承知いただき、下書き等を御用意下さい。

1. 講演締切（昭和60年11月30日）の直後に講演申込者に原稿用紙をお送りし、特別講演・シンポジウム講演は2ページ分（本文約1700字）、個人講演は1ページ分（本文約800字）の清書した原稿を行事係に折返し提出していただきます。
2. 清書原稿はそのまま印刷できるよう、タイプ・ワープロまたは楷書の手書きとし、表・線画を制限ページ内に入れても結構です。
3. プレプリントが新しい分類名の原記載となるのは好ましくないので、原稿の中で新名を提唱するのは避けて下さい。
4. プレプリントは会場で実費販売（1000円程度）となります。

なお、ポスターセッションや小集会なども会場のスペースの許す限り用意いたしますので、御希望の方やアイデアをお持ちの方は事務センターまたは行事係までお申出下さい。

行事係（東京大学・理・地質 速水 格）

○文部省科学研究費補助金（研究成果刊行費）による。

1985年7月10日 印刷	発 行 者	日本古生物学会
1985年7月15日 発行		文京区弥生2-4-16
ISSN 0031-0204		日本学会事務センター内
日本古生物学会報告・紀事		(振替口座東京84780番)
新 篇 138号	編 集 者	猪 郷 久 義・浜 田 隆 士
2,500 円	印 刷 者	東京都練馬区豊玉北2ノ13
		学術図書印刷株式会社 富 田 潔
		(電 話 03-991-3754)

Transactions and Proceedings of the Palaeontological
Society of Japan

New Series No. 138

July 15, 1985

CONTENTS

TRANSACTIONS

795. LING, Hsin Yi: Early Paleogene silicoflagellates and ebridians from the Arctic Ocean 79
796. KANEKO, Atsushi: A Middle Devonian trilobite fauna from the Kitakami Mountains, northeast Japan-II. The Calymenidae 94
797. MAJIMA, Ryuichi: Intraspecific variation in three species of *Glossaulax* (Gastropoda: Naticidae) from the Late Cenozoic strata in central and southwest Japan 111
798. HU, Chung-Hung: Ontogenies of two Middle Cambrian corynexochid trilobites from the Canadian Rocky Mountains 138